COPY 1

LIBRARY
AUG 12 '74
RECEIVED

RD
74/7

Report No. FAA-RD-74-7

SLANT VISUAL RANGE (SVR)/APPROACH LIGHT CONTACT HEIGHT(ALCH) MEASUREMENT SYSTEM: EVALUATION IN FOG

JULY 1974

FINAL REPORT
PHASE II

Document is Available to the Public Through the
National Technical Information Service,
Springfield, Virginia 22151

Prepared for

U.S. DEPARTMENT OF TRANSPORTATION
FEDERAL AVIATION ADMINISTRATION
Systems Research & Development Service
Washington, D.C. 20590

The contents of this report reflect the views of the Research and Development Department, Naval Ammunition Depot, which is responsible for the facts and the accuracy of the data presented herein. The contents do not necessarily reflect the official views or policy of the FAA. This report does not constitute a standard, specification, or regulation.

Technical Report Documentation Page

1. Report No.	2. Government Accession No.	3. Recipient's Catalog No.
FAA-RD-74-7		

4. Title and Subtitle	5. Report Date
Slant Visual Range (SVR)/Approach Light Contact Height (ALCH) Measurement System: Evaluation in Fog	July 1974
	6. Performing Organization Code
7. Author(s)	8. Performing Organization Report No.
9. Performing Organization Name and Address Department of Defense Research and Development Department Naval Ammunition Depot Crane, Indiana 47522	10. Work Unit No. (TRAIS)
	11. Contract or Grant No. DOT-FA71WAI-213
12. Sponsoring Agency Name and Address Department of Transportation Federal Aviation Administration Systems Research and Development Service Washington, D. C. 20591	13. Type of Report and Period Covered Final Report
	14. Sponsoring Agency Code

15. Supplementary Notes

16. Abstract

Systems with potential for predicting SVR/ALCH were tested at the National Aviation Facilities Experimental Center (NAFEC), Federal Aviation Administration, Department of Transportation, Atlantic City, New Jersey.

These systems' estimation of the slant path transmittance were compared to data being generated by NBS transmissometers located at several levels on nearby 160-foot towers. The transmittance values predicted by the systems being evaluated were used to compute RVR and SVR data. The results of these computations were compared to the actual RVR-SVR calculated based upon NBS transmissometer measurement.

The report contains data on the stratification of the fogs observed at NAFEC during the test duration.

Pilot eye response is considered with emphasis on techniques of determining the pilot's adaptation level. The pilot's adaptation level calculation is combined with (1) the extinction rate measurements, (2) pilot's eye response and (3) the geometry of the scenario in order to form ALCH and SVR algorithms. (NOTE: This July 1974 report supersedes report of identical title and number, dated January 1974.)

17. Key Words	18. Distribution Statement
Slant visual range Fog visibility Adaptation level	Document is available to the public through the National Technical Information Service, Springfield, Virginia 22151.

19. Security Classif. (of this report)	20. Security Classif. (of this page)	21. No. of Pages	22. Price
UNCLASSIFIED	UNCLASSIFIED	132	

Form DOT F 1700.7 (8-72) Reproduction of completed page authorized

TABLE OF CONTENTS

		PAGE
MANAGEMENT SUMMARY		ix
1.	INTRODUCTION	1
2.	EXPERIMENTAL FACILITY	3
	Physical Description	3
	Baseline Data Instrumentation	8
	Luminance and Illuminance Meters	8
	Data Acquisition System	10
3.	BASELINE FOG DATA	12
4.	TEST RESULTS OF BACKSCATTER VISUAL RANGE SYSTEM	23
5.	FORWARD SCATTER METER VISUAL RANGE SYSTEM CONCEPT	29
	Forward Scatter Meter	30
	Candidate System Evaluation	38
6.	EVALUATION OF METHODS OF DETERMINING SLANT TRANSMITTANCE	51
	Comparison of Horizontal and Slant Visual Range for Radiative Fogs	51
	Comparison of Horizontal and Slant Visual Range for Advective Fogs	56
7.	LUMINANCE MEASUREMENTS AND ANALYSIS	64
	NAFEC Measurements	64
	Determination of Background Luminance	76
	Computer Program Description	76
	Analysis of Computer Generated Luminance Data	77
8.	ALCH/SVR CALCULATIONS	102
	ALCH Algorithm	102
	SVR Algorithm	110
9.	SYSTEM DEMONSTRATION	116
	ALCH/SVR System	116
	Display Panel	117
10.	REFERENCES	120
11.	APPENDIX	121

LIST OF FIGURES

FIGURE NO.		Page
2-1	MAP OF NAFEC TOWER INSTALLATION	4
2-2	NAFEC TOWER INSTALLATION	5
2-3	NAFEC TOWER INSTALLATION	6
2-4	MET TOWER	7
2-5	LUMINANCE METER	9
3-1	FOG DENSITY CONTOURS (JANUARY 26)	13
3-2	VERTICAL PROFILE OF TRANSMISSION FOR RADIATION FOG	14
3-3	FOG DENSITY CONTOURS (MARCH 15)	16
3-4	VERTICAL PROFILE OF TRANSMISSION FOR ADVECTIVE FOG	17
3-5	FOG DENSITY CONTOURS (MARCH 16)	18
3-6	VERTICAL PROFILE OF TRANSMISSION FOR ADVECTIVE FOG	19
3-7	FOG DENSITY CONTOURS (MARCH 31)	20
3-8	TRANSMISSION CHARACTERISTICS	21
4-1	VIDEOGRAPH	24
4-2	VIDEOGRAPH SAMPLING VOLUME	25
4-3	COMPARISON OF BACKSCATTER INSTRUMENT AND TRANSMISSOMETERS	26
4-4	COMPARISON OF BACKSCATTER INSTRUMENT AND TRANSMISSOMETERS	27
4-5	COMPARISON OF BACKSCATTER INSTRUMENT AND TRANSMISSOMETERS	28
5-1	FORWARD SCATTER METER	31

LIST OF FIGURES, CONTD.

FIGURE NO.		PAGE
5-2	EG&G FORWARD SCATTER VISIBILITY METER	33
5-3	FORWARD SCATTER METER OUTPUT CHARACTERISTIC	34
5-4	RATIO OF TRANSMISSOMETER TO FSM	36
5-5	RATIO OF TRANSMISSOMETER TO FSM	37
5-6	COMPARISON OF FSM AND NBS TRANSMISSOMETER FOR PERCENT T<89	39
5-7	COMPARISON OF FSM AND NBS TRANSMISSOMETER	40
5-8	COMPARISON OF FSM AND NBS TRANSMISSOMETER FOR PERCENT TRANSMISSION <89	41
5-9	COMPARISON OF FSM AND NBS TRANSMISSOMETER FOR PERCENT TRANSMISSION <89; 464 OBSERVATIONS	42
5-10	RATIO OF 5-FOOT TRANSMISSOMETER TO REMOTE TRANSMISSOMETER	43
5-11	COMPARISON OF 5-FOOT LEVEL TRANSMISSOMETERS	44
5-12	COMPARISON OF NBS TRANSMISSOMETERS SEPARATED BY 1500 FEET FOR PERCENT T≥60	45
5-13	COMPARISON OF FSM AT 95 FEET AND NBS TRANSMISSOMETER AT 87 FEET SEPARATED BY 1500 FEET	47
5-14	COMPARISON OF FSM AT 95 FEET AND NBS TRANSMISSOMETER AT 87 FEET SEPARATED BY 1500 FEET FOR PERCENT T<60	48
5-15	COMPARISON OF TWO AND THREE POINT SYSTEMS	50
6-1	VERTICAL PROFILE OF TRANSMISSION FOR RADIATION FOG	52
6-2	COMPARISON OF VISUAL RANGE	54
6-3	COMPARISON OF VISUAL RANGE	55

LIST OF FIGURES, CONTD.

FIGURE NO.		PAGE
6-4	COMPARISON OF VISUAL RANGE	57
6-5	COMPARISON OF VISUAL RANGE	58
6-6	COMPARISON OF VISUAL RANGE	60
6-7	COMPARISON OF VISUAL RANGE	61
6-8	COMPARISON OF VISUAL RANGE	62
7-1	15' LUMINANCE READINGS 74TH DAY	65
7-2	50' LUMINANCE READINGS 74TH DAY	66
7-3	100' LUMINANCE READINGS 74TH DAY	67
7-4	150' LUMINANCE READINGS 74TH DAY	68
7-5	15' TRANSMISSION READINGS	69
7-6	50' TRANSMISSION READINGS 74TH DAY	70
7-7	123' TRANSMISSION READINGS 74TH DAY	71
7-8	154' TRANSMISSION READINGS 74TH DAY	72
7-9	EFFECT OF THRESHOLD ILLUMINANCE ON SVR	74
7-10	FREQUENCY DISTRIBUTION OF SVR PERCENT ERRORS	75
7-11	HAZE M AND ELDRIDGE PHASE FUNCTIONS	78
7-12	EFFECT OF DIFFERENT SOLAR ZENITH ANGLES	80
7-13	EFFECT OF DIFFERENT SOLAR ZENITH ANGLES	81
7-14	EFFECT OF DIFFERENT SOLAR ZENITH ANGLES	82
7-15	EFFECT OF DIFFERENT SOLAR ZENITH ANGLES	83
7-16	EFFECT OF DIFFERENT AZIMUTH ANGLES	85
7-17	EFFECT OF DIFFERENT AZIMUTH ANGLES	86
7-18	EFFECT OF DIFFERENT AZIMUTH ANGLES	87

LIST OF FIGURES, CONTD.

FIGURE NO.		PAGE
7-19	EFFECT OF DIFFERENT AZIMUTH ANGLES	88
7-20	EFFECT OF DIFFERENT OPTICAL DEPTHS	89
7-21	EFFECT OF DIFFERENT OPTICAL DEPTHS	90
7-22	EFFECT OF DIFFERENT OPTICAL DEPTHS	91
7-23	EFFECT OF GROUND REFLECTIVITY	92
7-24	PILOT-SUN GEOMETRY	93
7-25	REGRESSION PREDICTION OF LUMINANCE	95
7-26	REGRESSION PREDICTION OF LUMINANCE	96
7-27	EFFECT OF ILLUMINANCE ON OPTICAL DEPTH	97
7-28	EFFECT OF OPTICAL DEPTH IN PREDICTING BREAKOUT ALTITUDE	98
7-29	PREDICTION ERROR OF TOP OF FOG VS. ERROR IN ILLUMINANCE MEASUREMENT	101
8-1	EFFECT OF LUMINANCE ON ALCH	103
8-2	EFFECT OF LUMINANCE ON ALCH	104
8-3	ALCH VALUES FOR DIFFERENT FOG DENSITIES FOR A 1000 FT-L ADAPTATION	107
8-4	ALCH PREDICTIONS FOR DIFFERENT FOG DENSITIES FOR AN ILLUMINANCE THRESHOLD OF 1000 MILE CANDLES	109
8-5	ALCH ALGORITHM	111
8-6	SVR ALGORITHM	115
9-1	DISPLAY PANEL	118

LIST OF TABLES

TABLE NO.		PAGE
7-1	EFFECT OF BREAKOUT ALTITUDE ON ALCH	100
8-1	ADAPTATION EFFECT ON SVR	112

MANAGEMENT SUMMARY

Under contract by the FAA Weather and Flight Service Station Branch, an experimental program was conducted to evaluate techniques of determining approach zone visibility. The results were used in evaluating and refining a system concept which would predict the SVR at the 100-foot decision height and ALCH.

The data used to evaluate proposed concepts were collected at the National Aviation Facilities Experimental Center (NAFEC). Measurements required two 160-foot towers with horizontal transmissometers mounted at six levels, and one measuring the slant path between the base of one tower and the top of the other. Luminance meters were mounted on one tower at four levels. In addition, a 100-foot tower was remotely located 1,500 feet from both towers to provide data from a forward scatter meter, located at the top and a transmissometer at the 5-foot level. These data measurements served as "baseline" information defining atmospheric conditions to evaluate proposed system concepts.

The results of the field program indicate that meaningful predictions of glide path visibility cannot be obtained with presently configured RVR transmissometers. The vertical variation of the atmosphere must be sampled. In every situation observed during the field program, vertical sampling provided an accurate measure of slant visual range, as determined by comparison with baseline data. At onset and dissipation of advective fogs, the data is subject to error due to the position of the remote tower; however, even during these times, the vertical sampling system provided a better estimate of SVR than did a horizontal transmissometer at the 15-foot level. For visibility reduction which occurs during the day, the determination of adaptation level, using luminance meters, significantly improves the visibility prediction.

The system proposed to yield this vertical sampling would make use of fully developed operational instruments and a small special purpose

computer for handling the data processing. The field structure would consist of two forward scatter visibility meters and two luminance meters, mounted on a 100-foot tower, offset 1,300 feet perpendicular to the runway centerline at the tenth approach light bar (1,000 feet from threshold). The inherent flexibility of this system will allow changes to algorithms used in signal processing when new and better data are available. It would be easy to incorporate into the system any additional sensors for special situations or improvements in instrumentation such as new ceilometers.

An engineering model of the proposed system was demonstrated at NAFEC on 23 August 1973.

Future plans include flight tests to evaluate a development system at NAFEC during the 1973-1974 fog season.

Acknowledgments

The following NAD Crane Research and Development Department personnel have contributed to the SVR/ALCH program:

F. Bagrash
G. Bradley
M. Brown
F. Burton
R. Chipman
D. Johnson
C. Lohkamp
C. Luetzelschwab
D. Montgomery
L. Simonton
R. Sparks
R. Stovall
L. Wheelock
R. Williams

The cooperation and guidance of Messrs. E. Bromley, A. Larsson and K. Kraus of the FAA Weather and Flight Service Station Branch and Mr. E. Schlatter's group at NAFEC are gratefully acknowledged.

1. INTRODUCTION

This report describes the results of work performed by the Research and Development Department, Naval Ammunition Depot, Crane, Indiana, in the second phase of a multi-phase program to develop and implement a slant visual range/approach light contact height measurement system. This system, utilizing state-of-the-art hardware and technology, is intended primarily to be used at airports with Category II or lower landing minima. Measurements will be made which, after processing, will provide the pilot an assessment of the approach zone visibility.

The current phase of this program had several objectives. The predominant portion was the design and implementation of a test program to be conducted at NAFEC, Atlantic City, New Jersey. This program was to evaluate the ability of proposed systems to determine slant path transmittance. A major feature of the test facility was a pair of towers with transmissometers mounted at various levels. Data recorded by these instruments established the vertical variation of visibility in the atmosphere. Thus determinations of slant transmittance by proposed systems could be compared with that determined from the tower facility.

Incorporated in any of the proposed systems are algorithms for calculation of slant visual range (SVR) and approach light contact height (ALCH). The development of these algorithms was one of the objectives of this effort. The working definition of ALCH used is the height on the glide path at which a pilot will see and should continue to see a minimum of five light bars of approach lights at 100-foot spacings, if extended to touchdown, assuming a standard cockpit cut-off angle of 15 degrees. The working definition of SVR is the slant distance to the farthest high intensity runway edge light or approach light which a pilot will see at an altitude of 100 feet on the approach path

or, if larger, the slant distance which would have a transmittance of 5.5 percent.

A data processing system was also an objective of the effort. The system included a minicomputer, interface equipment and a display panel. The interface electronics and the digital display panel were designed and built during this phase of the project. At the completion of the NAFEC tests, the data processing system was demonstrated at NAFEC using input data recorded during the tests.

2. EXPERIMENTAL FACILITY

Physical Description

A test facility for evaluating SVR/ALCH candidate systems and for measuring true atmospheric conditions in fogs, including vertical variation, was established at the National Aviation Facilities Experimental Center (NAFEC) in the fall of 1972. The facility consisted of a two-tower site used to record baseline fog data, and a remote site with a single tower used for system evaluation. The baseline site had two 160 foot towers separated by 250 feet. One of the towers, henceforth to be called the "met" tower, was triangular with each face 40 feet across and very sturdily constructed (Hochreiter, 1968). The rigidity was necessary to provide a stable platform for the NBS transmissometer receivers. The second tower, rectangular base four feet by six feet, was a lightweight upright scaffolding tower of much lighter construction than the met tower. It was felt that this would provide a platform stable enough for mounting the transmissometer projectors.

NBS transmissometers were mounted at six levels sampling the transmission over horizontal paths at 5, 15, 51, 87, 123 and 154.5 feet above the surface. A seventh transmissometer measured the slant path from the top of one tower to the bottom of the other. A series of meters were installed to measure luminance and illuminance at various altitudes. Luminance was measured at 15, 50, 100 and 150 feet. Illuminance was measured at five feet and 150 feet. A rotating beam ceilometer was located with the projector mounted at the base of the met tower. Figure 2-1 shows the location of the test facility on a map of NAFEC. Figures 2-2 and 2-3 show schematically the two-tower test facility. Figure 2-4 is a photograph of the met tower.

The baseline data tower complex was established to give an accurate record of the visibility in fogs and their vertical variation. With

MAP OF NAFEC TOWER INSTALLATION

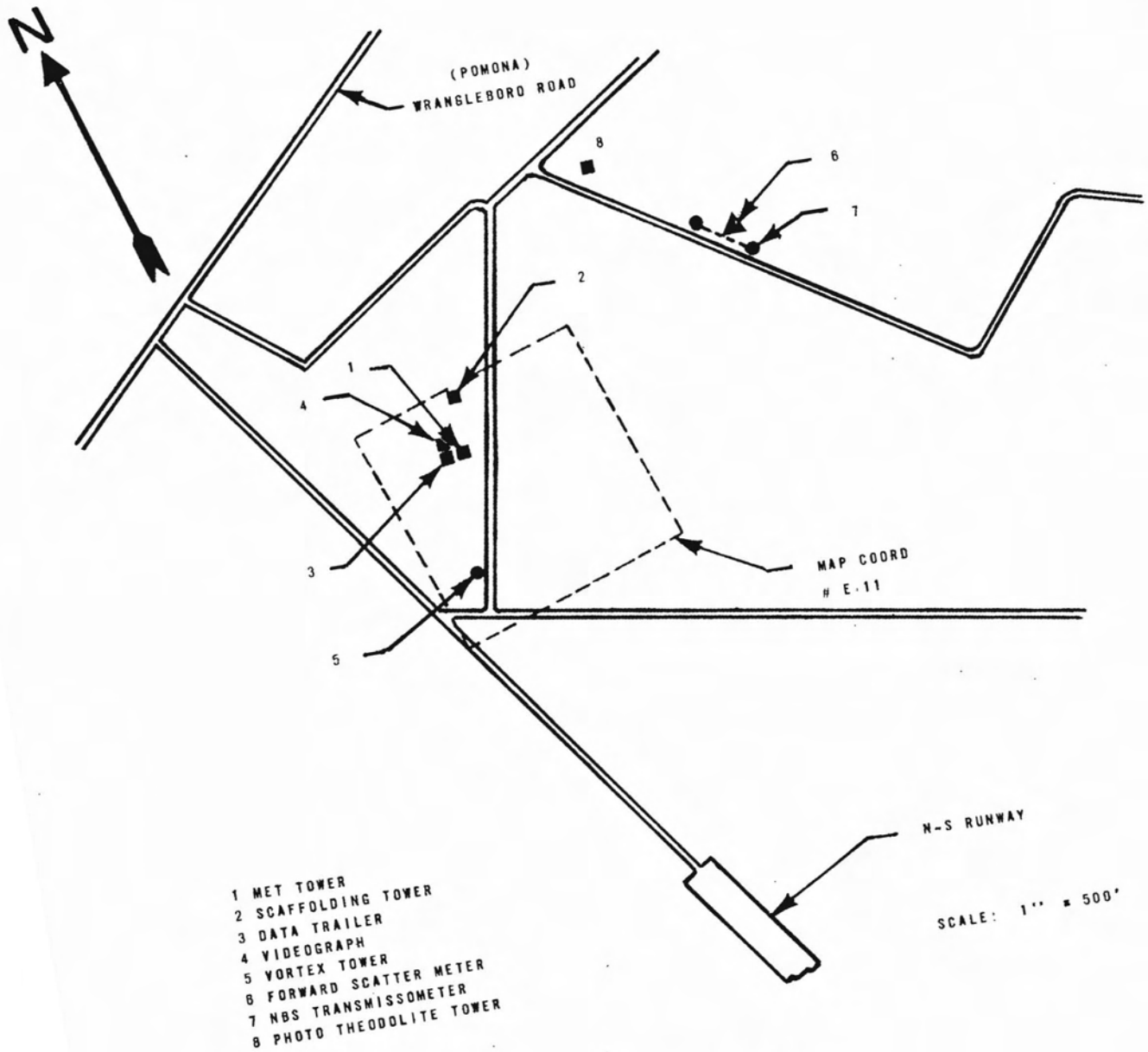

Figure 2-1

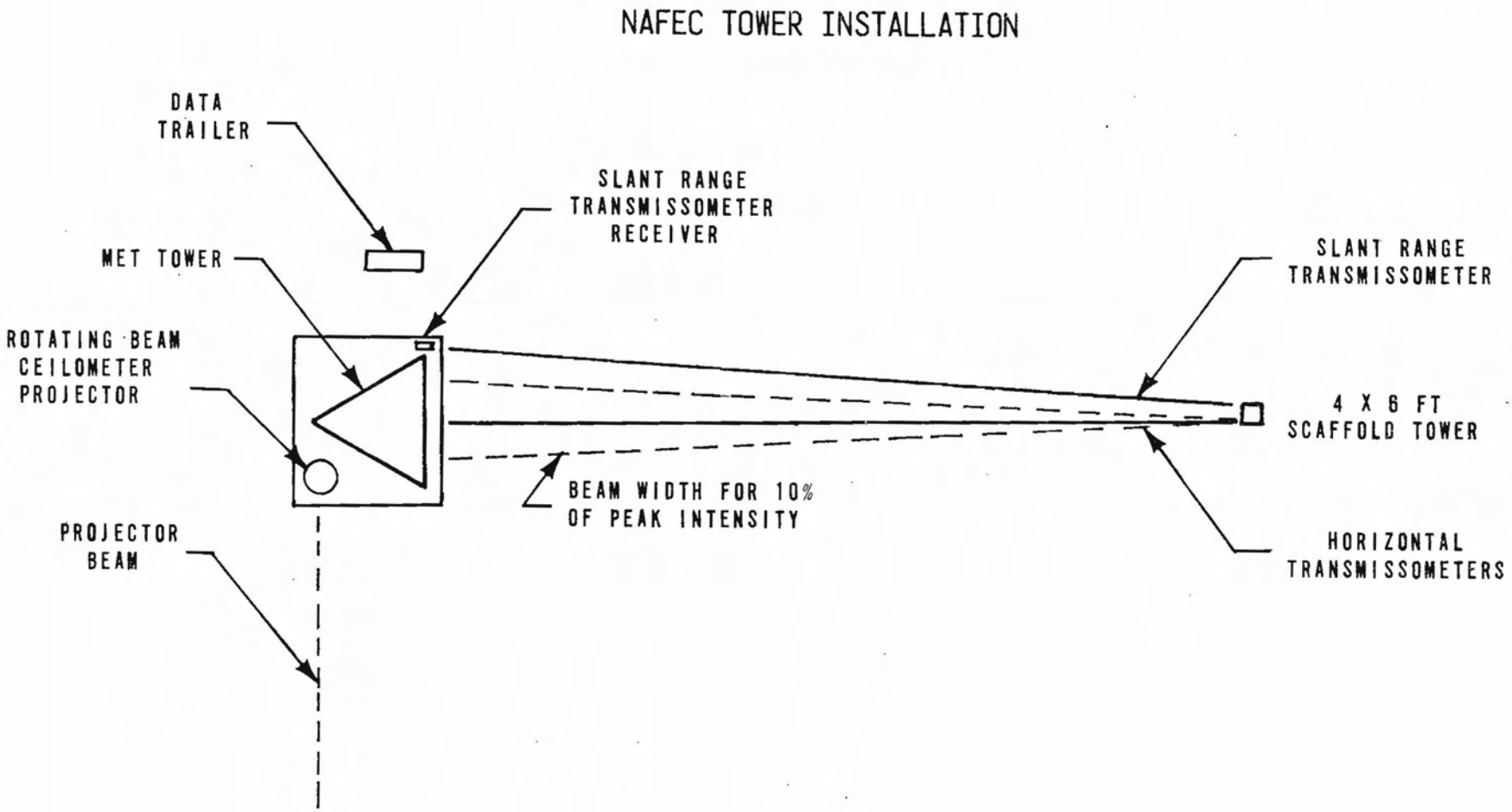
NAFEC TOWER INSTALLATION
DATA TRAILER
SLANT RANGE TRANSMISSOMETER RECEIVER
MET TOWER
SLANT RANGE TRANSMISSOMETER
ROTATING BEAM CEILOMETER PROJECTOR
4 X 6 FT SCAFFOLD TOWER
BEAM WIDTH FOR 10% OF PEAK INTENSITY
PROJECTOR BEAM
HORIZONTAL TRANSMISSOMETERS

Figure 2-2

NAFEC TOWER INSTALLATION

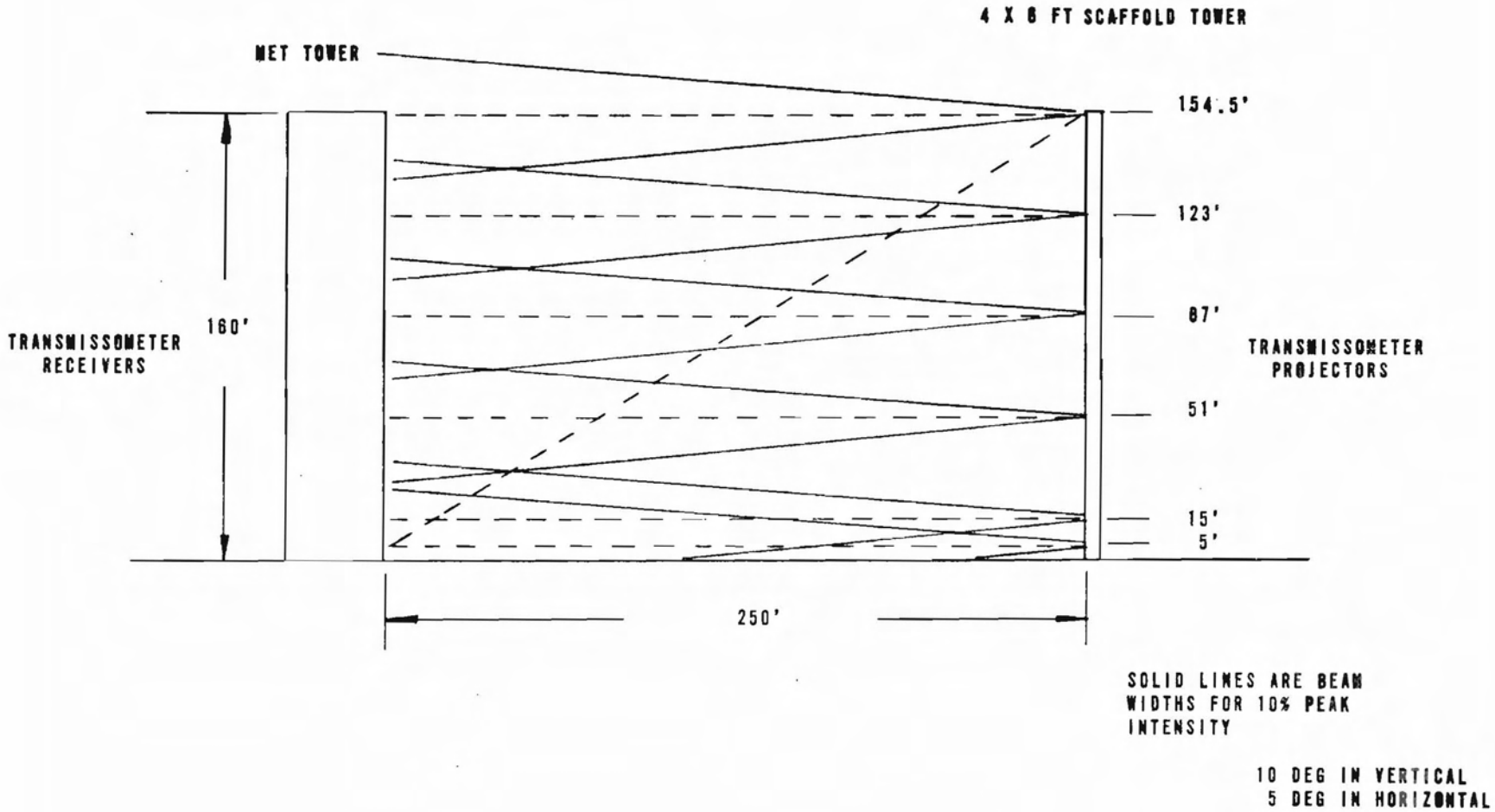

Figure 2-3

MET TOWER

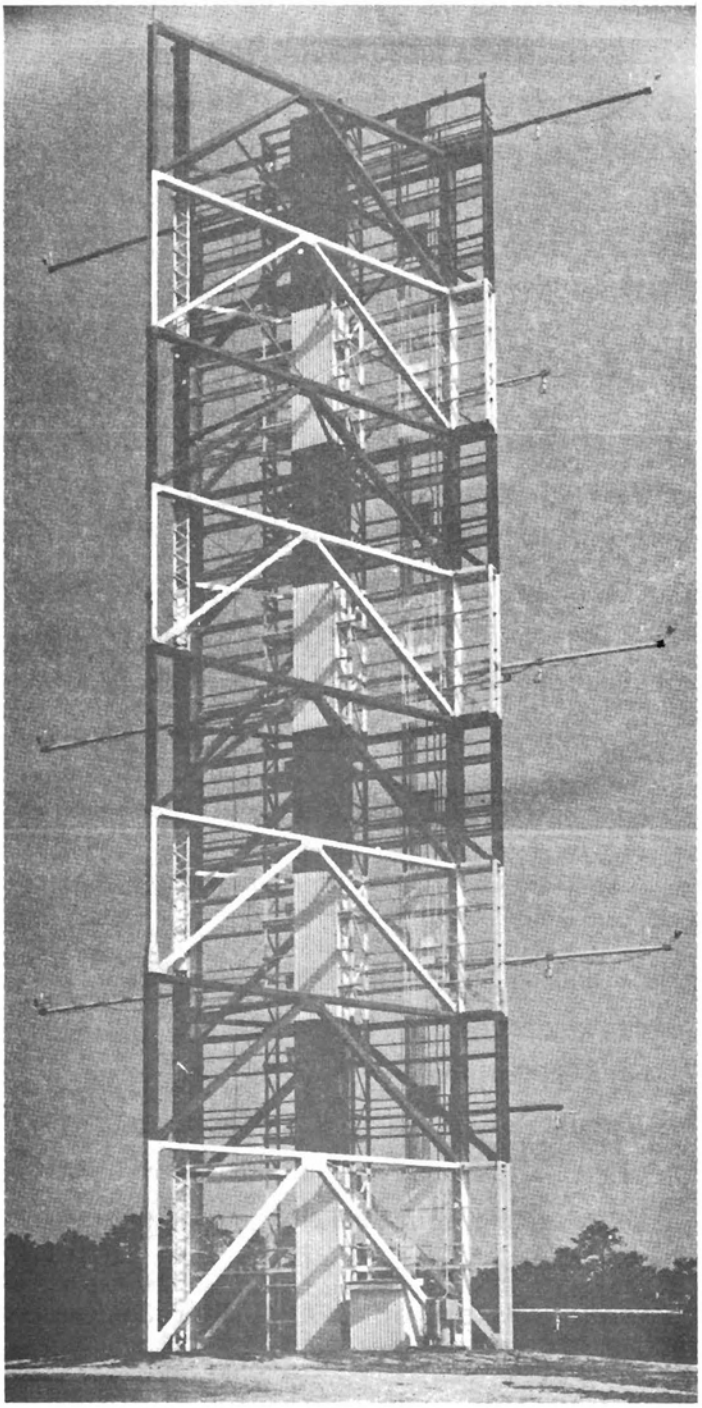

FIGURE 2-4

this description of the fog, it was possible to assess the performance of various candidate systems used to predict slant visual range.

Baseline Data Instrumentation

The NBS transmissometers used were set with 250-foot baselines with the exception of the slant path unit which had a 290-foot baseline. A detailed description of the NBS transmissometer has been given by Douglas and Young (1945). The transmittance data was recorded on punch cards, punched paper tape and strip charts. The strip charts are those normally used with the transmissometers; the punched paper tape was the data recording facility to be used with the candidate systems and served as a backup for the punch card system. The punch card equipment, provided by NAFEC, was the primary data recording system for the NBS transmissometers. Both the card and paper tape data recording systems were equipped with automatic turn-on and turn-off features enabling unattended operation.

The rotating beam ceilometer was configured to give an indication of angle when the return signal reached a prescribed level. This angle was recorded on the punch cards. The ceilometer was set up with a 200-foot baseline.

Luminance and Illuminance Meters

The luminance and illuminance meters were fabricated at NAD Crane using silicon photocells. Each unit was equipped with a photoptic filter so that intensities measured are directly applicable to that seen by an observer. Figure 2-5 shows a diagram of the basic luminance meter. A cover glass keeps dust and moisture off the beam defining lens; to eliminate moisture condensation on this glass, a small heater assembly is mounted firmly against the edges of this glass. The remainder of the unit consists of an amplifier and two power supplies, one for the amplifier and one for the heater. The luminance meters

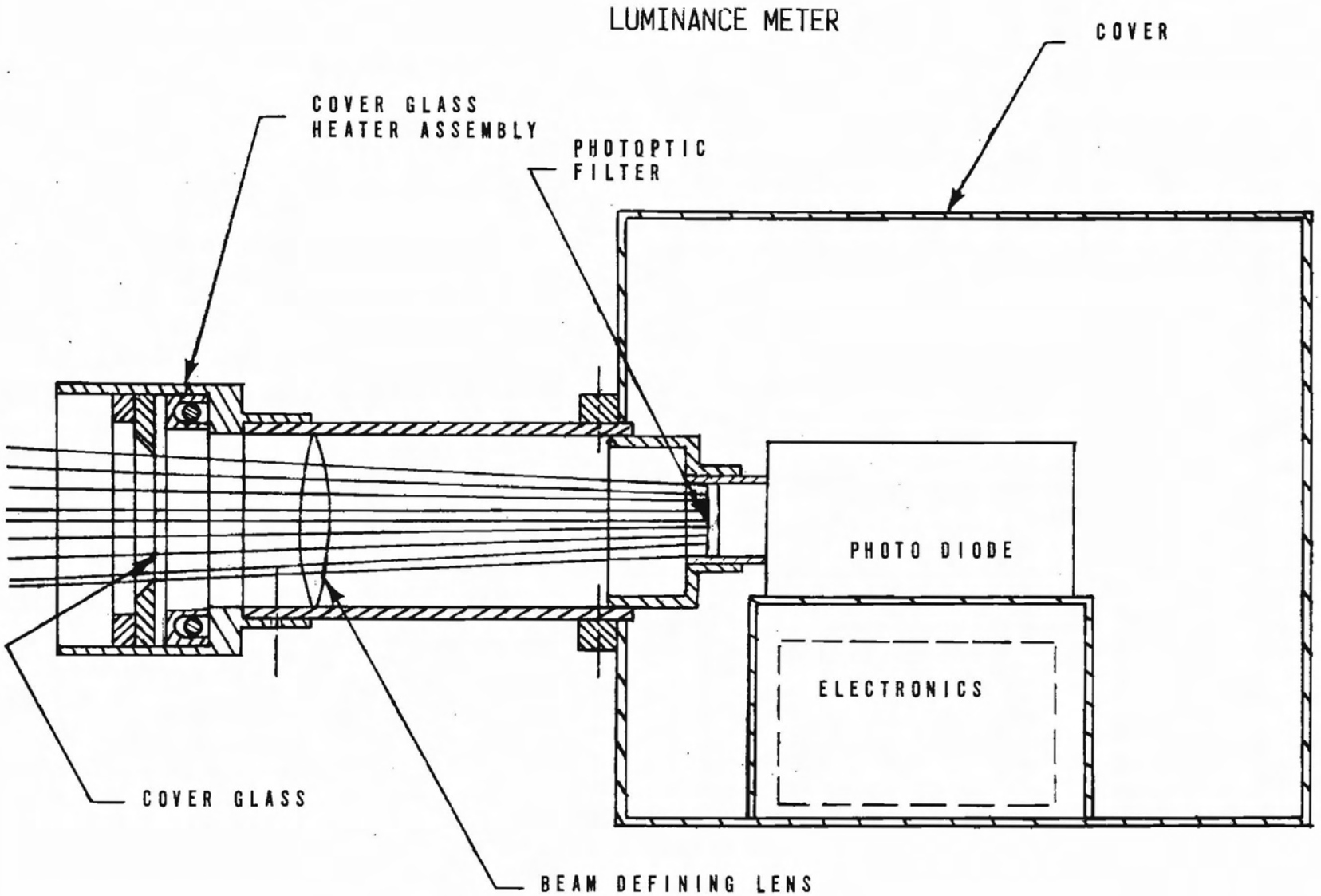
LUMINANCE METER
COVER
COVER GLASS
HEATER ASSEMBLY
PHOTOPTIC
FILTER
PHOTO DIODE
ELECTRONICS
COVER GLASS
BEAM DEFINING LENS

Figure 2-5

were set up with a 6° degree field of view, and a linear operating range from approximately 50 to 1,000 foot-lamberts. The illuminance meters made use of the same sensors and electronics, but the optics were set up to give the maximum field of view possible, about 60°, consistent with the packaging geometry.

Data Acquisition System

Data processing and recording was accomplished using a mini-computer and paper tape punch. The computer is a Nova 1220, manufactured by Data General Corporation; its physical dimensions are 19 inches wide, 10 inches high and 24 inches deep. The central processor has four 16-bit accumulators; memory capacity is 8,000 words with full memory cycle time of 1,200 nanoseconds. The computer executes arithmetic and logical instructions in 1,350 nanoseconds. A teletype was used to update information such as date and time, to change system operating modes, to enter calibration correction factors, to output selected portions of the data and as a backup for data recording. A high speed paper tape punch and reader is used to program the computer and record the output data.

The signals from the NBS transmissometers in the form of 250 volt pulses were applied to circuitry which made them compatible with the computer interface. These pulses were counted by the computer for one minute, and the percent transmittance calculated based on 4,000 pulses representing 100% transmittance. All the other signals recorded were scaled in analog form to 0-10 volts; these signals were applied to the analog-to-digital converter and then processed by the computer.

The system was set up with automatic turn-on and turn-off capability for data recording. The computer continually scanned the transmissometers, and when any of the six levels of horizontal trans-

missometers read less than 85%, data recording commenced. When the slant transmissometer read greater than 85% for ten consecutive minutes, data recording was terminated.

3. BASELINE FOG DATA

The experimental facility was in operation from 12 September 1972 to 10 June 1973. The automatic data collection system was operating from 26 January 1973 to the end of the recording period. Data gathered before the installation of the minicomputer was recorded only on the strip chart recorders used with the NBS transmissometers. A complete catalog of fog data recorded and a sample of the transmissometer data is shown in the appendix.

The majority of the fogs observed had predominant characteristics of advection fogs, although some radiation fogs were recorded before the facility was complete. In this section, examples of the data recorded will be presented.

Figure 3-1 shows an altitude-time-density contour plot for a fog recorded 26 January. The variation in the vertical was measured by the six levels of transmissometers, and linear interpolation was used between levels. The range of transmittance was then divided into several categories and a gray scale applied. This fog has the basic characteristics of a radiation fog, denser near the surface than aloft, and graphically illustrates the spatial and temporal variability of the fog. Figure 3-2 shows vertical profiles of transmittance for four times during the fog. This clearly illustrates the characteristic of a fairly shallow radiation fog. At 2301, the 15-foot level transmissometer indicated about 3%; this would give an RVR of 1,200 feet (below Category II minima) based on light setting 4, night conditions. At this same time, the slant transmissometer yielded a visual range of 1,800 feet (corresponding to 29% transmittance). The values measured by the slant transmissometer were adjusted to account for the 290-foot rather than 250-foot baseline. Light setting 4, night conditions, was used in calculations of visual range merely to convert percent transmittance to visual range. The choice was arbitrary and any light setting could have been selected for this purpose.

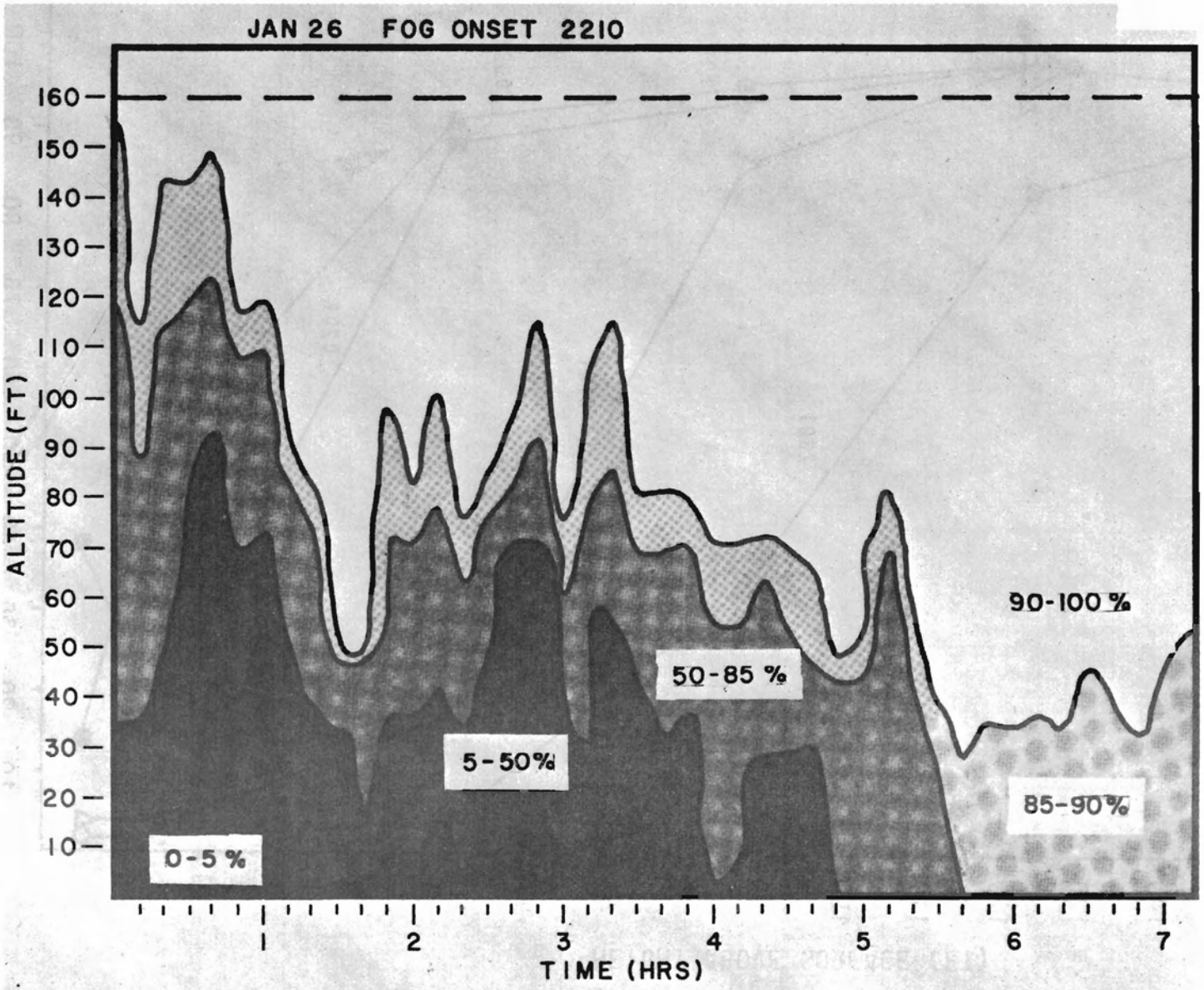

FIGURE 3-1
FOG DENSITY CONTOURS

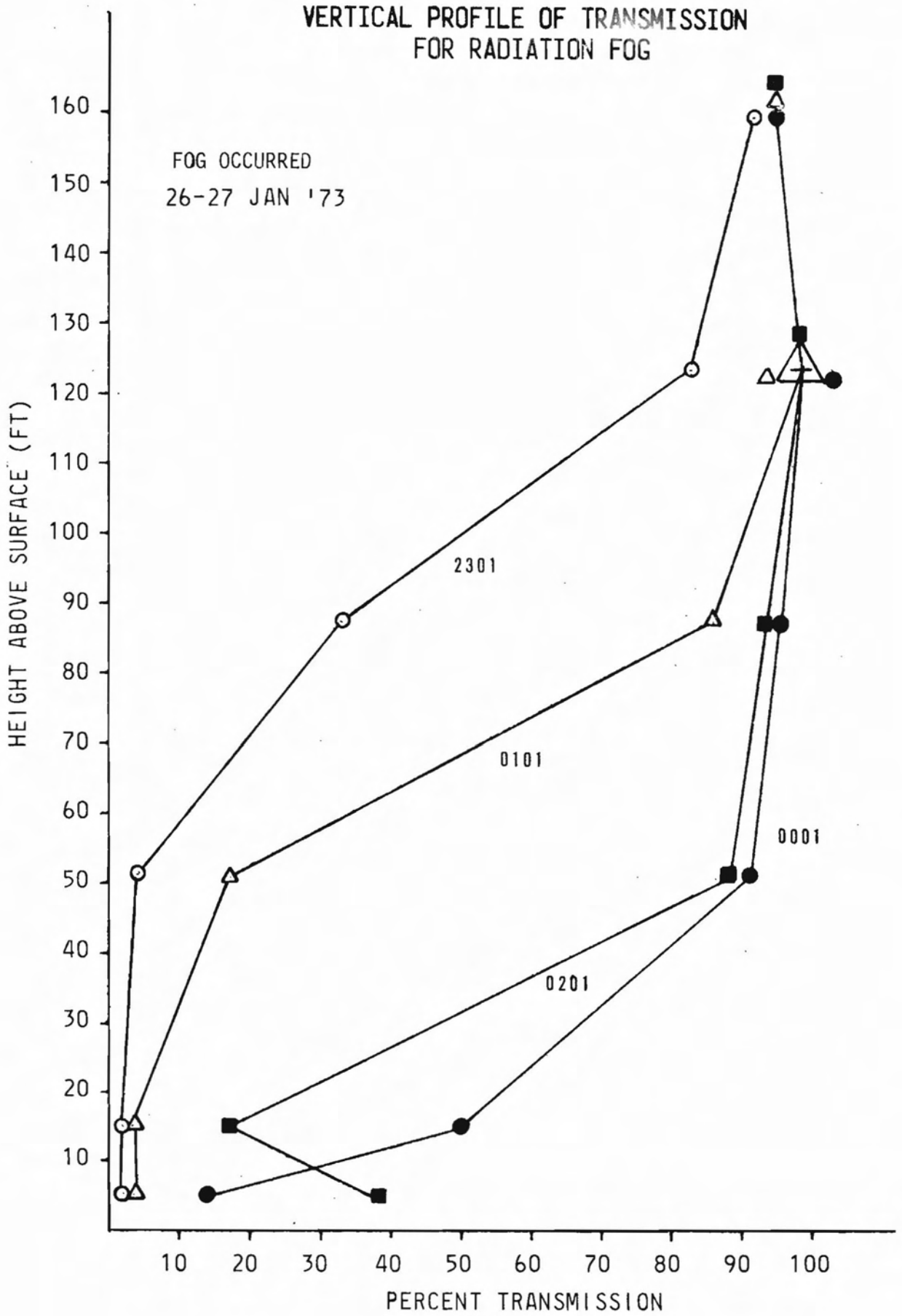
VERTICAL PROFILE OF TRANSMISSION
FOR RADIATION FOG
FOG OCCURRED
26-27 JAN '73
HEIGHT ABOVE SURFACE (FT)
160
150
140
130
120
110
100
90
80
70
60
50
40
30
20
10
2301
0101
0001
0201
10
20
30
40
50
60
70
80
90
100
PERCENT TRANSMISSION

FIGURE 3-2

Figure 3-3 is an altitude-time-density contour plot with density divided into eight divisions. This fog illustrates characteristics of an advection fog, fog density increasing upward. Several profiles of transmittance versus height are shown for this fog in Figure 3-4. At 0915 hours, the 15-foot level transmissometer showed 27% transmission, corresponding to an RVR of 1,750 feet (high intensity light setting 4, night conditions). The slant transmissometer displayed 8.5% yielding an SVR of about 1,000 feet (high intensity light setting 4, night conditions).

Figures 3-5 and 3-6 show similar characteristics to those in Figures 3-3 and 3-4. For this advective fog occurring on 16 March 1973, the 15-foot level transmissometer would again yield an unrealistic assessment of the slant visual range.

Figure 3-7 shows an altitude-time-density plot for a fog occurring 31 March 1973. This fog has the characteristics of the lowering of a stratus deck. In the segment shown, the primary reduction to visibility existed above 120 feet. Above that level, transmission was less than 15%, but the slant transmittance measured from the 159-foot level was varying from 70 to 80%. This type of fog lends itself to ceiling measurement. Data recorded from the rotating beam ceilometer for this time indicated a ceiling of 140 feet. Figure 3-7 shows that this was a good estimate. However, the lowering of a stratus deck is transitory, and as the fog thickens below, the rotating beam ceilometer is unable to give meaningful results.

Figure 3-8 shows a plot of transmittance versus time for a typical fog. This fog occurred on 23 May 1973 and was predominantly advective in character. Data from five levels of transmissometers are shown. Rapid large scale fluctuations appear and can be found at all levels except the 5-foot level. This figure illustrates

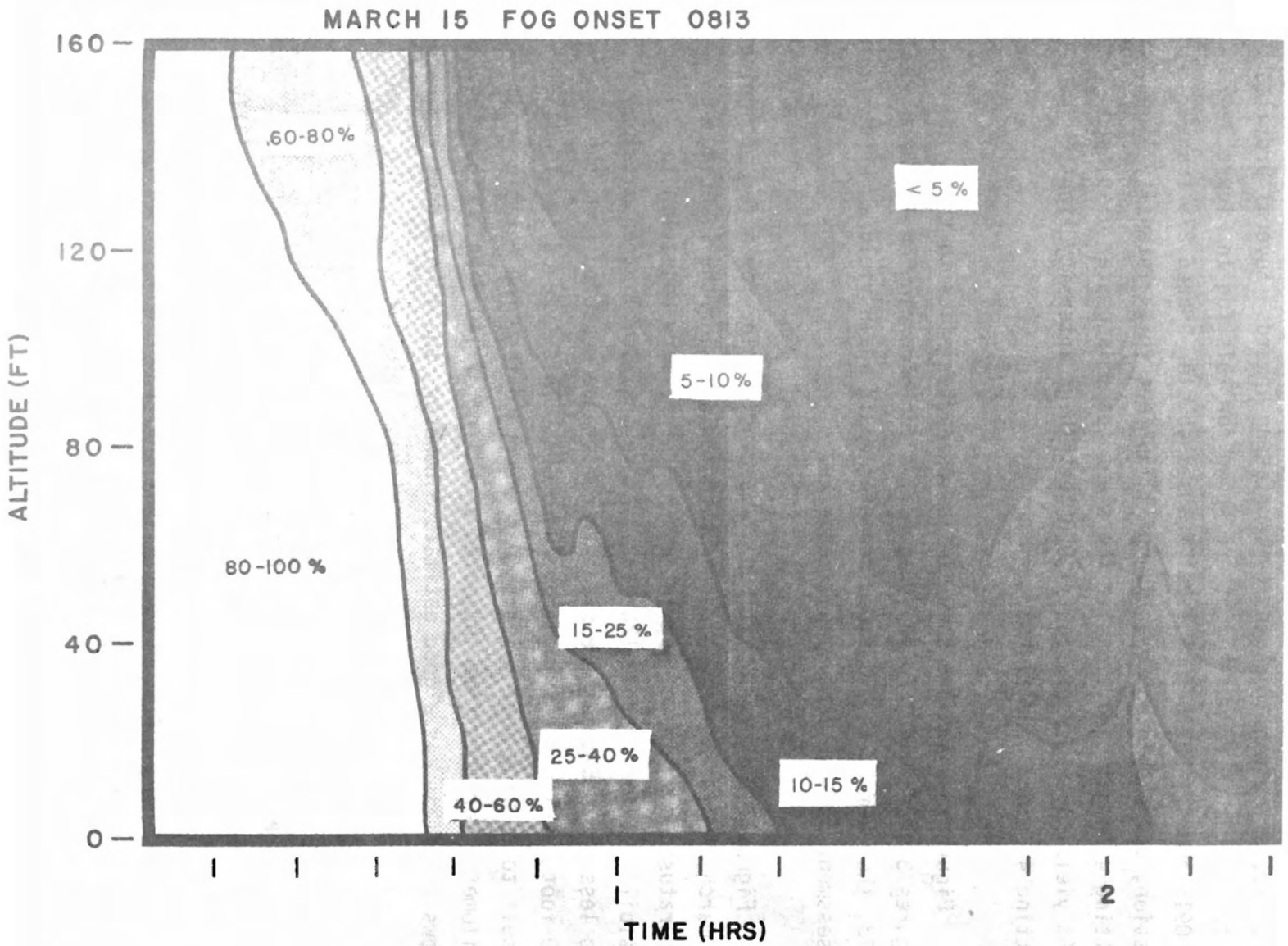

FIGURE 3-3
FOG DENSITY CONTOURS

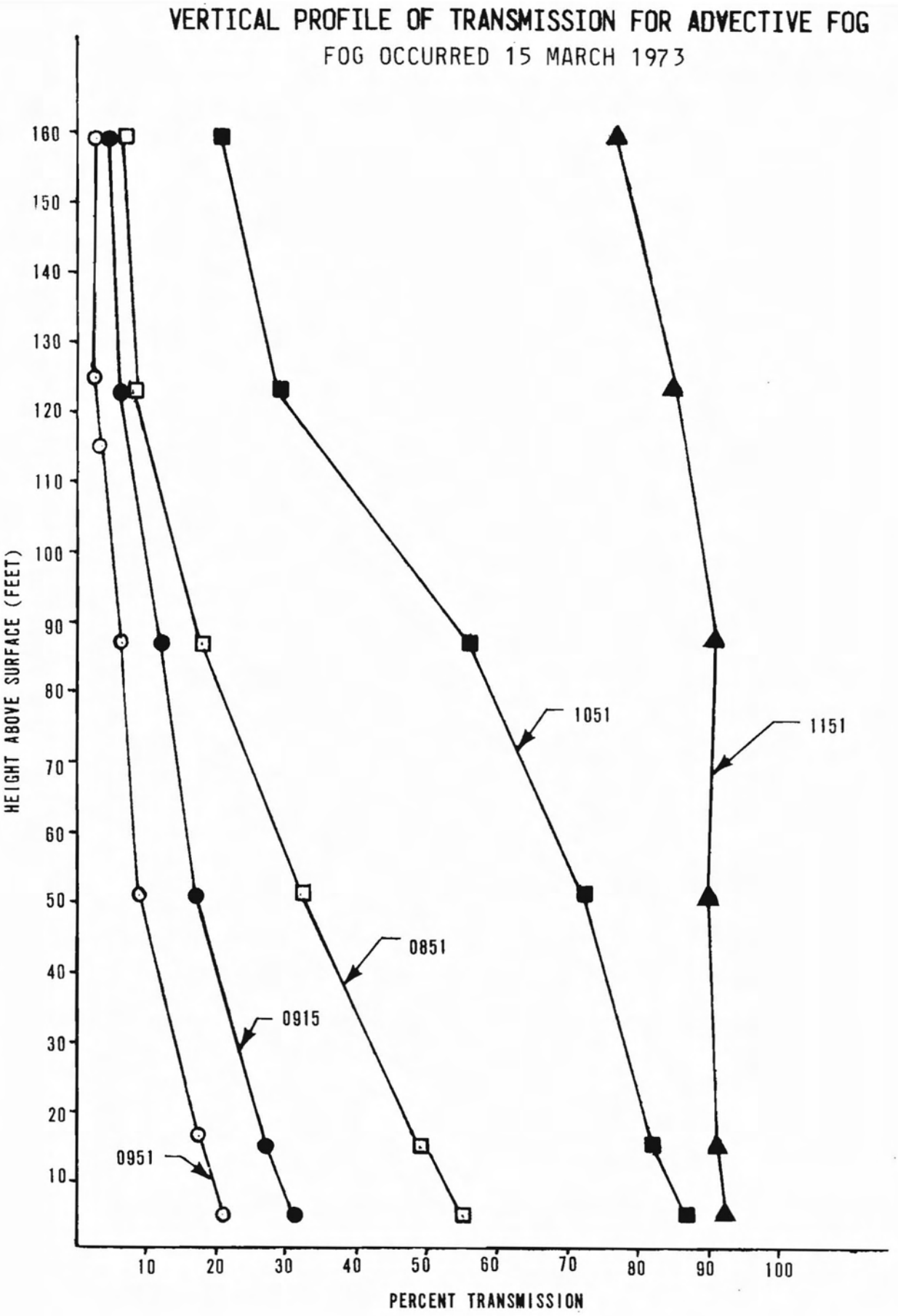
VERTICAL PROFILE OF TRANSMISSION FOR ADVECTIVE FOG
FOG OCCURRED 15 MARCH 1973
HEIGHT ABOVE SURFACE (FEET)
160
150
140
130
120
110
100
90
80
70
60
50
40
30
20
10
1051
1151
0851
0915
0951
10
20
30
40
50
60
70
80
90
100
PERCENT TRANSMISSION

FIGURE 3-4

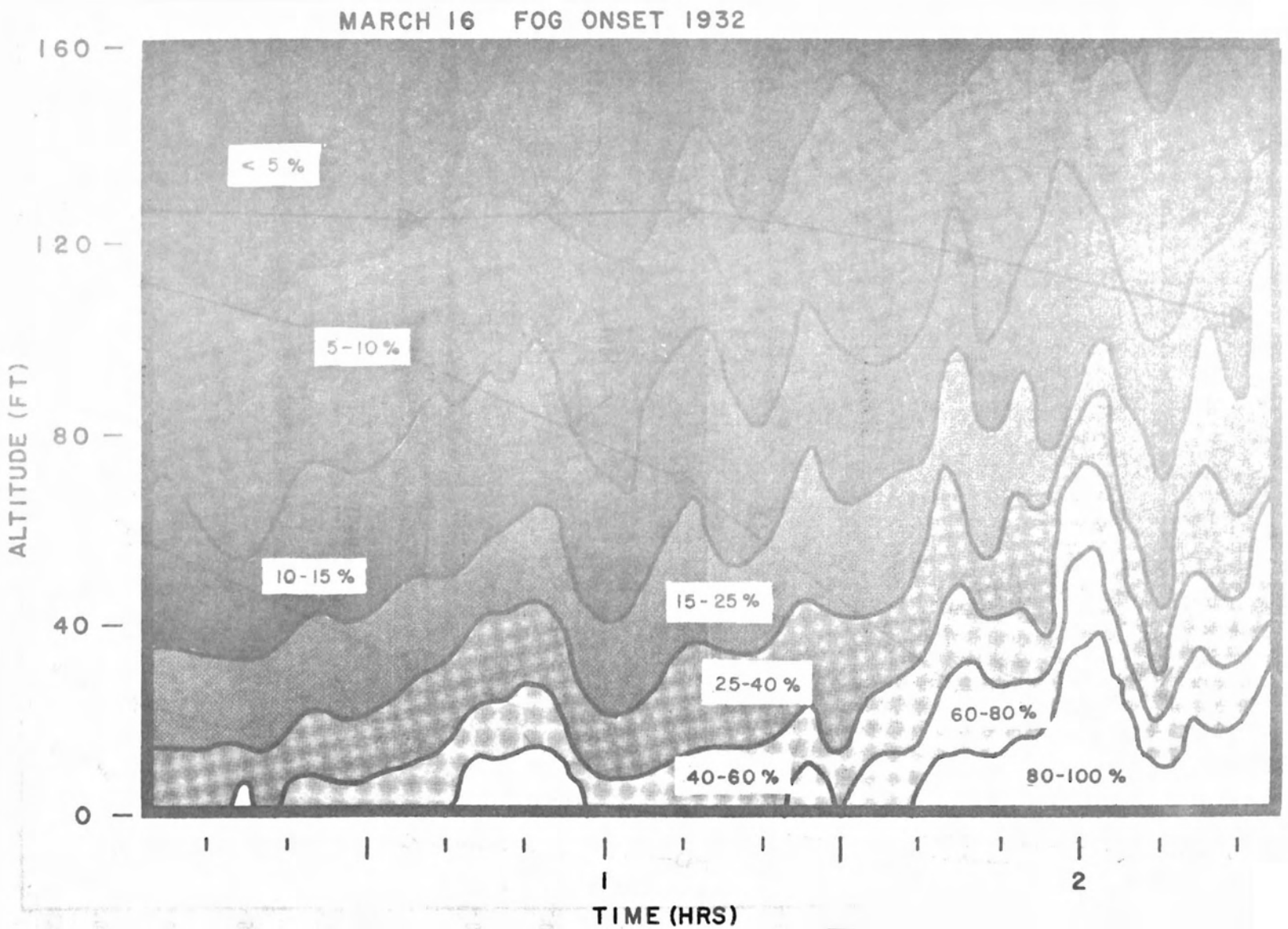

FIGURE 3-5

FOG DENSITY CONTOURS

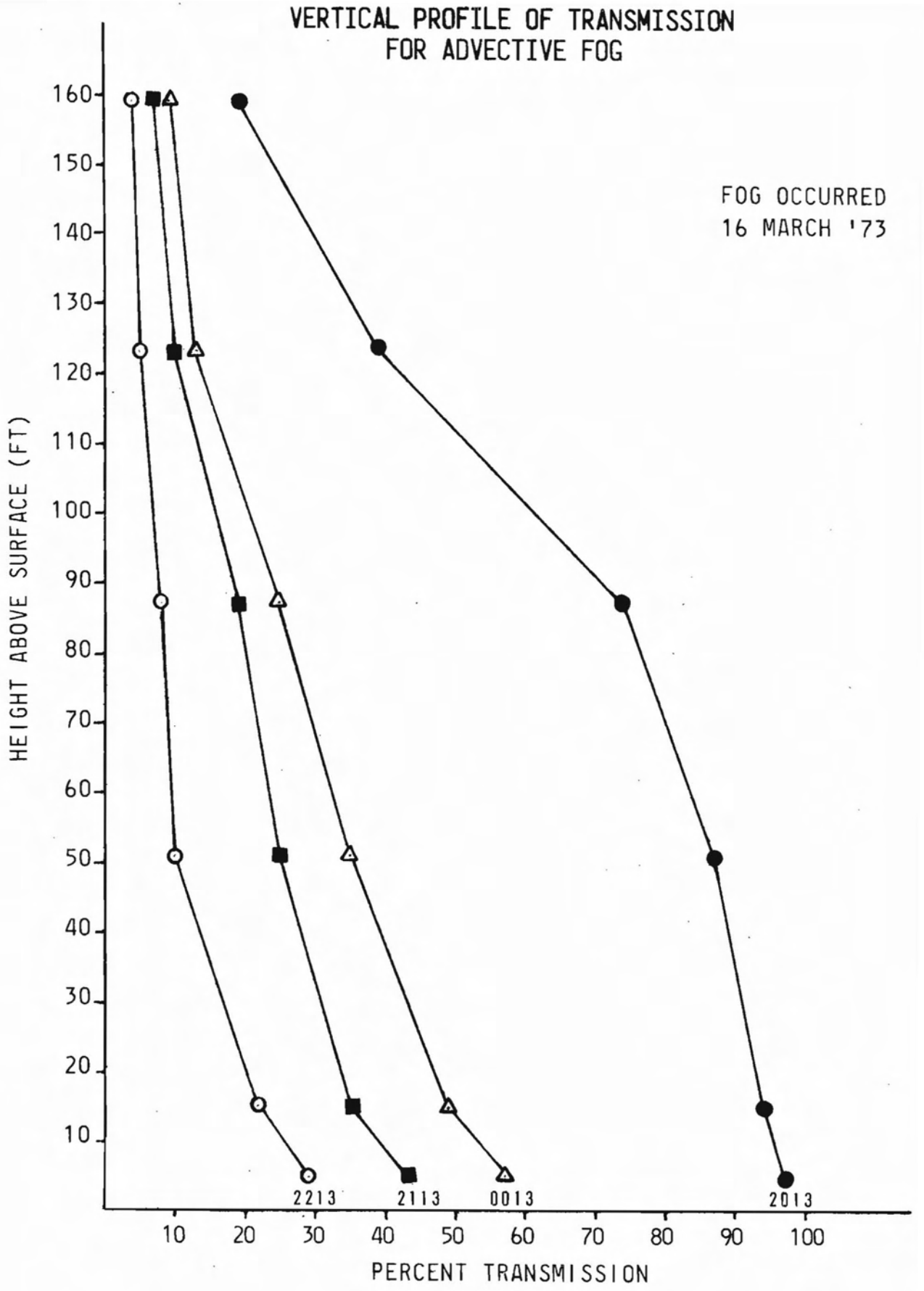
VERTICAL PROFILE OF TRANSMISSION
FOR ADVECTIVE FOG
FOG OCCURRED
16 MARCH '73
HEIGHT ABOVE SURFACE (FT)
160
150
140
130
120
110
100
90
80
70
60
50
40
30
20
10
2213
2113
0013
2013
10
20
30
40
50
60
70
80
90
100
PERCENT TRANSMISSION

FIGURE 3-6

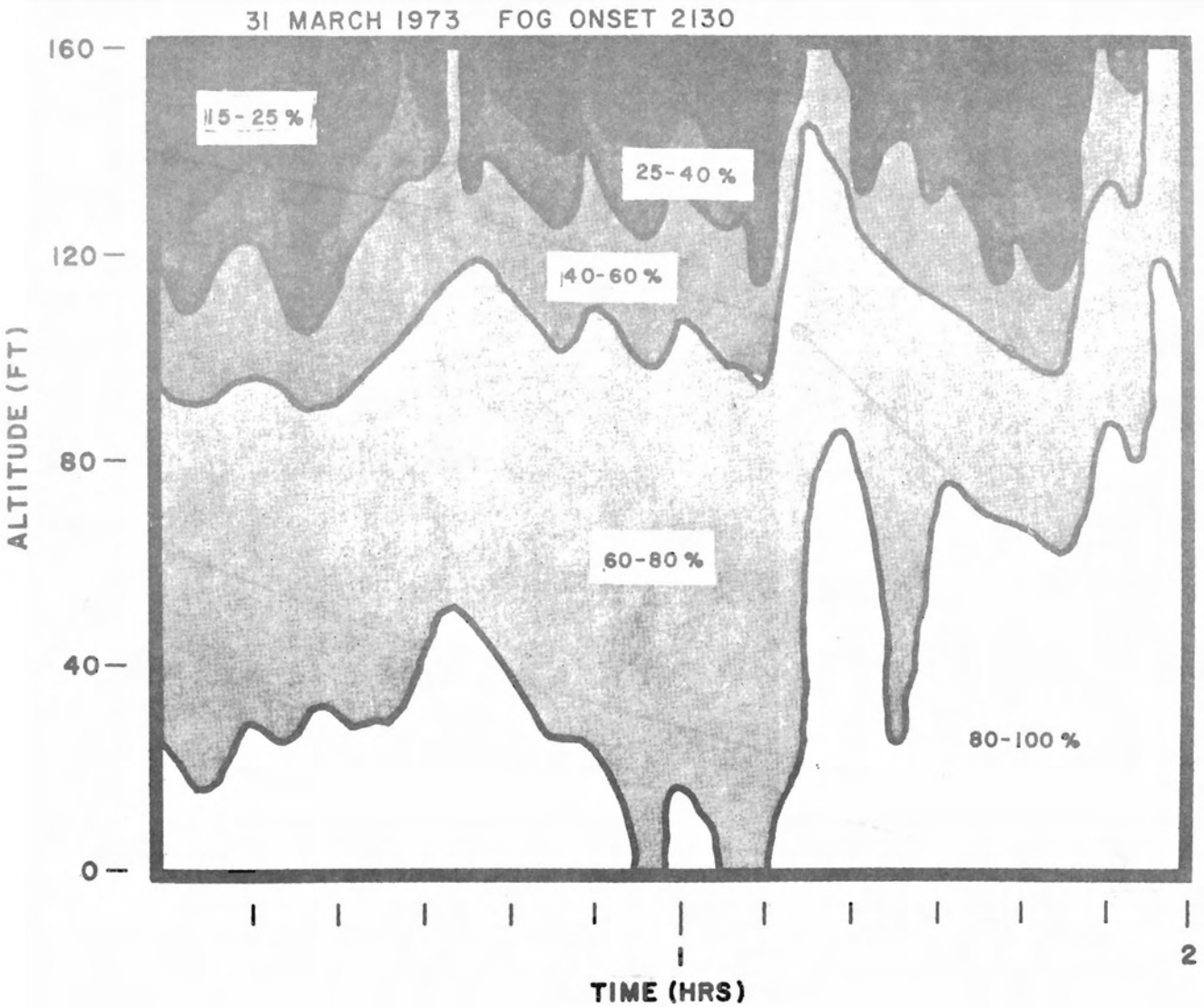

Figure 3-7

FOG DENSITY CONTOURS

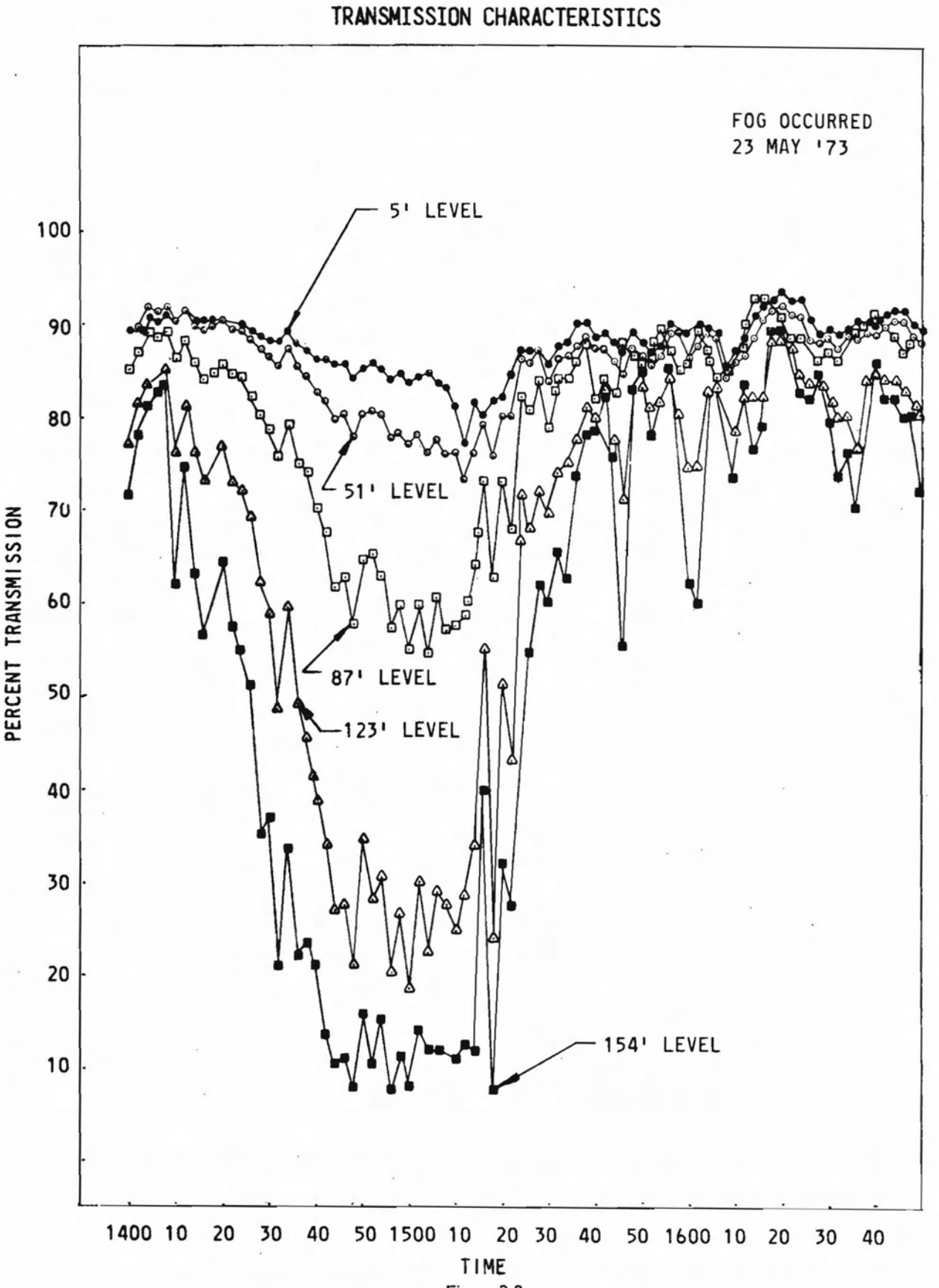
TRANSMISSION CHARACTERISTICS
FOG OCCURRED
23 MAY '73
5' LEVEL
51' LEVEL
87' LEVEL
123' LEVEL
154' LEVEL
PERCENT TRANSMISSION
100
90
80
70
60
50
40
30
20
10
1400 10 20 30 40 50 1500 10 20 30 40 50 1600 10 20 30 40
TIME

Figure 3-8

typical results as they would appear on the transmissometer strip chart records.

The baseline data recorded at NAFEC allows one to compare the performance of proposed systems for determining approach zone visibility. It further permits comparison of how well measurements taken at various heights characterize the total slant path visual range. A result which emerges from the data recorded is that measurements made near the surface are inadequate for determining slant visual range. It is felt that a similar result would be found at almost any location, perhaps varying in degree of inadequacy; however, this result was obtained from measurements taken at NAFEC during a six-month period.

In addition to the primary objective of the field test, data was acquired on the vertical structure of fogs. This data should be useful to people working on other aspects of the microphysics of fog.

4. TEST RESULTS OF BACKSCATTER VISUAL RANGE SYSTEM

One system which was tested at NAFEC made use of the Videograph to determine the slant path transmission. The Videograph, designed and manufactured by Impulsphysik Gmbh, Hamburg, Germany, bases its operation on atmospheric backscatter. Transmitter and receiver are housed in a single unit mounted on a pedestal. The projector light source is a xenon flash lamp with peak luminance of 3×10^6 candelas/cm^2. The axis of the projector is inclined upward with respect to the receiver's axis allowing intersection to occur at a known distance from the housing. Figure 4-1 is a photograph of the instrument.

Figure 4-2 illustrates schematically how the projector and receiver fields of view overlap. The backscatter instrument used at NAFEC was installed with the projecting/receiving head inclined five degrees above the horizontal. Although the sampled volume extends out approximately 75 feet, nearly 90% of the return signal originates in the first 20 feet of the volume (Lohkamp, et al, 1972). Considering the inclination and the length of the path sampled, the transmission determined is that at about the five-foot level. Figures 4-3, 4-4 and 4-5 show plots of percent transmission versus time for the slant and five-foot level transmissometers and the Videograph. Our results indicate that for atmospheres with transmission greater than about 70% (RVR 4900, light setting 4, night conditions), the backscatter instrument does provide an estimate of transmission which compares well with the NBS transmissometer. Unfortunately, the range of the instrument tested was insufficient for many of the denser fogs encountered at NAFEC.

VIDEOGRAPH

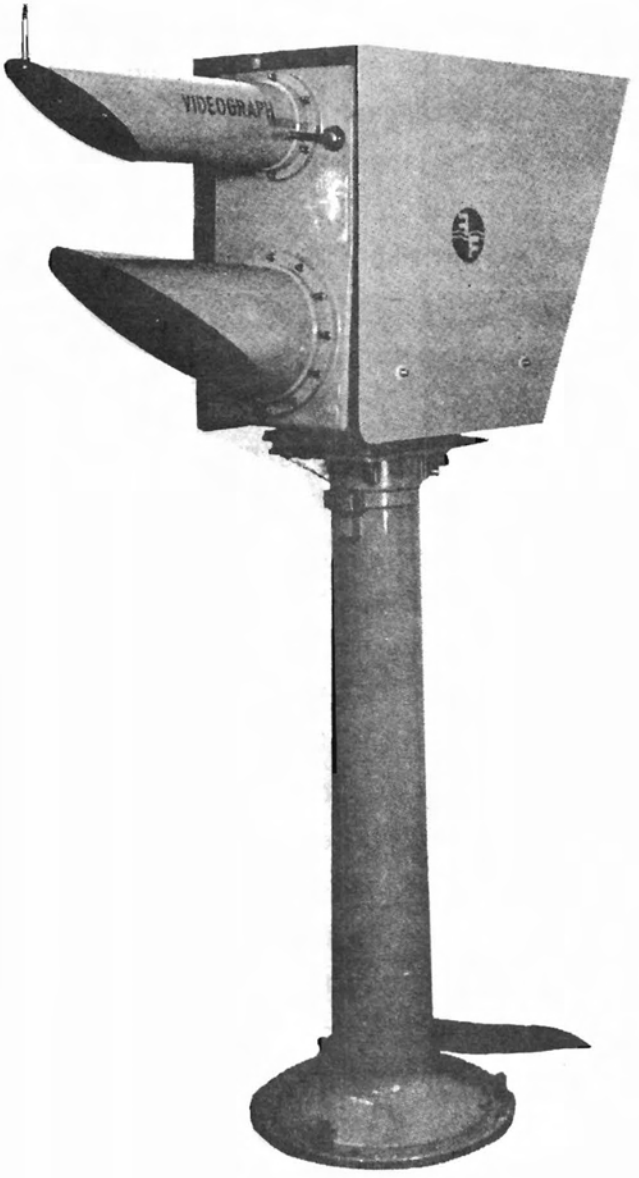

FIGURE 4-1

VIDEOGRAPH SAMPLING VOLUME

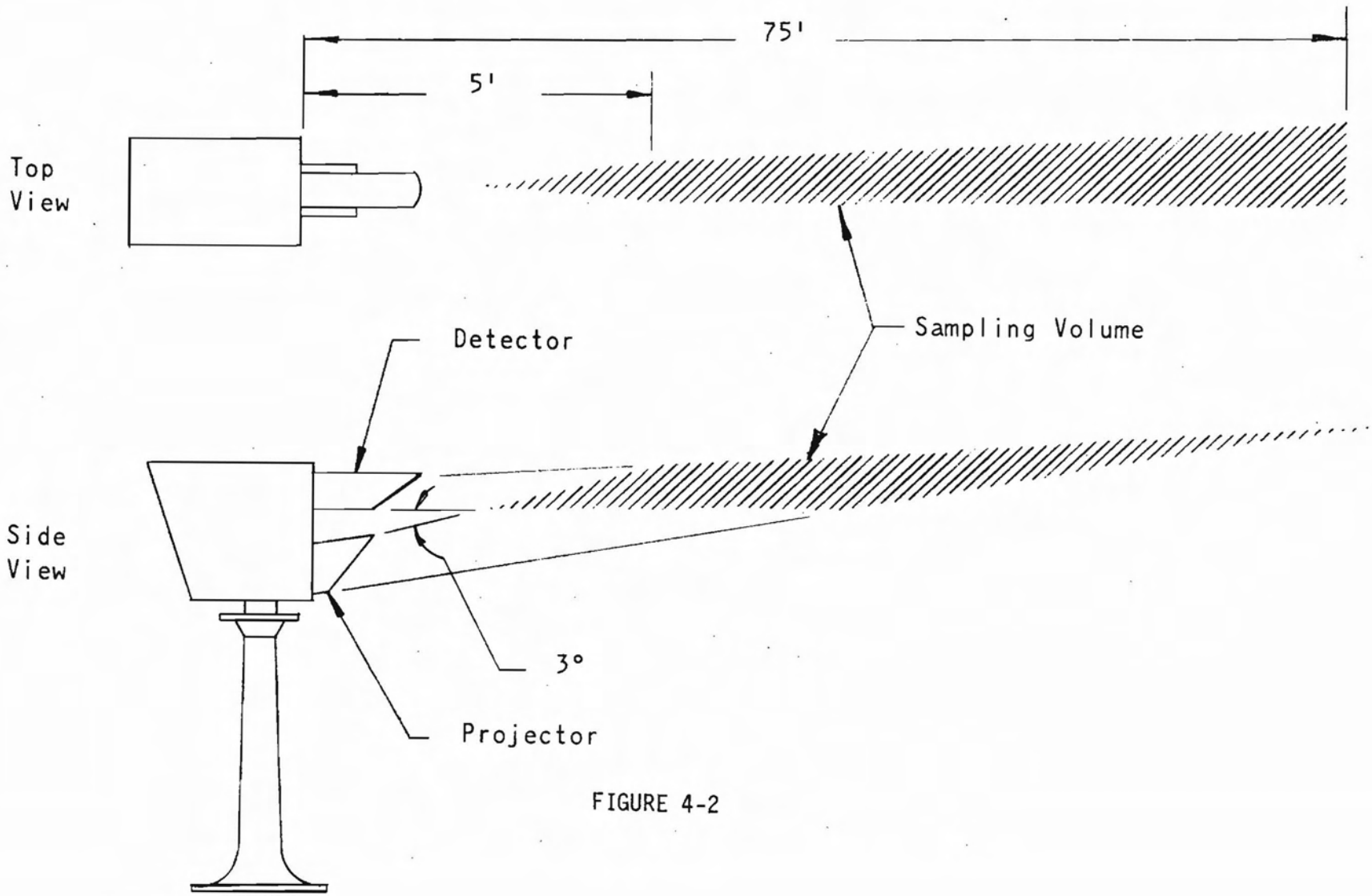

FIGURE 4-2

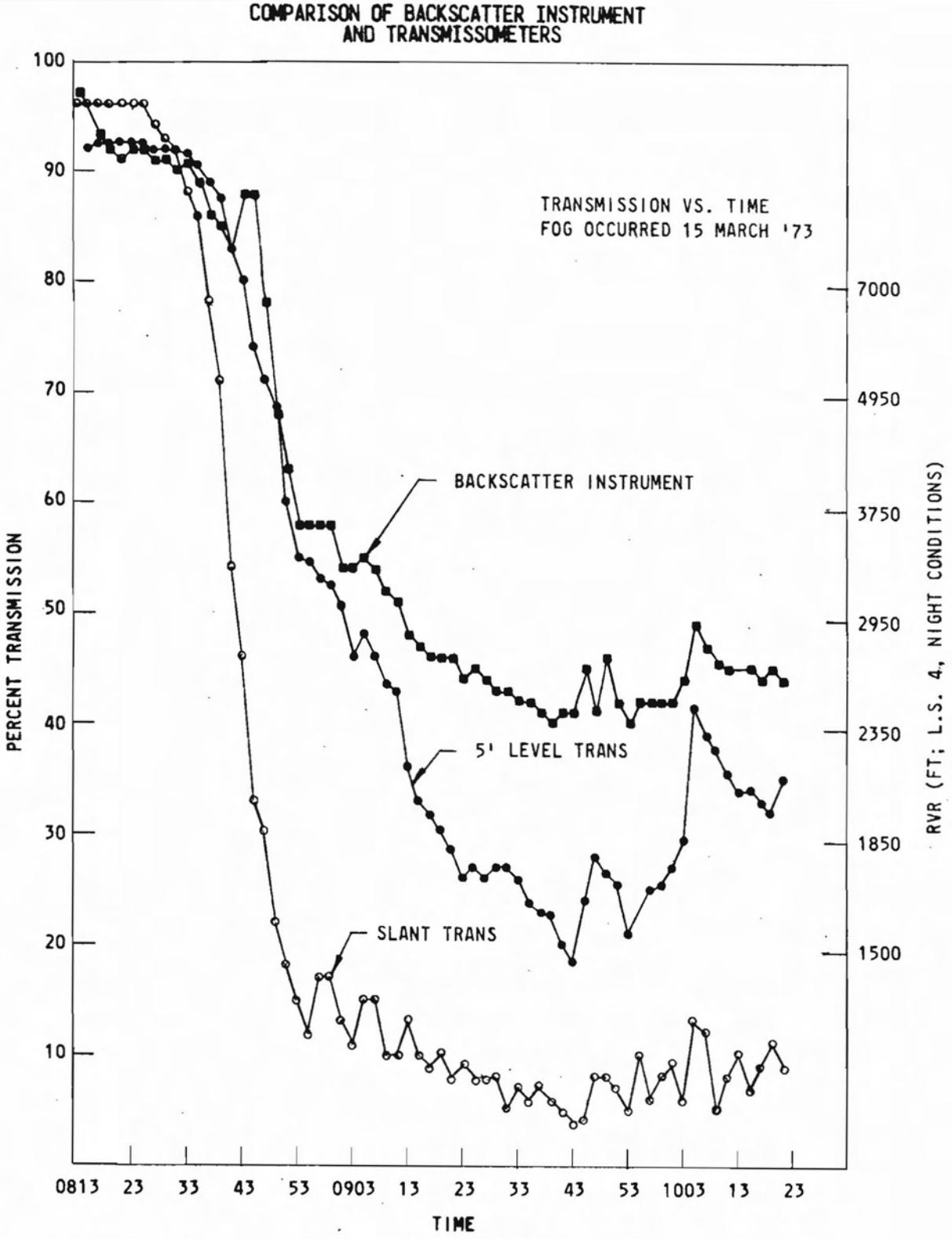
COMPARISON OF BACKSCATTER INSTRUMENT
AND TRANSMISSOMETERS
TRANSMISSION VS. TIME
FOG OCCURRED 15 MARCH '73
BACKSCATTER INSTRUMENT
5' LEVEL TRANS
SLANT TRANS
PERCENT TRANSMISSION
RVR (FT; L.S. 4, NIGHT CONDITIONS)
TIME
100
90
80
70
60
50
40
30
20
10
7000
4950
3750
2950
2350
1850
1500
0813
23
33
43
53
0903
13
23
33
43
53
1003
13
23

FIGURE 4-3

COMPARISON OF BACKSCATTER INSTRUMENT
AND TRANSMISSOMETERS

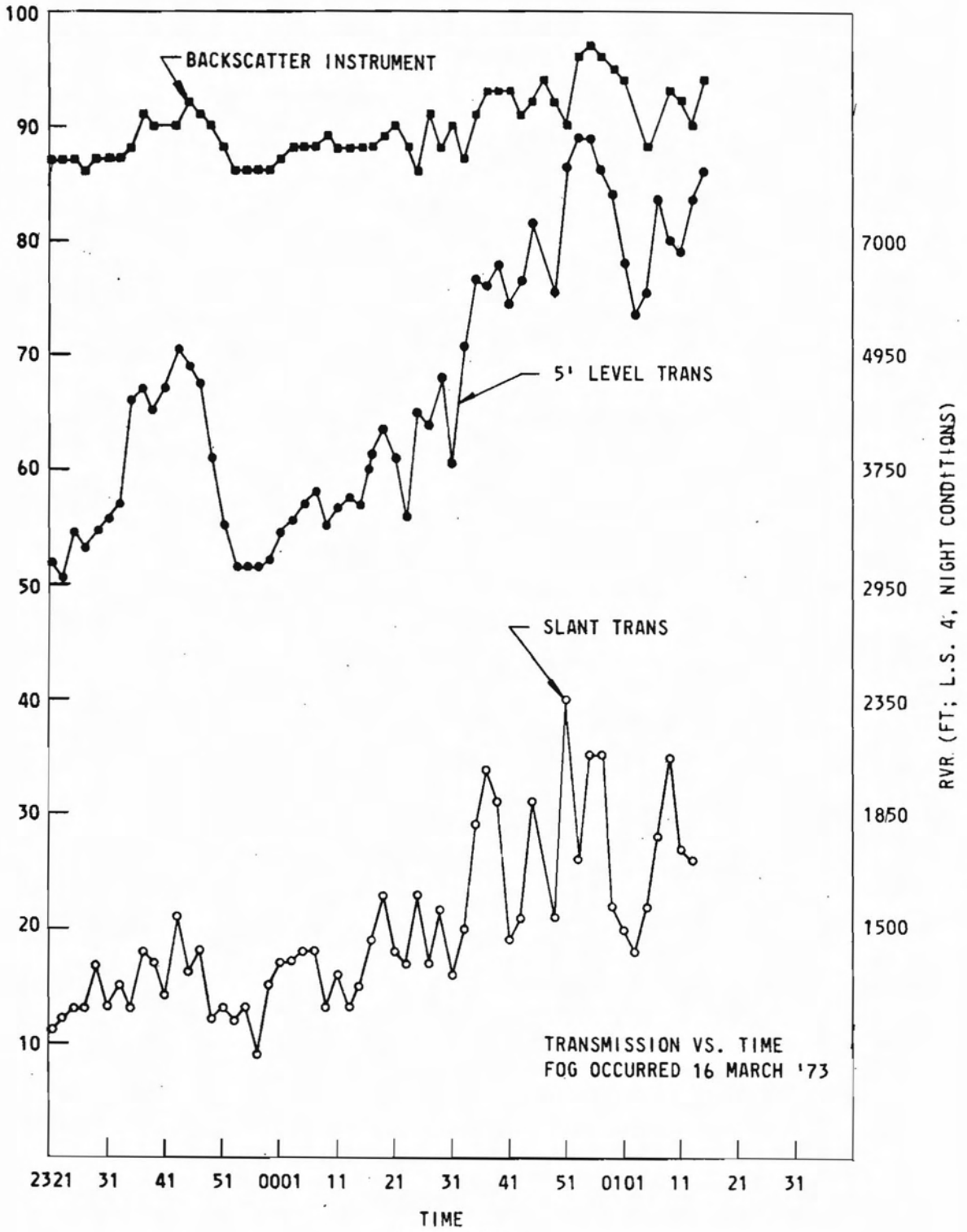

FIGURE 4-4

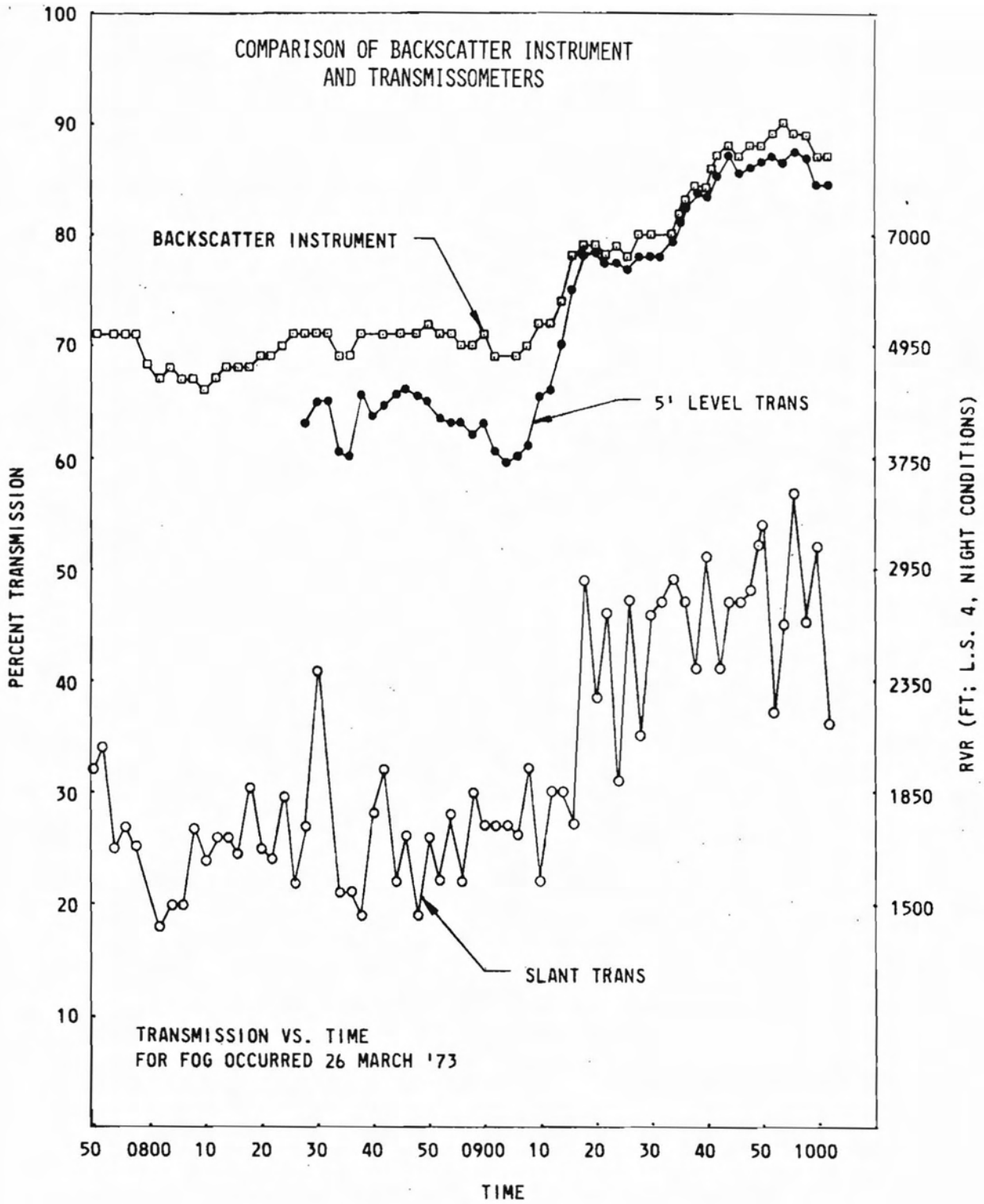
COMPARISON OF BACKSCATTER INSTRUMENT
AND TRANSMISSOMETERS
BACKSCATTER INSTRUMENT
5' LEVEL TRANS
SLANT TRANS
TRANSMISSION VS. TIME
FOR FOG OCCURRED 26 MARCH '73
PERCENT TRANSMISSION
RVR (FT; L.S. 4, NIGHT CONDITIONS)
TIME
100
90
80
70
60
50
40
30
20
10
7000
4950
3750
2950
2350
1850
1500
50
0800
10
20
30
40
50
0900
10
20
30
40
50
1000

FIGURE 4-5

5. FORWARD SCATTER METER VISUAL RANGE SYSTEM CONCEPT

At the initiation of Phase II, the proposed systems under consideration were those employing a tower offset from the approach zone. Although these systems may have some restrictive features, particularly in their configuration, they do offer advantages of simplicity in measurement technique and data interpretation and direct use of fully developed, operational instrumentation.

Several concepts were explored and rejected. The final concept would measure horizontal and vertical variations of visibility independently, and slant path transmittance would be determined analytically using the separate measurements. Vertical variation of visibility would be detected by short baseline instrument at various levels on a tower. Horizontal variations would be measured by instruments located at the base of the tower and near the extended runway centerline.

The basic assumption inherent in the system concept is that relative vertical variation of transmittance remains constant over horizontal distances of several thousand feet. The horizontal distance for constancy can be strongly affected by local conditions; this will be investigated using the test data obtained. Based on this assumption, vertical variation in the approach zone would be found by taking the measurements on the tower displaced from the runway and correcting them by the ratio of the readings on the ground transmissometers at the tower and approach zone centerline. Using a system which relies on this assumption will entail scrutiny of proposed sites to effect minor modifications dictated by such features as terrain.

The feasibility of this system and associated assumptions were tested at NAFEC. The height of the tower was chosen as 100 feet to coincide with the 100-foot decision height. Instruments to be mounted

on the tower to determine transmittance must be rugged, require infrequent maintenance and must utilize a measurement technique insensitive to tower vibration and sway. Several instruments are available which generally satisfy these requirements. An EG&G Forward Scatter Visibility Meter was selected because it not only satisfied the requirements but also had been extensively compared with the NBS transmissometer by the Air Force.

One approach considered installation of visibility meters at several levels on the tower; however, it was decided that the system could be tested with a meter at the top of the tower and one near the ground. With the instrumentation available at the met tower complex, assessment of the need for more levels of measurement could be made. The possible delivery date of a second visibility meter would have jeopardized the completion of the system in time for the fog season at NAFEC; therefore, an NBS transmissometer mounted five feet above the ground was used to measure visibility at the tower base. Regulations (Federal Aviation Regulations, Vol. XI, Part 77; Objects Affecting Navigable Airspace) require that a 100-foot high obstruction must be offset approximately 1,300 feet from the extended runway centerline. At NAFEC a temporary tower was erected about 1,500 feet from the met tower facility. For the purposes of analysis, the met tower provided measurement of visibility in a region simulating an approach zone and the offset of the temporary tower was that required by regulation.

Forward Scatter Meter

Description and Operating Characterisitics

The EG&G Model 207 Forward Scatter Meter, shown in Figure 5-1, is designed to determine the amount of light scattered in the forward direction by water droplets in the atmosphere. The FSM is a nephelometer type instrument which has the advantage of small size and ease of calibration and installation as compared to the extinction type instrument.

FORWARD SCATTER METER

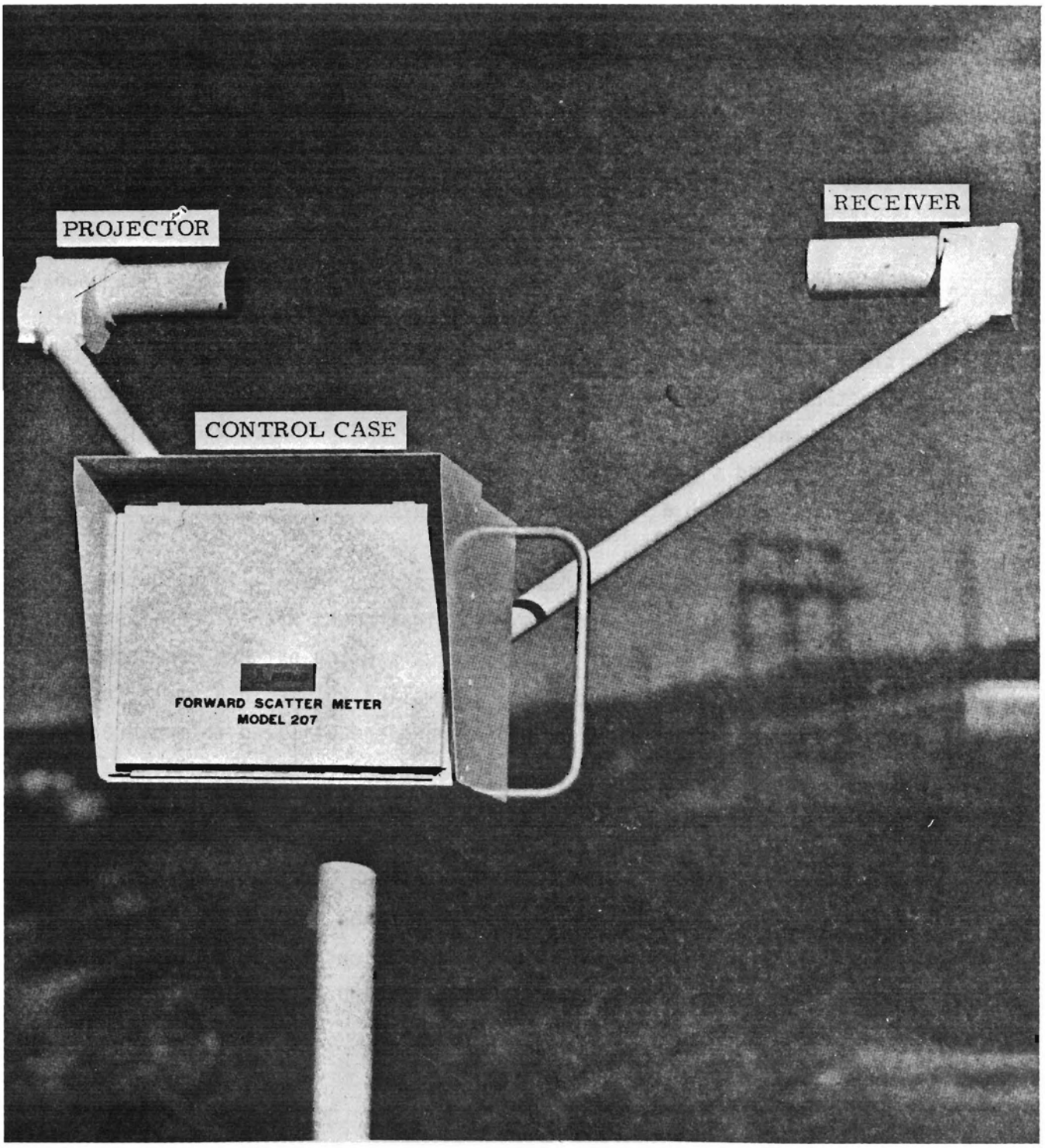

FIGURE 5-1

The forward scatter meter (FSM) utilizes a 1.7 cubic feet volume between a projector and receiver separated by 48 inches to measure the visual range (see Figure 5-2). An optical system in the projector assembly provides the desired beam pattern of high intensity light, while another optical system in the receiver assembly collects the desired scattered light onto a light sensitive detector. Interference from external light (e.g., sunlight, street lights) is prevented by modulation of the projected light and synchronous demodulation of the received light.

The unit is a self-contained, AC line powered instrument designed for unattended operation at an unprotected site under all weather conditions. Fabricated in a single unit, the instrument consists of a cabinet housing the control unit, control panel and associated electronics, and two support arms holding the projector and receiver assemblies. Power input and signal output terminals are located at the rear of the cabinet beneath a removable access cover.

The FSM is designed to measure the scattering of light in the atmosphere from a single, post-mounted instrument with a four-foot optical baseline. A unique conical torus sensing pattern, as shown in Figure 5-2, provides a reasonable sampling volume in a small instrument. Wavelengths from 0.4 to 1.1 microns are utilized to measure the forward scattered light over the angles of 20° to 50° inclusive. Solid state electronics with regulated power supplies and regulated modulated halogen incandescent source provide stable, long-term, drift-free analog outputs over a range of scattering coefficients equivalent to the range of 200 to 20,000 feet visual range. The theoretical correlation of integrated scattering coefficient to visual range based on 5% liminal contrast ratio and the corresponding output voltage of the FSM is shown in Figure 5-3.

EG&G FORWARD SCATTER VISIBILITY METER

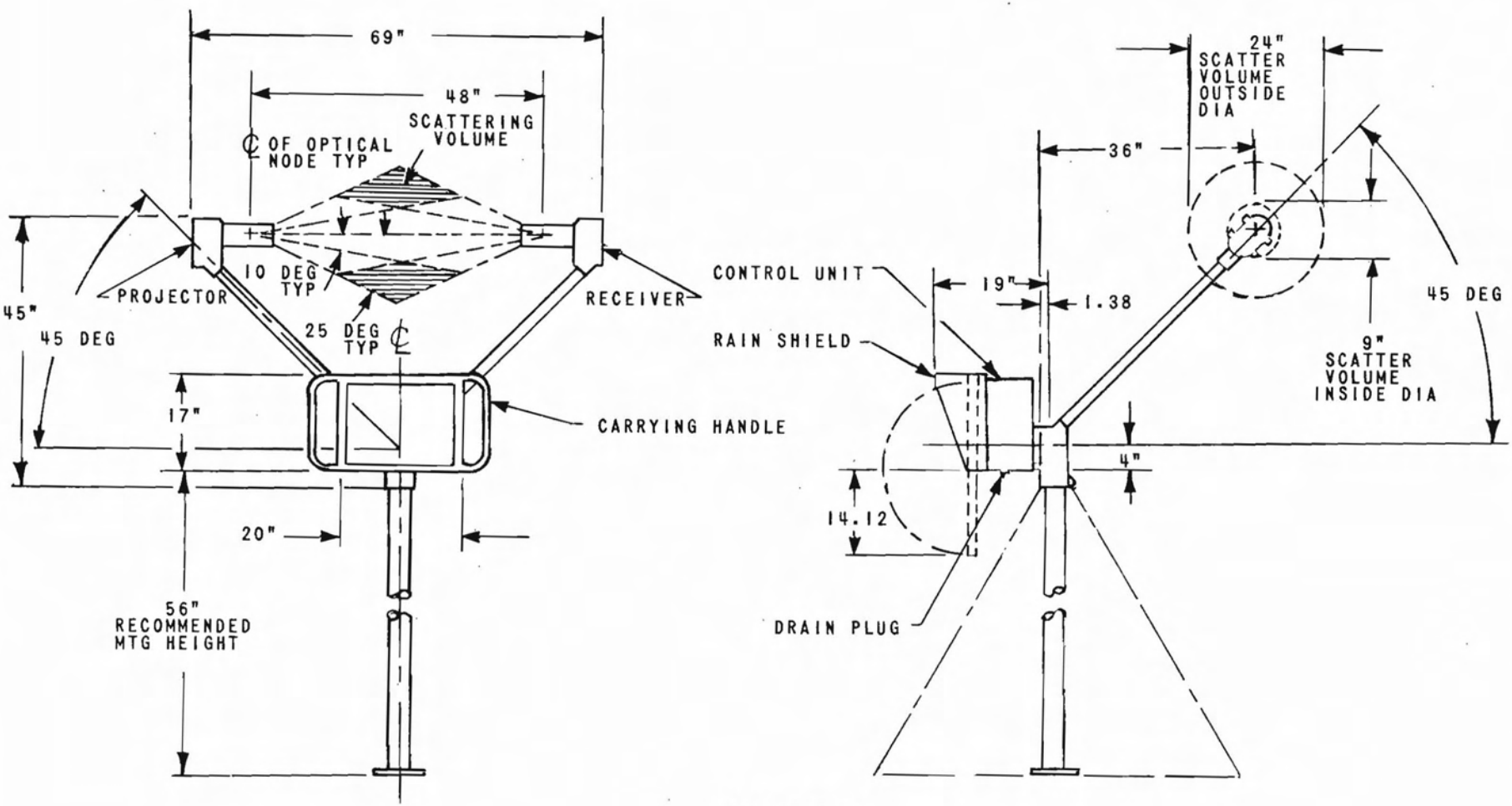

FIGURE 5-2

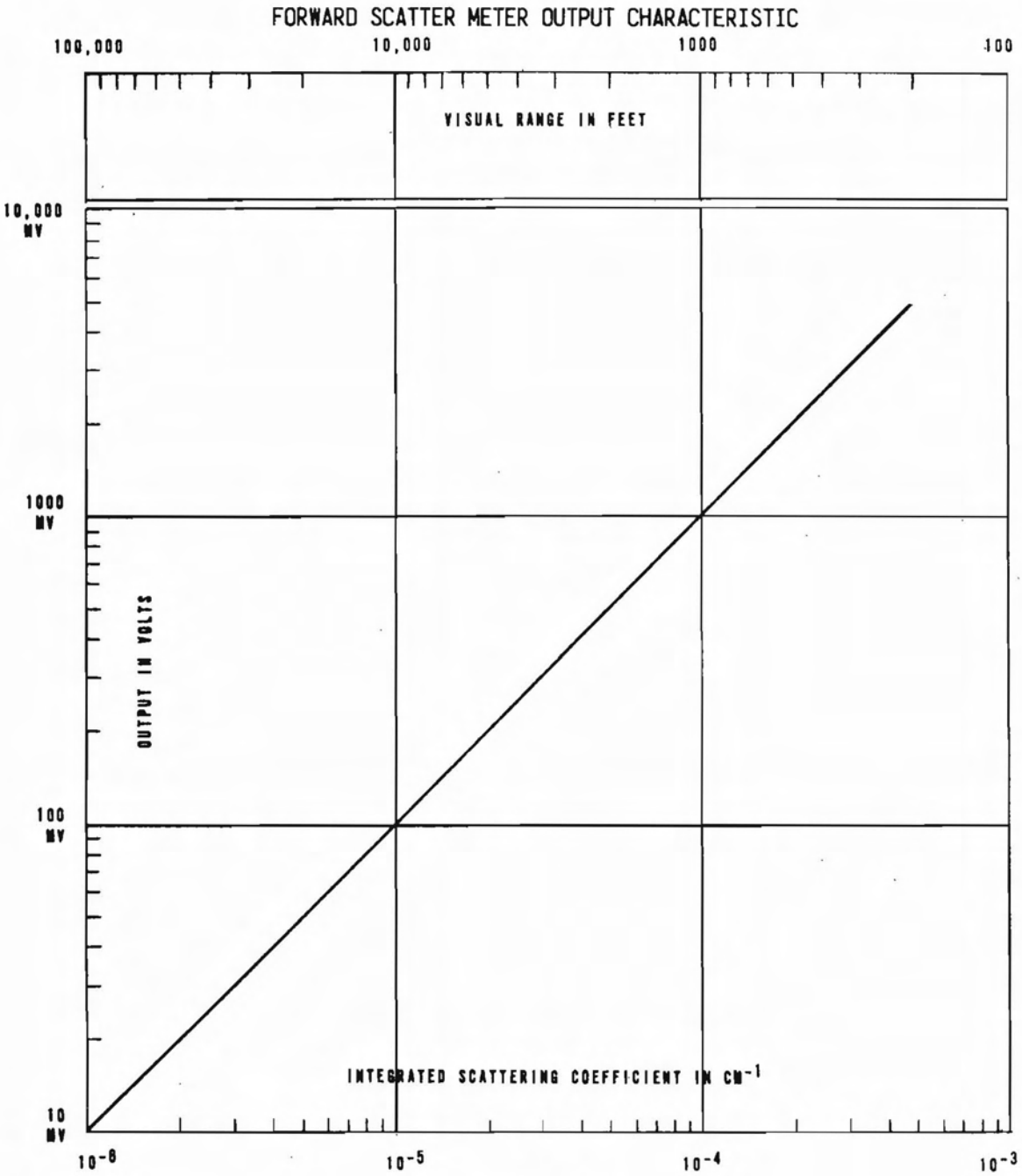
FORWARD SCATTER METER OUTPUT CHARACTERISTIC
100,000
10,000
1000
100
VISUAL RANGE IN FEET
10,000 MV
1000 MV
100 MV
10 MV
OUTPUT IN VOLTS
INTEGRATED SCATTERING COEFFICIENT IN CM-1
10-6
10-5
10-4
10-3

FIGURE 5-3

Comparison of Forward Scatter Meter and NBS Transmissometer

Extensive comparison of the FSM and the NBS transmissometer has been done by Air Force Cambridge Research Laboratory. Hering, Muench and Brown (1971) found the correlation coefficient between the FSM and transmissometer measurements was 0.91 with a standard error of estimate of 26%. They found disparities between simultaneous measurements were caused primarily by high frequency fluctuations in fog density that were detected by the small volume measurements with the FSM, but were smoothed out by the measurements of transmittance over a 500-foot baseline. The measurements were made in fairly dense advection fog at Cutler, Maine. Measurements made in snow gave similar results to those obtained in fog.

In the early stages of the field program at NAFEC, the FSM was mounted at the base of the met tower. The sampled volume was at about the same height as the first NBS transmissometer, and data recorded during this period gives additional comparison of the FSM and the NBS transmissometer.

The results of the comparison of the FSM and the NBS transmissometer are illustrated in two distinct ways. Figures 5-4 and 5-5 show the ratio of transmittance measured by the NBS transmissometer to transmittance determined by the FSM. The ratios are plotted versus time. For the examples shown in Figure 5-5, the ratio is nearly constant but shows a small bias, i.e., the FSM gives a lower value of transmittance than the NBS, yielding a ratio greater than one. The data shown in Figure 5-4 is for a period of time characterized by very rapid fluctuations in transmittance readings for both instruments. During this time, instantaneous readings do not show good agreement yielding large rapidly changing ratios. Most of the large ratios result from small transmittance reading, less than 5%.

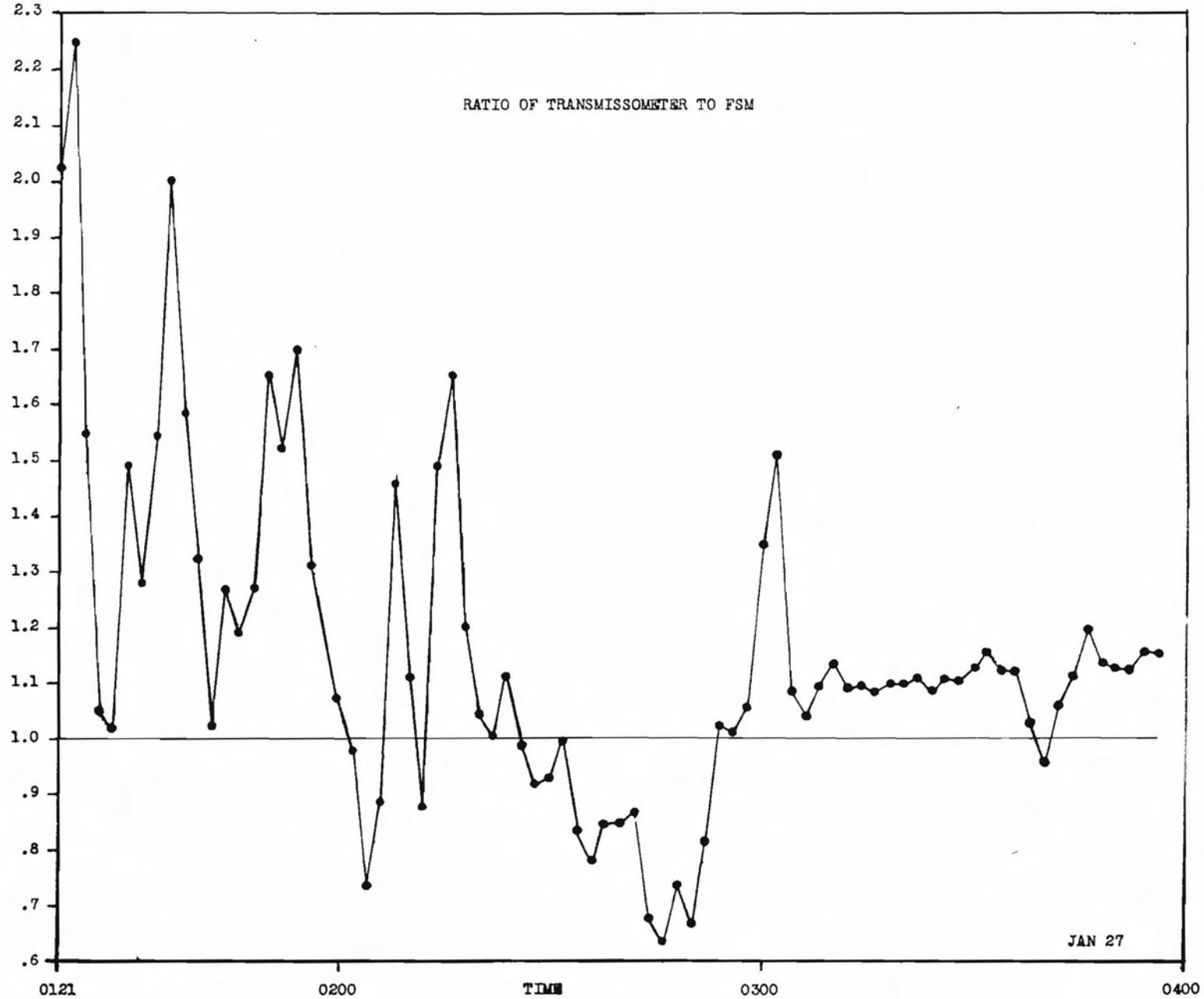
RATIO OF TRANSMISSOMETER TO FSM
2.3
2.2
2.1
2.0
1.9
1.8
1.7
1.6
1.5
1.4
1.3
1.2
1.1
1.0
.9
.8
.7
.6
0121
0200
TIME
0300
0400
JAN 27

Figure 5-4

RATIO OF TRANSMISSOMETER TO FSM

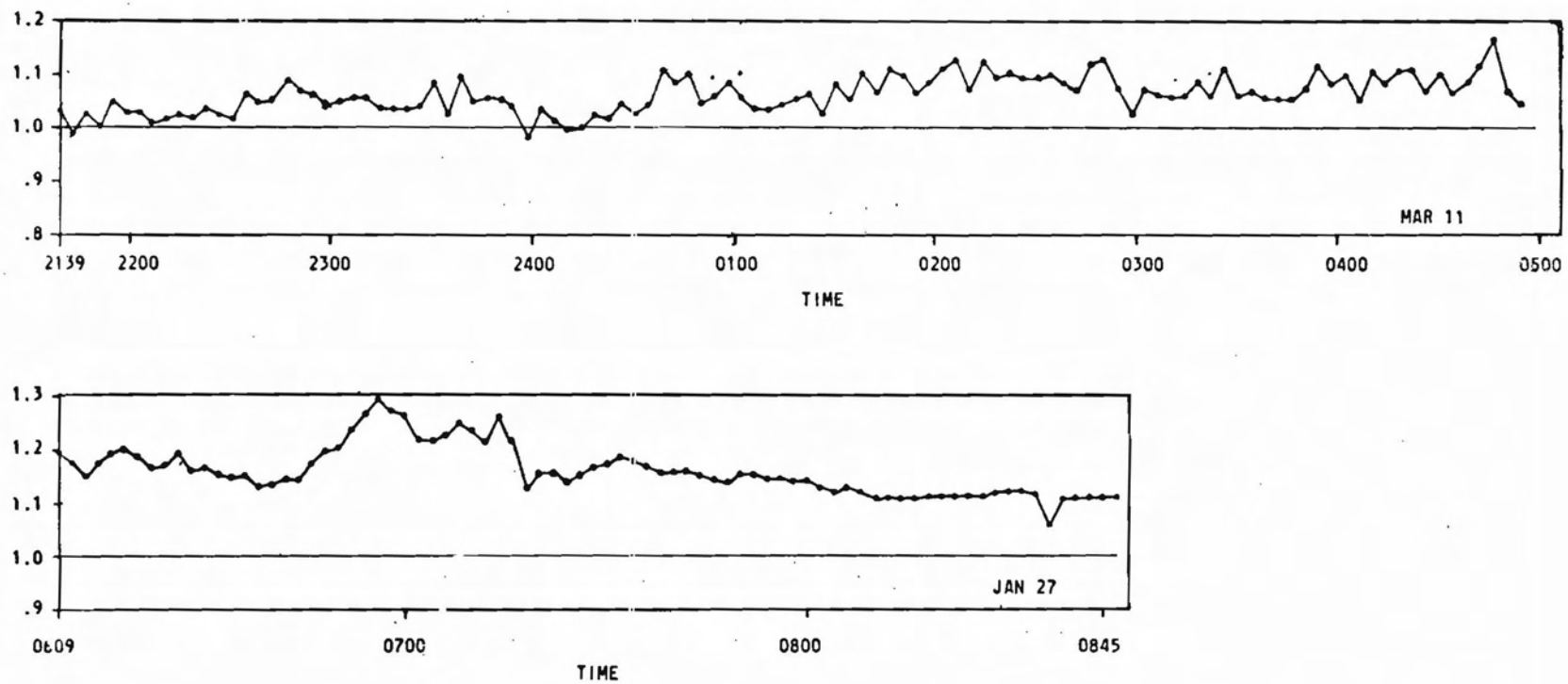

FIGURE 5-5

The comparison, on percent transmittance for five separate incidents was run, and the percent error between instruments was found. This is shown in Figure 5-6; the comparison was limited to observations with transmittances less than 89%. The data represents 572 minutes of observations; the peak error falls in the 3 to 4% range. Figure 5-7 is a plot of one of the above incidents showing percent transmittance for the FSM plotted versus percent transmission for the NBS instrument. Figure 5-8 shows a similar comparison to Figure 5-6 but for a fog not included in the above cumulative summary. This shows the largest difference of any of the results of the two instruments. Figure 5-9 shows a composite of all of the above cases. The results found show good agreement between the FSM and the NBS transmissometer.

Candidate System Evaluation

Various analyses were performed on the data taken at NAFEC to evaluate aspects of the proposed system. One analysis of horizontal variation was made by comparing the transmission reading of the five-foot transmissometer at the test site with the reading of the transmissometer at the remote site, 1,500 feet away, which was also at the five-foot level. For two fogs, the comparison of the two instruments with time is shown by plotting the ratio of their readings, Figure 5-10. Except for a few observations in these fogs, the ratio is close to one. The extreme readings show less than 30% difference. Figure 5-11 illustrates the comparison in the form of a histogram of percent error. Some care must be used in analyzing these results. Much of the data recorded was for advection type fogs with fairly high percent transmission near the surface. In these cases, agreement was good, although the more significant tests were for conditions with much more limited visibility near the surface. A histogram was also made for those cases for which percent transmission was less than 60, shown in Figure 5-12. Again the agreement between the instruments was quite good, although a larger population appeared in the higher percent errors. The good

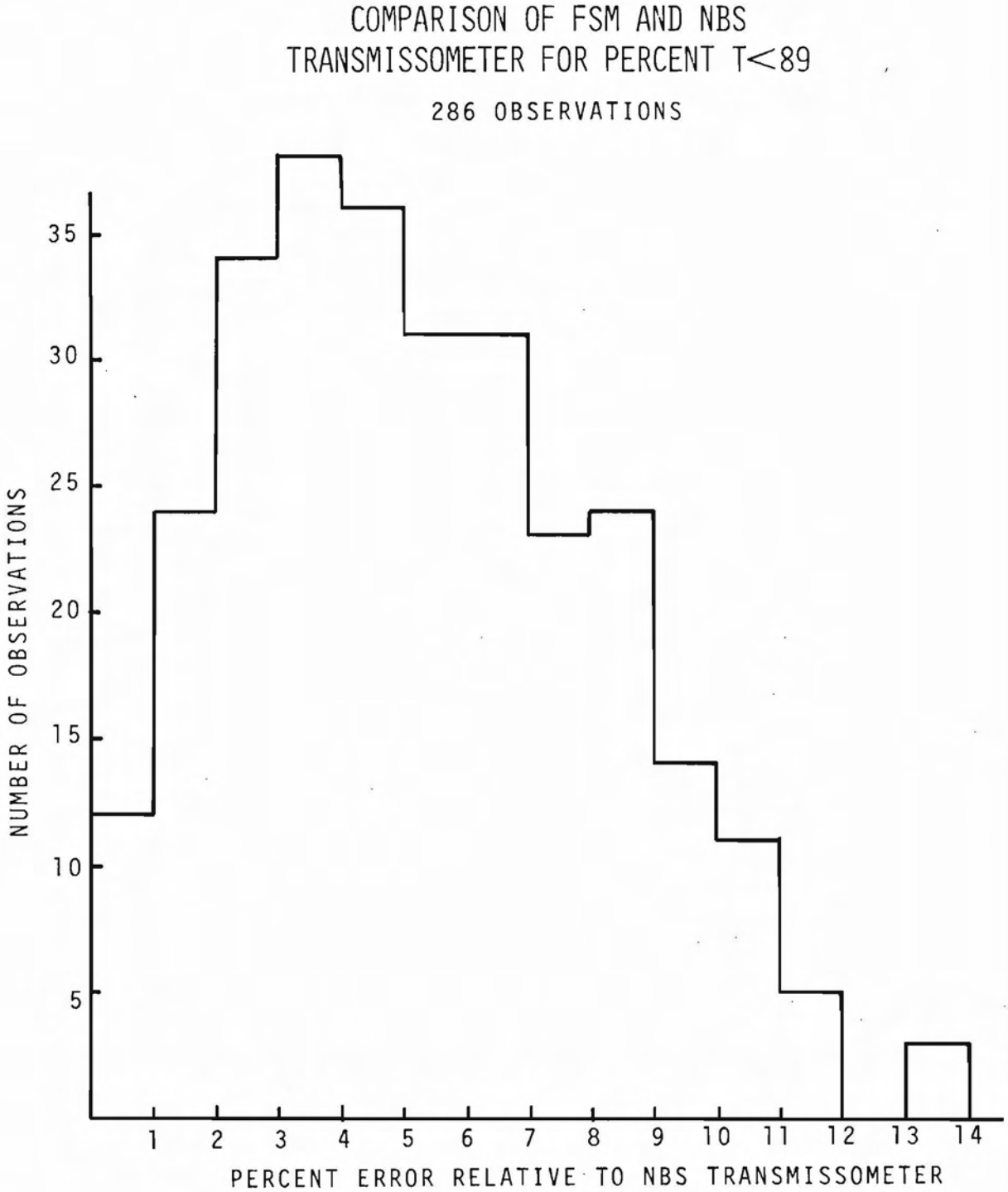
COMPARISON OF FSM AND NBS
TRANSMISSOMETER FOR PERCENT T<89
286 OBSERVATIONS
NUMBER OF OBSERVATIONS
35
30
25
20
15
10
5
1
2
3
4
5
6
7
8
9
10
11
12
13
14
PERCENT ERROR RELATIVE TO NBS TRANSMISSOMETER

FIGURE 5-6

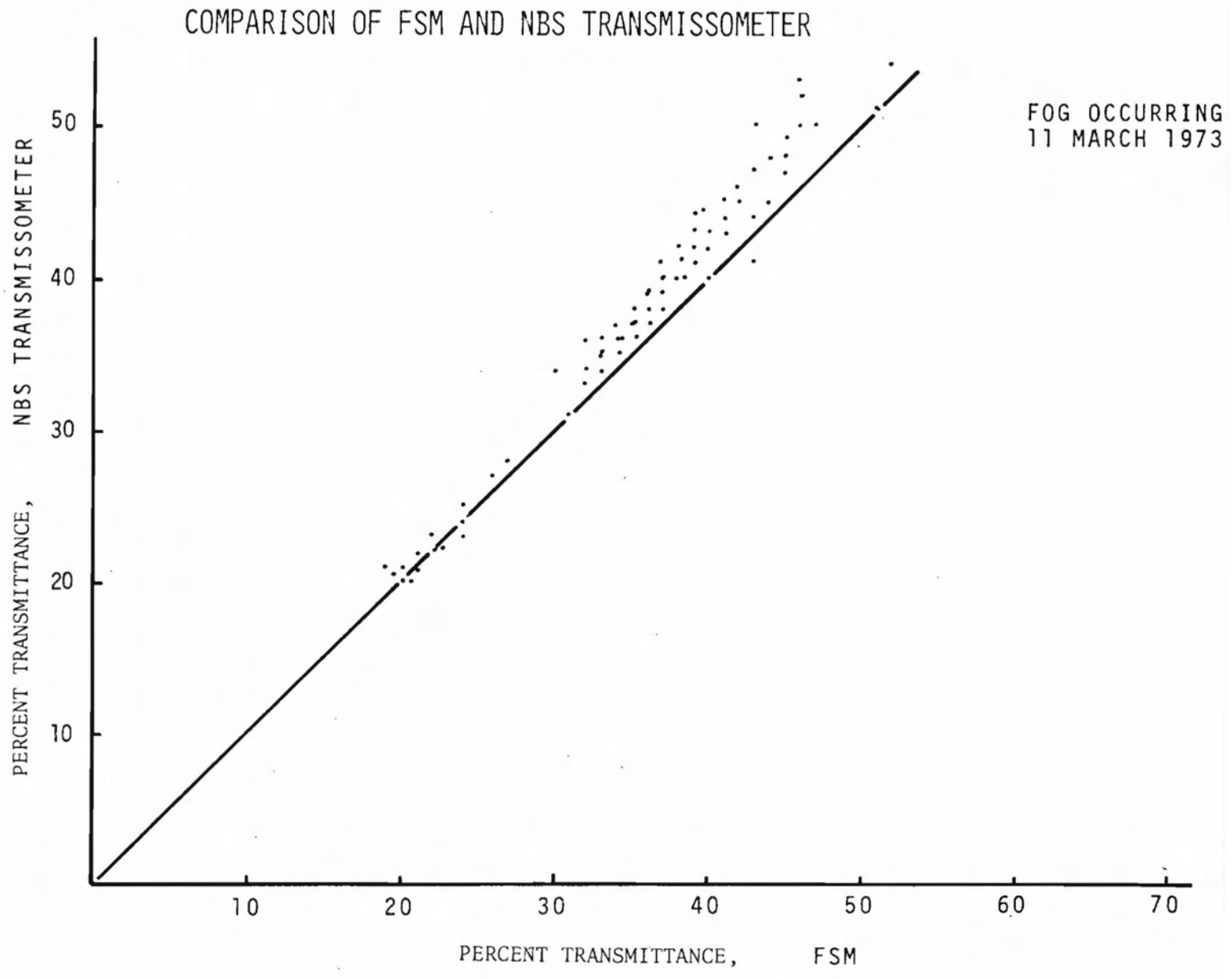
COMPARISON OF FSM AND NBS TRANSMISSOMETER
FOG OCCURRING
11 MARCH 1973
PERCENT TRANSMITTANCE, NBS TRANSMISSOMETER
10
20
30
40
50
10
20
30
40
50
60
70
PERCENT TRANSMITTANCE, FSM

FIGURE 5-7

COMPARISON OF FSM AND NBS
TRANSMISSOMETER FOR PERCENT TRANSMISSION<89

178 OBSERVATIONS

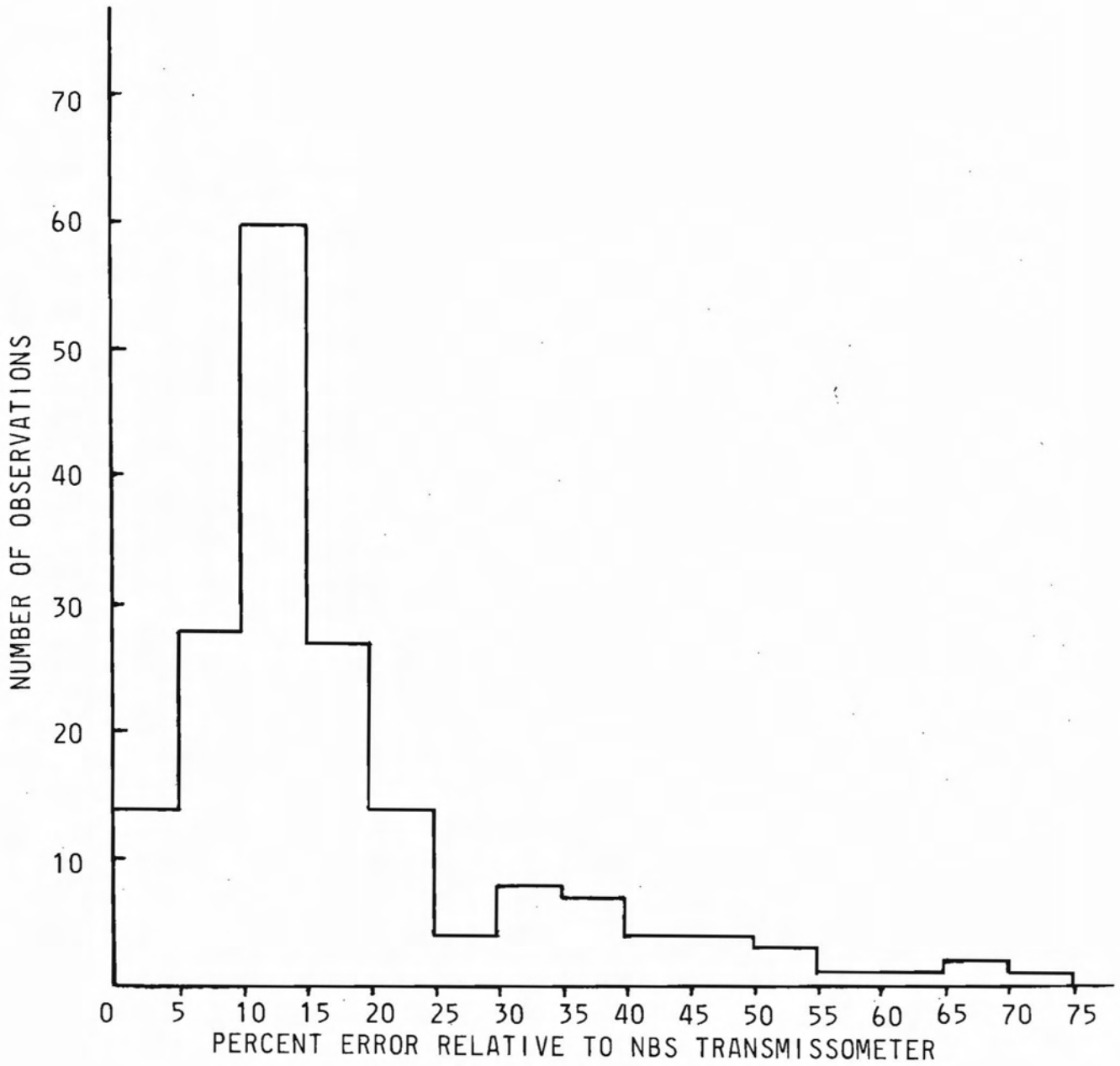

FIGURE 5-8

COMPARISON OF FSM AND NBS TRANSMISSOMETER
FOR PERCENT TRANSMISSION < 89; 464 OBSERVATIONS

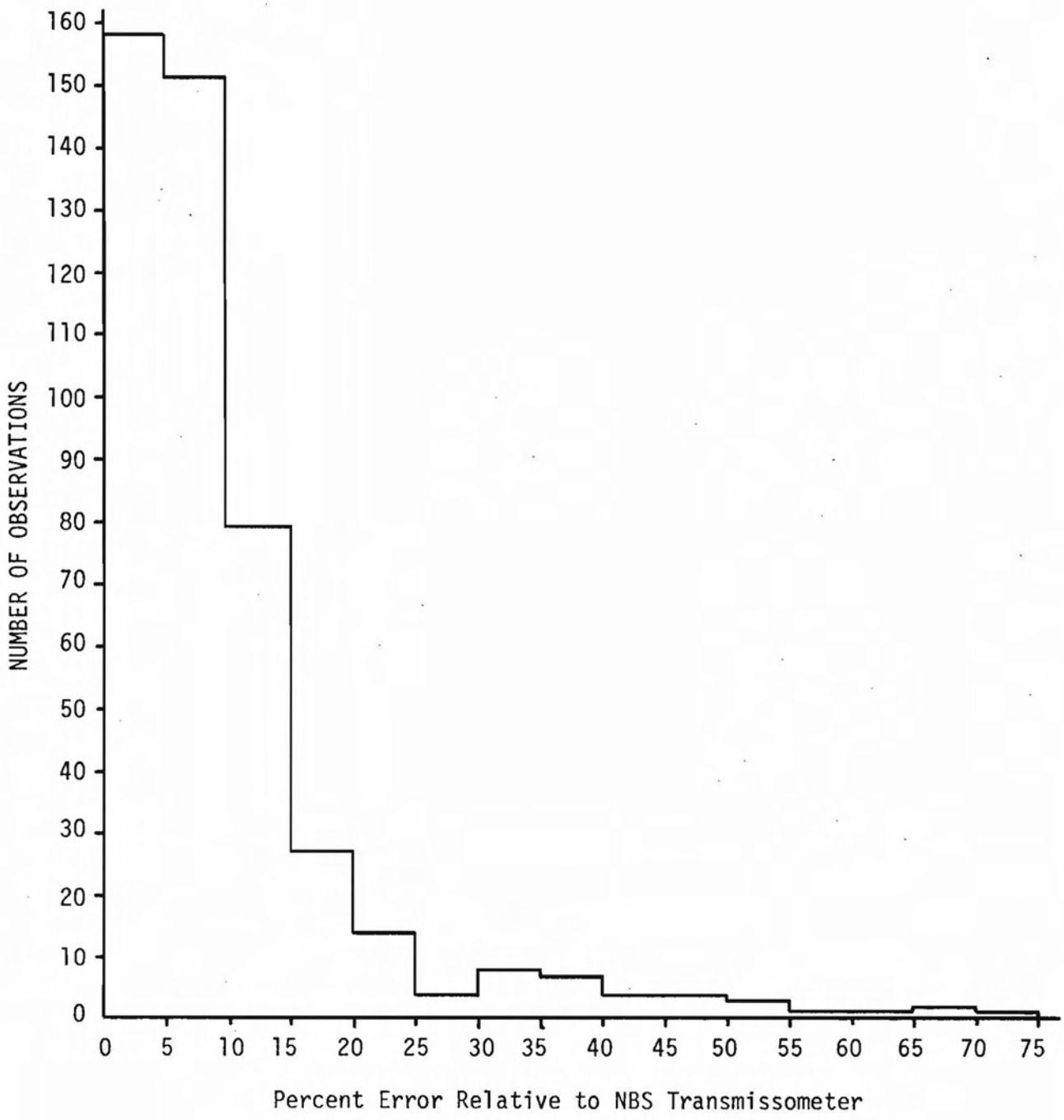

Figure 5-9

RATIO OF 250 FEET BASELINE TRANSMISSOMETERS AT 5 FOOT HEIGHTS 1500 FEET APART

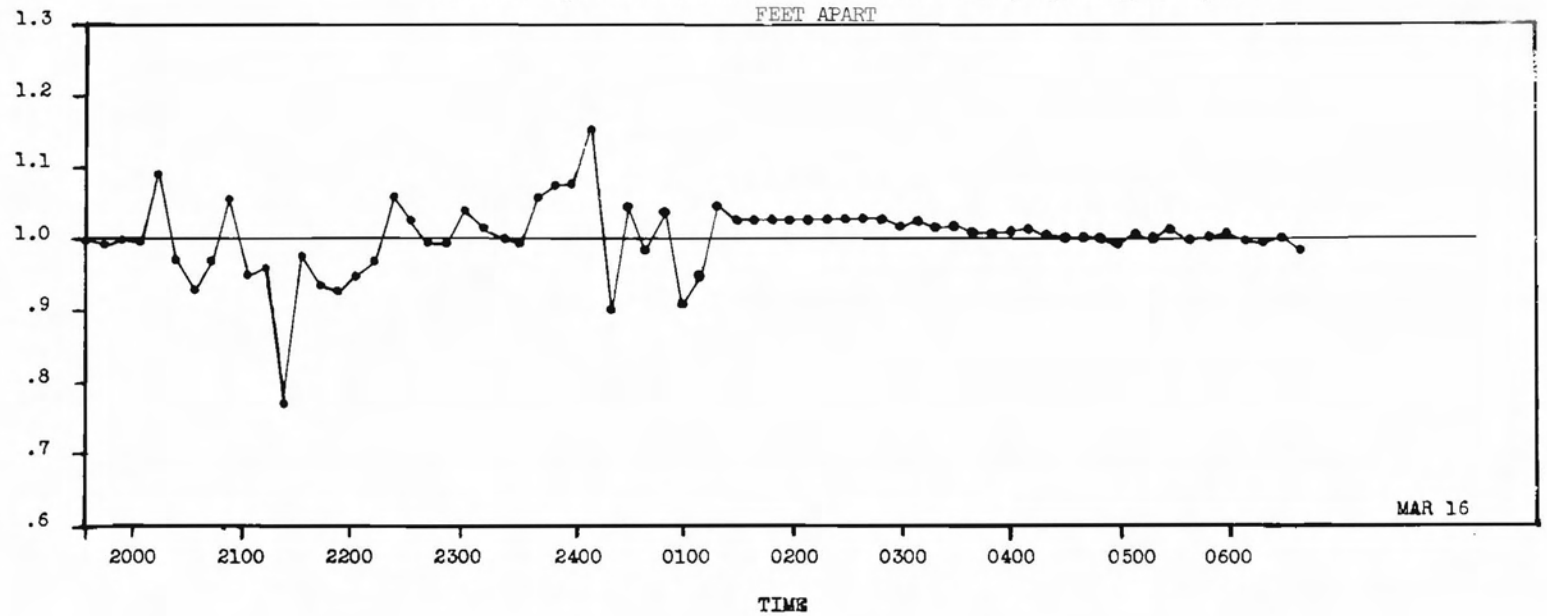

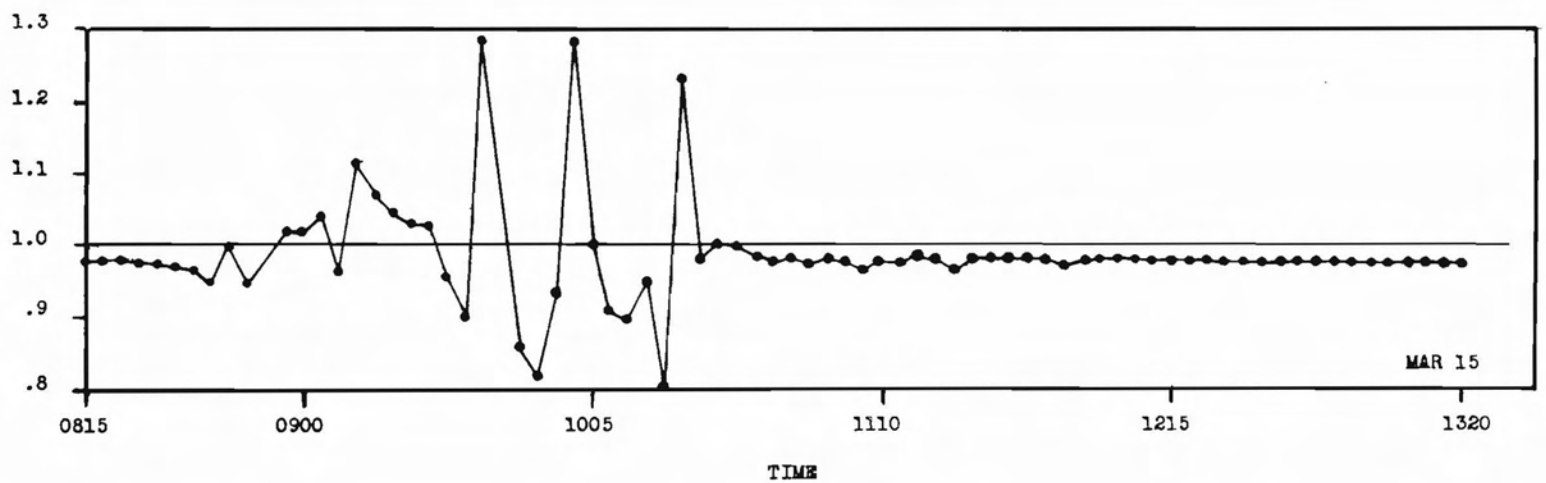

FIGURE 5-10

COMPARISON OF 5 FOOT LEVEL TRANSMISSOMETERS

1434 OBSERVATIONS; 2868 MINUTES OF FOG

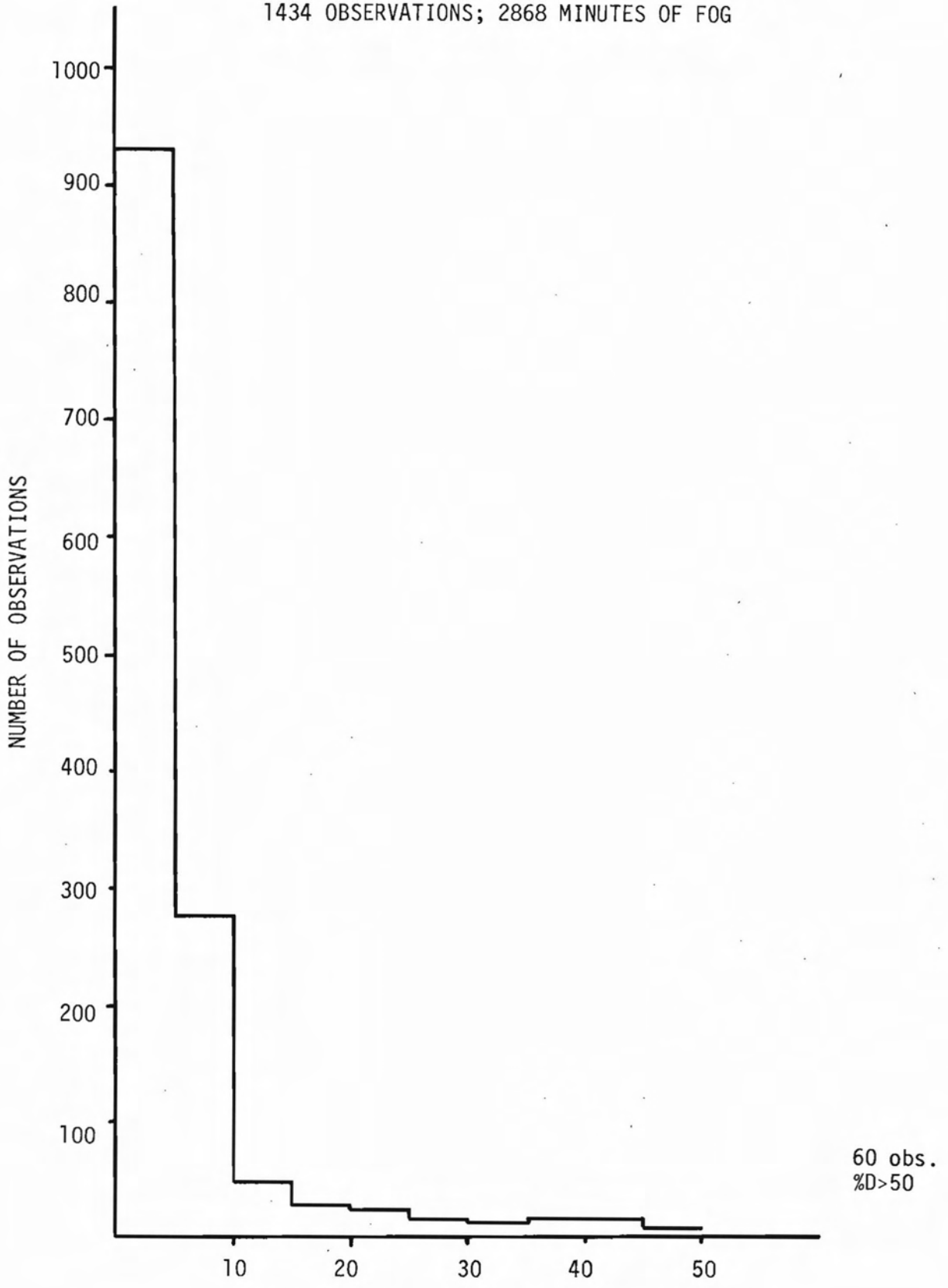

PERCENT ERROR RELATIVE TO MET TOWER

FIGURE 5-11

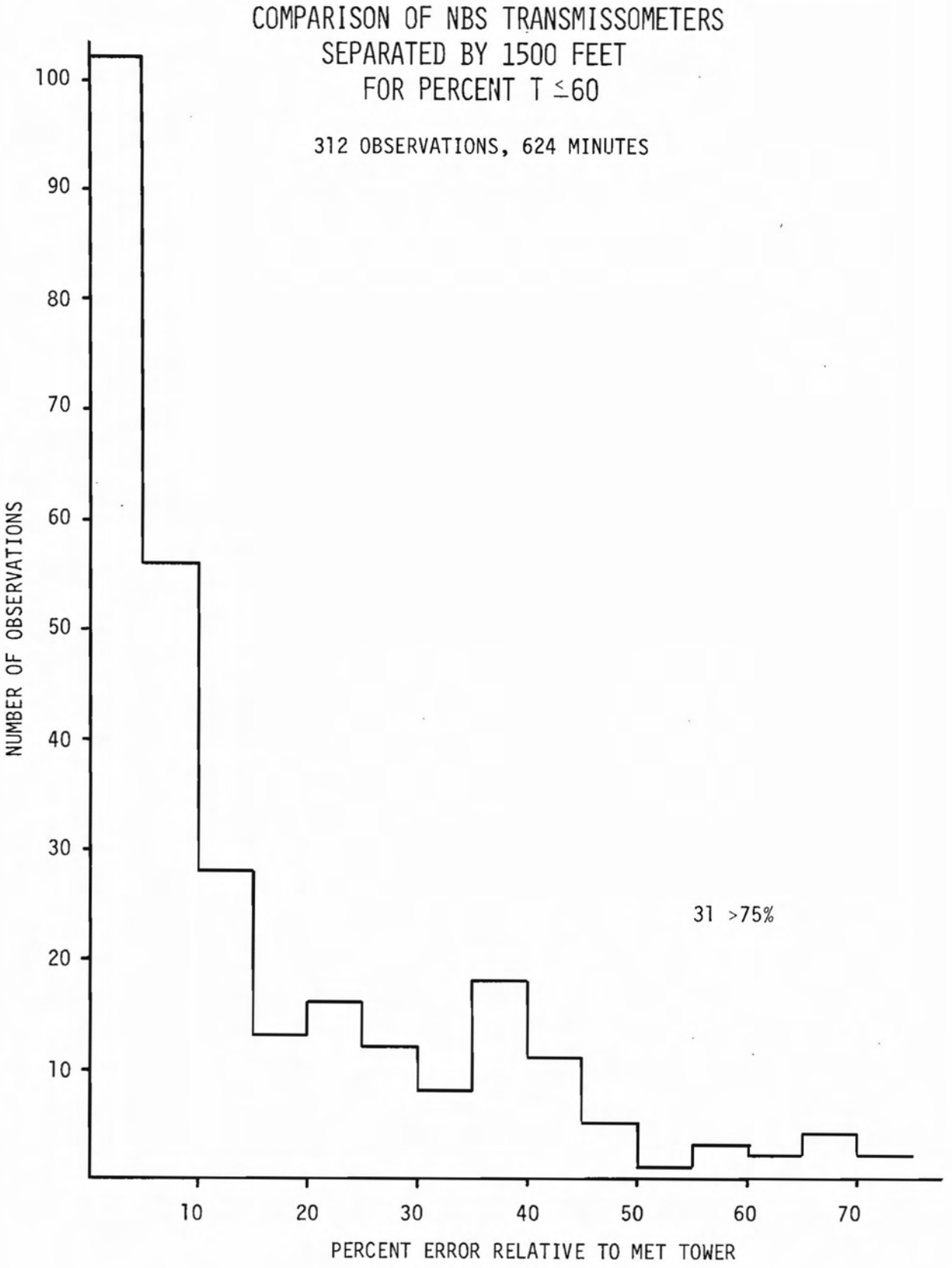
COMPARISON OF NBS TRANSMISSOMETERS
SEPARATED BY 1500 FEET
FOR PERCENT T ≤60
312 OBSERVATIONS, 624 MINUTES
NUMBER OF OBSERVATIONS
100
90
80
70
60
50
40
30
20
10
31 >75%
10
20
30
40
50
60
70
PERCENT ERROR RELATIVE TO MET TOWER

FIGURE 5-12

agreement of these two five-foot transmissometers presented a need to reconsider the concept of using the ratio of their readings as a correction factor to the transmittance readings at the different vertical levels at the remote tower. This would indicate that little would be lost by neglecting horizontal variation, eliminating the need for a transmissometer on the ground at the center line of the approach path.

An analysis of horizontal variation aloft was then made by comparing the transmittance reading of the 87-foot transmissometer at the test site with the transmittance reading obtained from the FSM at the remote site, at the 95-foot level. The altitude of the 87-foot transmissometer was closest to the altitude of the FSM. A histogram of the percent errors for this comparison is shown in Figure 5-13. There is reasonably good agreement between these readings, although the agreement is not as good as the agreement of the five-foot transmissometers. Also, many of these observations were for light fog conditions. Therefore, in Figure 5-14 a comparison is shown for those cases where the transmission was less than 60%.

An attempt was made to improve the agreement of the readings aloft by multiplying the tranmission reading obtained from the FSM by the ratio of the readings of the ground transmissometers. No improvement could be shown. Therefore, this was eliminated from the candidate system.

An analysis was made for the test data accumulated at NAFEC to estimate improvement to be gained by measuring transmission at more levels than two. The permissable tower height, without penetrating restricted zones defined in Federal Aviation Regulations, Part 77, is linearly related to the lateral offset from the approach zone centerline for heights to 150 feet. Since the objective is obtaining estimates of transmittance along the glide slope, a balance is sought between tower height and lateral displacement. The tower height decided on was 100 feet; therefore, consideration was given only to adding measuring instruments between the five- and 100-foot levels.

COMPARISON OF FSM AT 95 FEET AND
NBS TRANSMISSOMETER AT 87 FEET
SEPARATED BY 1500 FEET

734 OBSERVATIONS

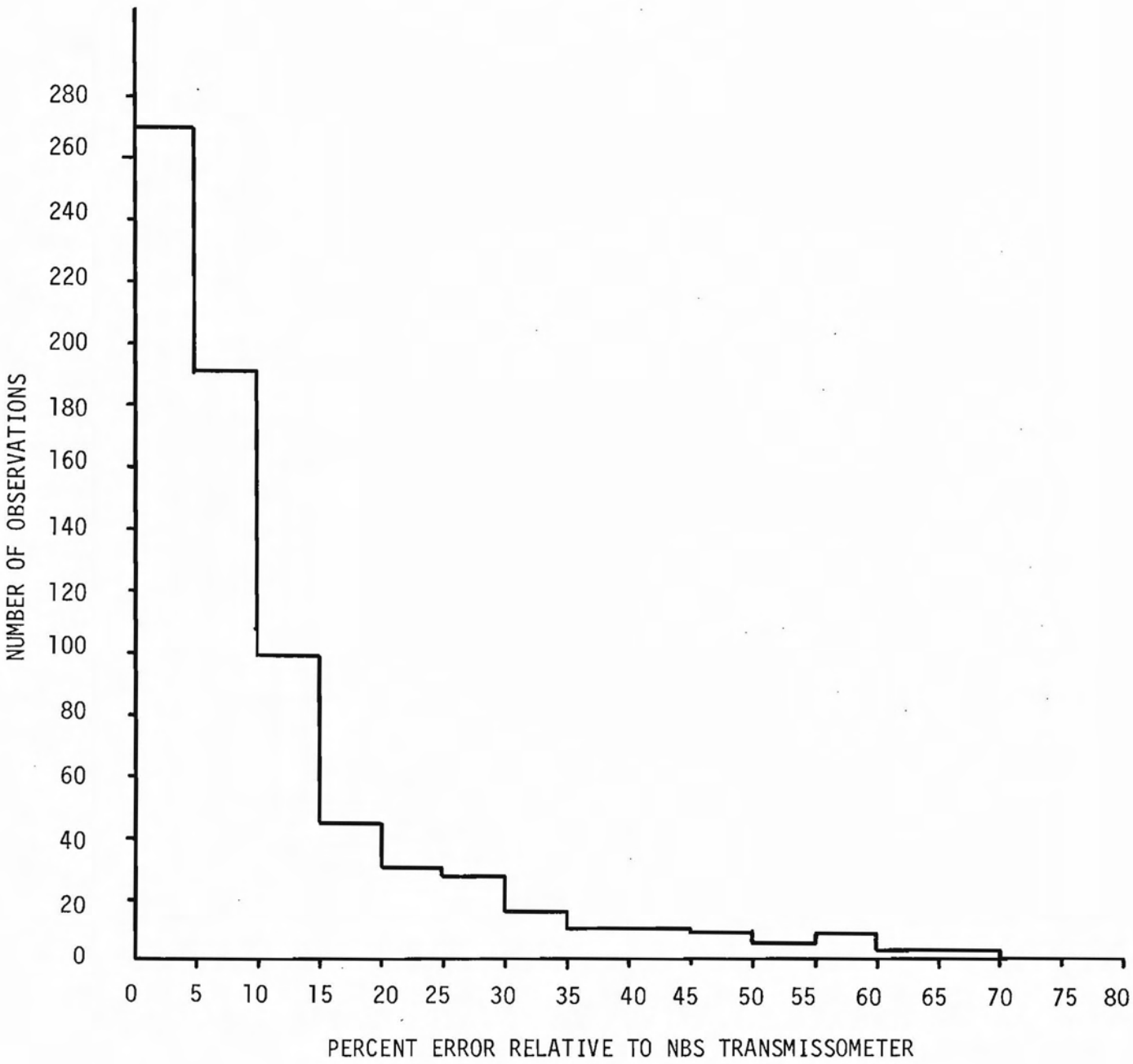

FIGURE 5-13

COMPARISON OF FSM AT 95 FEET
AND NBS TRANSMISSOMETER AT 87 FEET
SEPARATED BY 1500 FEET
FOR PERCENT T<60

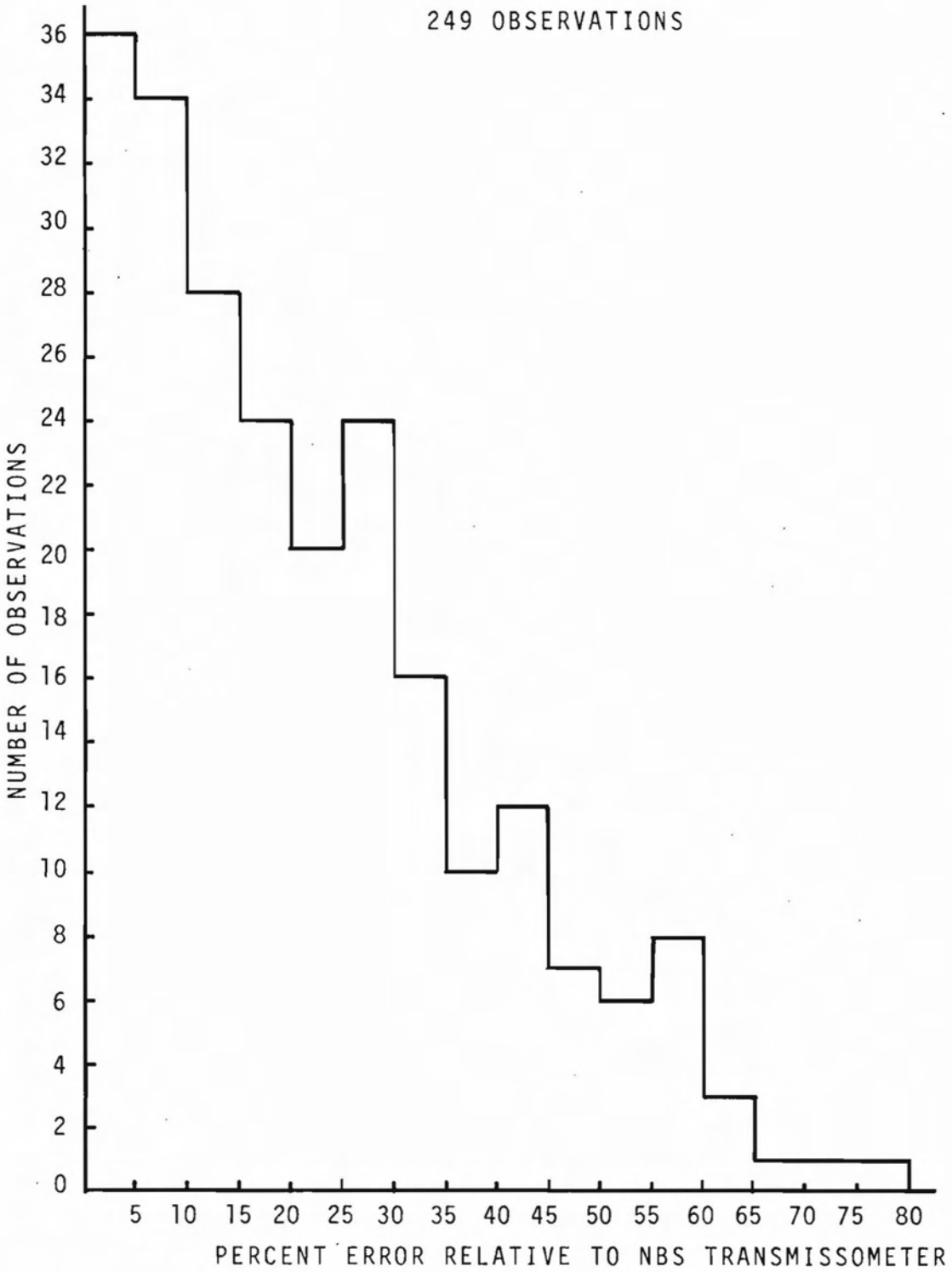

FIGURE 5-14

A study was made to determine how much improvement in performance of the minimum candidate system could be expected if an FSM were mounted at the 50-foot level on the tower. This would provide a measurement at 5, 50 and 100 feet above the surface. Since this kind of information was not taken at the remote tower, the comparison was made by using the results from the met tower transmissometers located at 5, 50 and 123 feet. Estimated RVR values were calculated using the transmittance data from all three transmissometers and from only the five-foot and the 123-foot transmissometers. An error was determined by comparing the two and three-point estimates with an RVR value calculated from the reading of the slant transmissometer. Figure 5-15 shows these results in bargraph form with the number of observations versus the error in RVR for each system. The three-point system shifts the population from larger to smaller error; however, the amount of improvement, never more than 10%, was felt to be on the borderline in justifying the additional complexity of the system. Caution must be exercised when extrapolating these results to other airports. Local effects frequently dominate the fog characteristics; however, it was decided that the two-point measurement system would be used for the further tests at NAFEC.

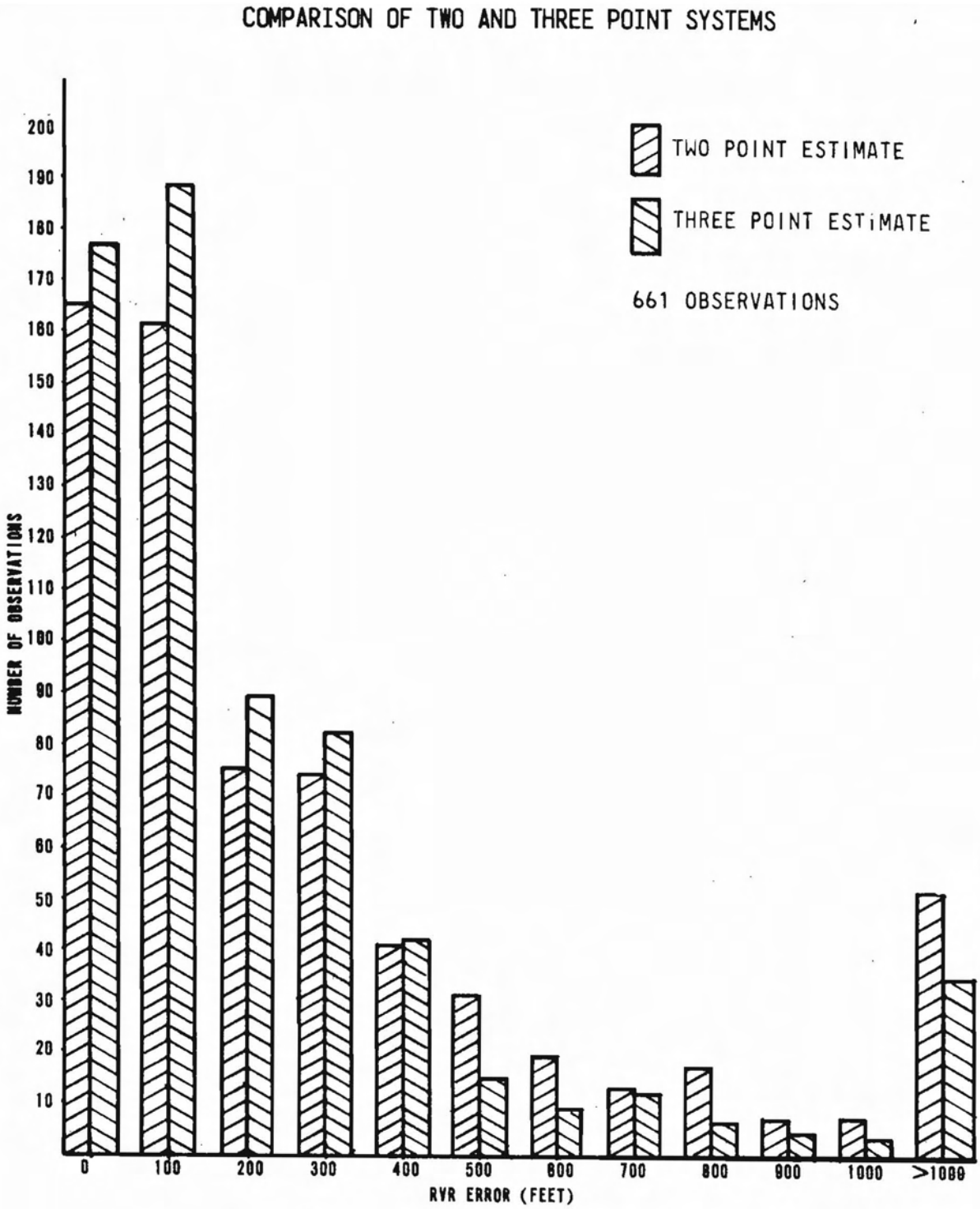
COMPARISON OF TWO AND THREE POINT SYSTEMS
TWO POINT ESTIMATE
THREE POINT ESTIMATE
661 OBSERVATIONS
NUMBER OF OBSERVATIONS
200
190
180
170
160
150
140
130
120
110
100
90
80
70
60
50
40
30
20
10
0
100
200
300
400
500
600
700
800
900
1000
>1000
RVR ERROR (FEET)

FIGURE 5-15

6. EVALUATION OF METHODS OF DETERMINING SLANT TRANSMITTANCE

One of the major objectives of the experiment at NAFEC was the collection of data which would allow a comparison of predictions of the present RVR system, the proposed system and the actual state of the atmosphere. For these comparisons, results from the transmissometers have been converted to RVR using Allard's law with light setting four and two mile-candle threshold illuminance. In all cases, illustrated visual range is rounded to the nearest 100 feet. The slant transmissometer provides a measure of the slant visual range from ground to 160 feet altitude and is the best description of the conditions which exist in the atmosphere. The comparisons examine how closely the present RVR system and the candidate system could predict the slant visual range at the met tower site. The candidate system consists of a transmissometer five feet above the surface and the FSM 95 feet above the surface. This system was located 1,500 feet from the met tower complex.

Comparison of Horizontal RVR and Slant Visual Range for Radiative Fogs

With the exception of one case, all of the fogs recorded after the installation of the mini-computer were primarily advective rather than radiative in character. When radiative fog occurred, fall and early winter, the only data recording systems operative were the transmissometer strip charts; however, exploration of relation between RVR and SVR would be incomplete without considering some of these cases.

Example 1

A fog occurred on 16 September 1972 lasting about three hours from 0300 to 0600. Figure 6-1 shows vertical transmission profiles at four times during the fog. The profiles are composed of data points

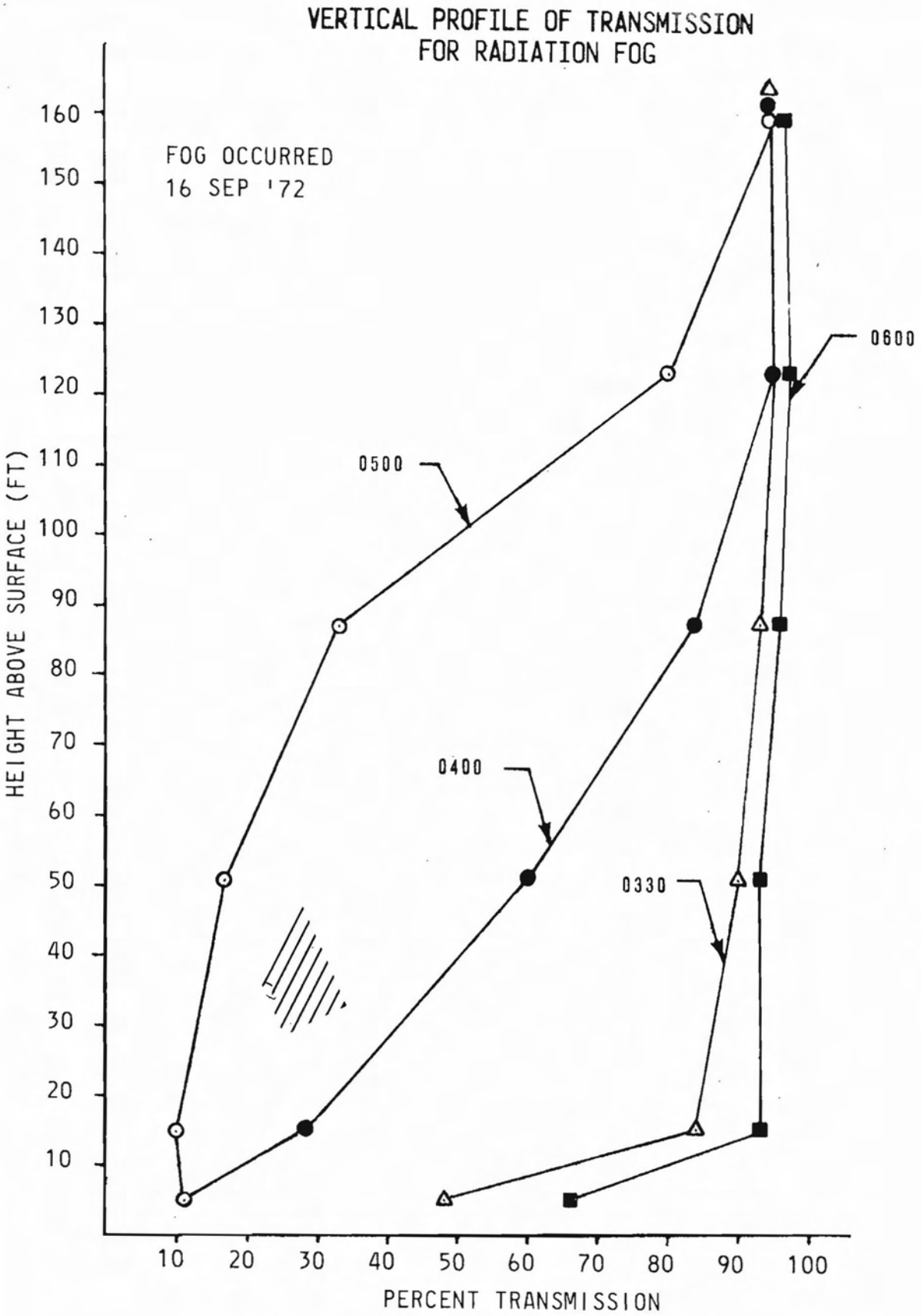
VERTICAL PROFILE OF TRANSMISSION
FOR RADIATION FOG
FOG OCCURRED
16 SEP '72
0600
0500
0400
0330
HEIGHT ABOVE SURFACE (FT)
160
150
140
130
120
110
100
90
80
70
60
50
40
30
20
10
10
20
30
40
50
60
70
80
90
100
PERCENT TRANSMISSION

Figure 6-1

at the six discrete levels on the towers joined by straight lines. The profiles indicate a substantial reduction in visibility occurred near the ground starting around 0330; the layer thickened and became more dense reaching its maximum obscuration at about 0500. From 0500 until 0600, the process very nearly reversed with clearing occurring aloft and more slowly at the surface. During the entire fog, the visibility reduction was primarily confined to the lowest 100 feet of the atmosphere.

Figure 6-2 shows the RVR and SVR records for the same period. RVR is found using the transmission measured at the 15-foot level; SVR is found using the slant transmissometer corrected to a 250-foot baseline. These curves indicate that RVR provides misleading information on the slant path transmission until about 0440; for the next forty minutes, the trends for the two instruments are the same but the values recorded are always significantly different. The best agreement existing exhibits a difference of 500 feet. The 15-foot level transmissometer is consistently conservative in its estimate of slant transmittance.

Example 2

These data were recorded on 26 January 1973. Similar characteristics to those in Example 1 are seen with even more dense conditions near the surface. The vertical transmission profiles, Figure 3-2, again illustrate that the restriction to visibility was primarily within the first 100 feet of the atmosphere. Figure 6-3 shows the comparison of the 15-foot and slant transmissometer converted to RVR. Again the RVR was alwyas a much more conservative estimate of visual range than that measured using the slant transmissometer. For several hours, the RVR was less than 1,200 feet, Category II minima at some airports, while the slant visual range was exhibiting rapid fluctuations but always well above the 1,200-foot level.

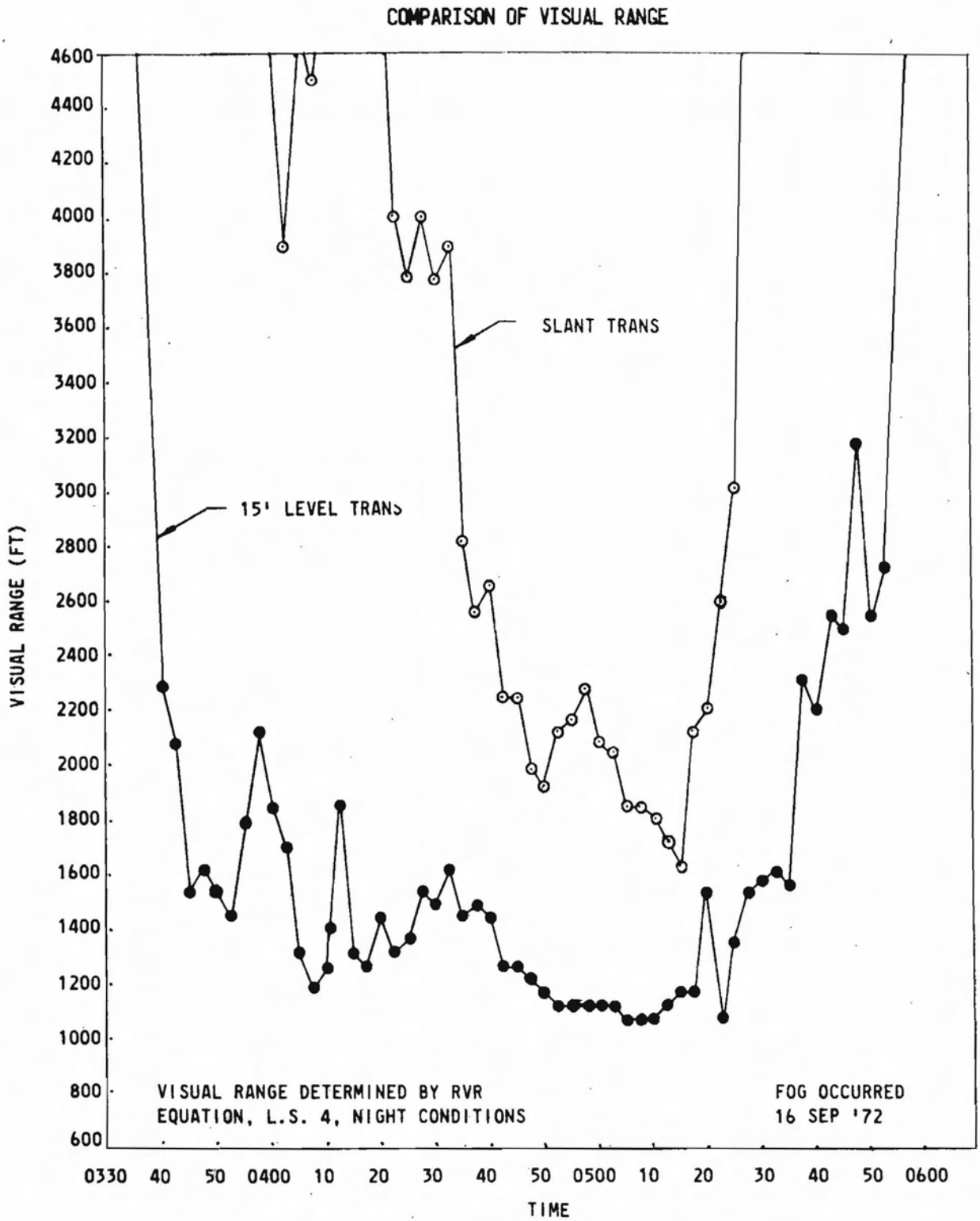
COMPARISON OF VISUAL RANGE
VISUAL RANGE (FT)
4600
4400
4200
4000
3800
3600
3400
3200
3000
2800
2600
2400
2200
2000
1800
1600
1400
1200
1000
800
600
SLANT TRANS
15' LEVEL TRANS
VISUAL RANGE DETERMINED BY RVR
EQUATION, L.S. 4, NIGHT CONDITIONS
FOG OCCURRED
16 SEP '72
0330
40
50
0400
10
20
30
40
50
0500
10
20
30
40
50
0600
TIME

Figure 6-2

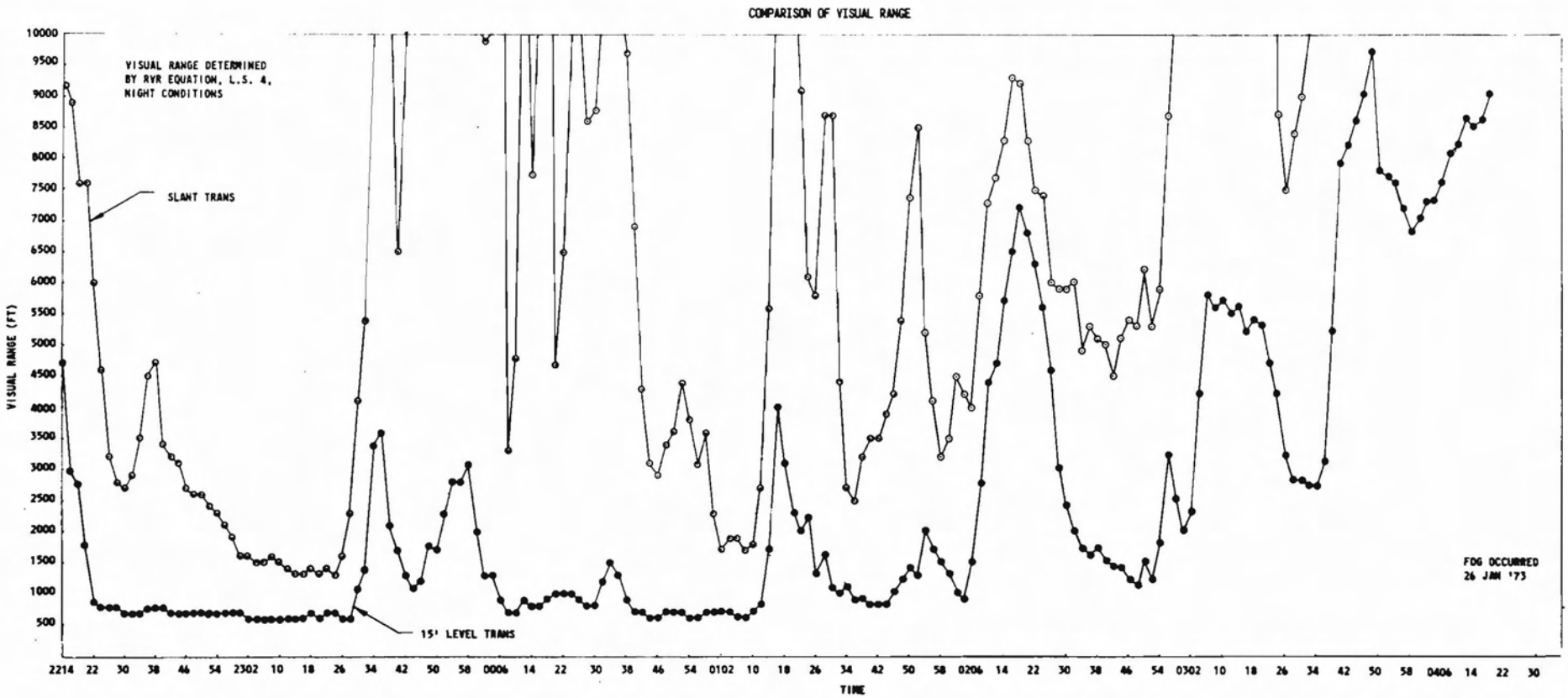
COMPARISON OF VISUAL RANGE
VISUAL RANGE DETERMINED BY RVR EQUATION, L.S. 4, NIGHT CONDITIONS
SLANT TRANS
15' LEVEL TRANS
FOG OCCURRED 26 JAN '73
VISUAL RANGE (FT)
10000
9500
9000
8500
8000
7500
7000
6500
6000
5500
5000
4500
4000
3500
3000
2500
2000
1500
1000
500
2214 22 30 38 46 54 2302 10 18 26 34 42 50 58 0006 14 22 30 38 46 54 0102 10 18 26 34 42 50 58 0206 14 22 30 38 46 54 0302 10 18 26 34 42 50 58 0406 14 22 30
TIME

Figure 6-3

Example 3

The results for this fog which occurred on 30 May 1973 differ from the other examples as the 15-foot transmissometer first gives a visual range greater than the slant transmissometer but later the visual range values reversed in magnitude. Figure 6-4 shows the RVR and SVR values for this fog.

Comparison of Horizontal and Slant Visual Range for Advective Fogs

After the proposed system was installed, no predominantly radiative fogs were recorded. The following comparisons will illustrate the visual ranges found from slant transmissometer, the 15-foot level transmissometer and the proposed system measurements of transmittance.

Example 1

The data recording commenced at about 0800 on 15 March 1973 for this predominantly advective fog. Figure 3-4 shows typical transmission profiles recorded. Those shown include several during the early phases when the fog density is increasing and several during the decay phases. Even in the early phases, the fog is very dense aloft. During dissipation, clearing occurs more rapidly at the surface than aloft. Figure 6-5 shows the corresponding visual ranges obtained by using the transmittance measurements in the RVR equation assuming night condition, light setting four. The results from the 15-foot level transmissometer are consistently higher than both the slant and the candidate system. The difference between the proposed system and the slant transmissometer during the steady state averages approximately 100 feet. During onset and dissipation, a much larger difference exists between these readings; however, this was anticipated due to their separation of about 1,500 feet. These differences occur for about ten minutes at the beginning and end of the fog.

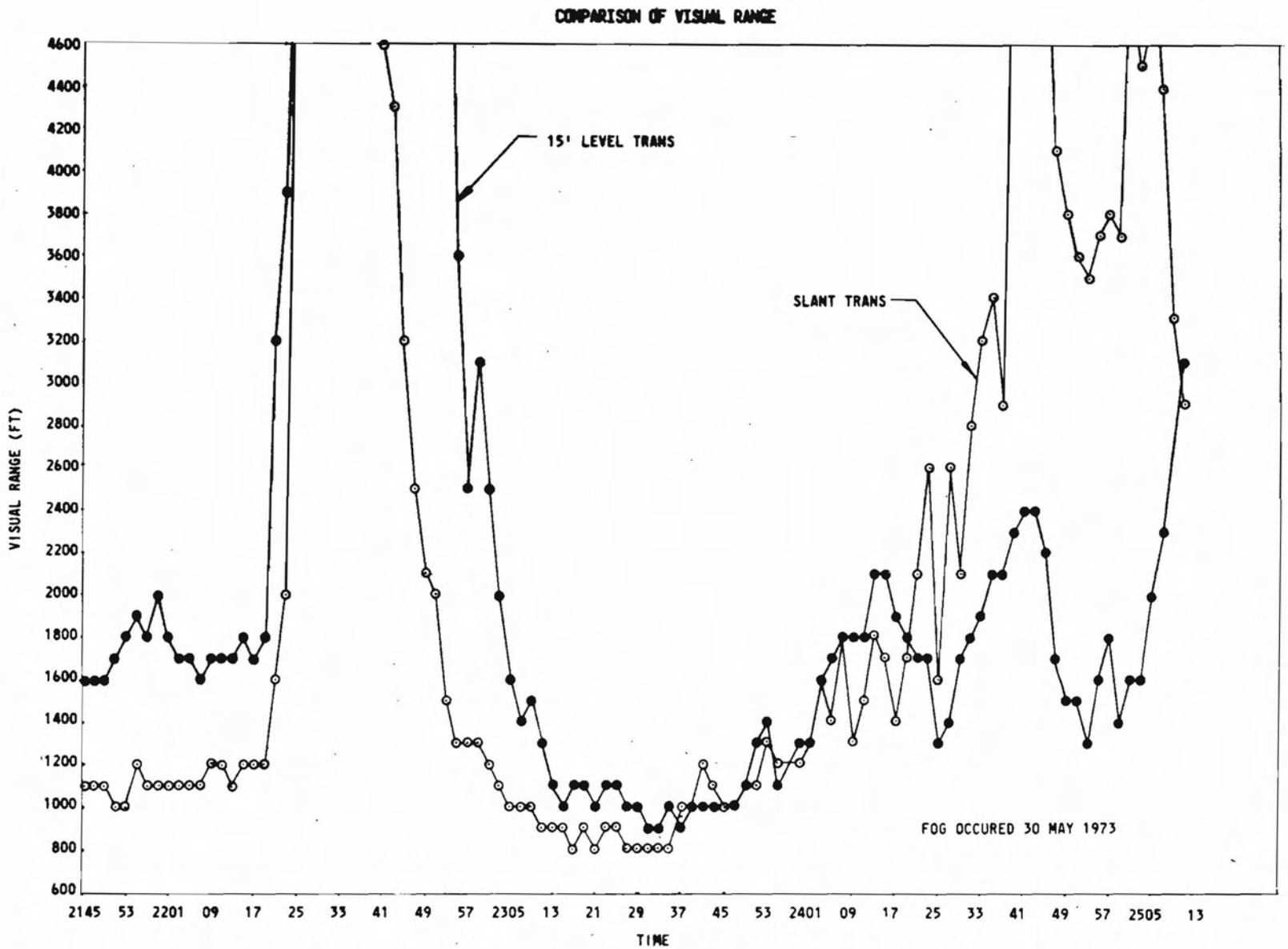
COMPARISON OF VISUAL RANGE
15' LEVEL TRANS
SLANT TRANS
FOG OCCURED 30 MAY 1973
VISUAL RANGE (FT)
4600
4400
4200
4000
3800
3600
3400
3200
3000
2800
2600
2400
2200
2000
1800
1600
1400
1200
1000
800
600
2145 53 2201 09 17 25 33 41 49 57 2305 13 21 29 37 45 53 2401 09 17 25 33 41 49 57 2505 13
TIME

Figure 6-4

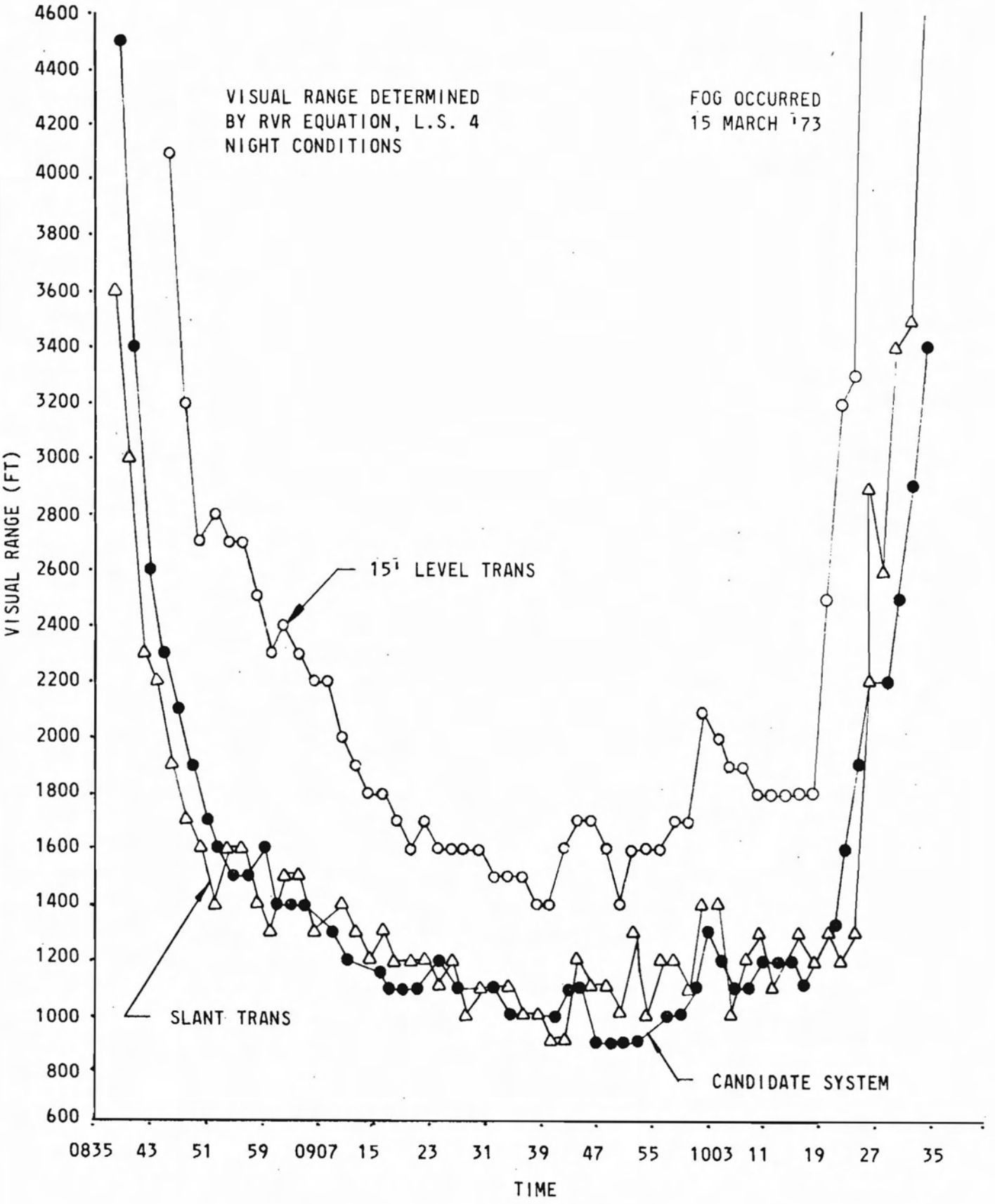
VISUAL RANGE DETERMINED
BY RVR EQUATION, L.S. 4
NIGHT CONDITIONS
FOG OCCURRED
15 MARCH '73
15' LEVEL TRANS
SLANT TRANS
CANDIDATE SYSTEM
VISUAL RANGE (FT)
4600
4400
4200
4000
3800
3600
3400
3200
3000
2800
2600
2400
2200
2000
1800
1600
1400
1200
1000
800
600
0835
43
51
59
0907
15
23
31
39
47
55
1003
11
19
27
35
TIME

Figure 6-5

Example 2

Two more occurrences of advective fogs which were recorded are presented in Figures 6-6 and 6-7. Figure 6-5 shows results for a fog occurring on 16 March 1973. Several vertical transmission profiles for this fog were shown in Figure 3-6. Their general shape does not differ greatly from those of Figure 3-4. Figure 6-7 includes results recorded on 26 March 1973. These data do not differ greatly from those shown in Example 1; the proposed system always shows much better agreement with the slant transmissometer than does the 15-foot level transmissometer.

Example 3

This incomplete record, Figure 6-8, is shown primarily because it is one of the relatively few records obtained. In the early stages of the fog, agreement between the proposed system and the slant transmissometer is not particularly good; however, it is in the formation when the separation between instruments probably accounts for this discrepancy. Similar discrepancies can occur during dissipation; however, they will be less frequent since dissipation can result from evaporation produced by radiative effects. The reading from the 15-foot transmissometer results in RVR's so large that they are off-scale on the graph. Unfortunately, the main portion of the record was lost to a malfunction of the recorder. Starting again at 0705, proposed system agrees well with the slant transmissometer.

In all these cases, the RVR calculated using the 15-foot level transmissometer was greater than that found with either the slant transmissometer or the candidate system. This consistency is an indication of the characteristic of the advective fogs, density increasing with altitude, and the fact that both the candidate system and the slant transmissometer provide data from levels higher than 15 feet.

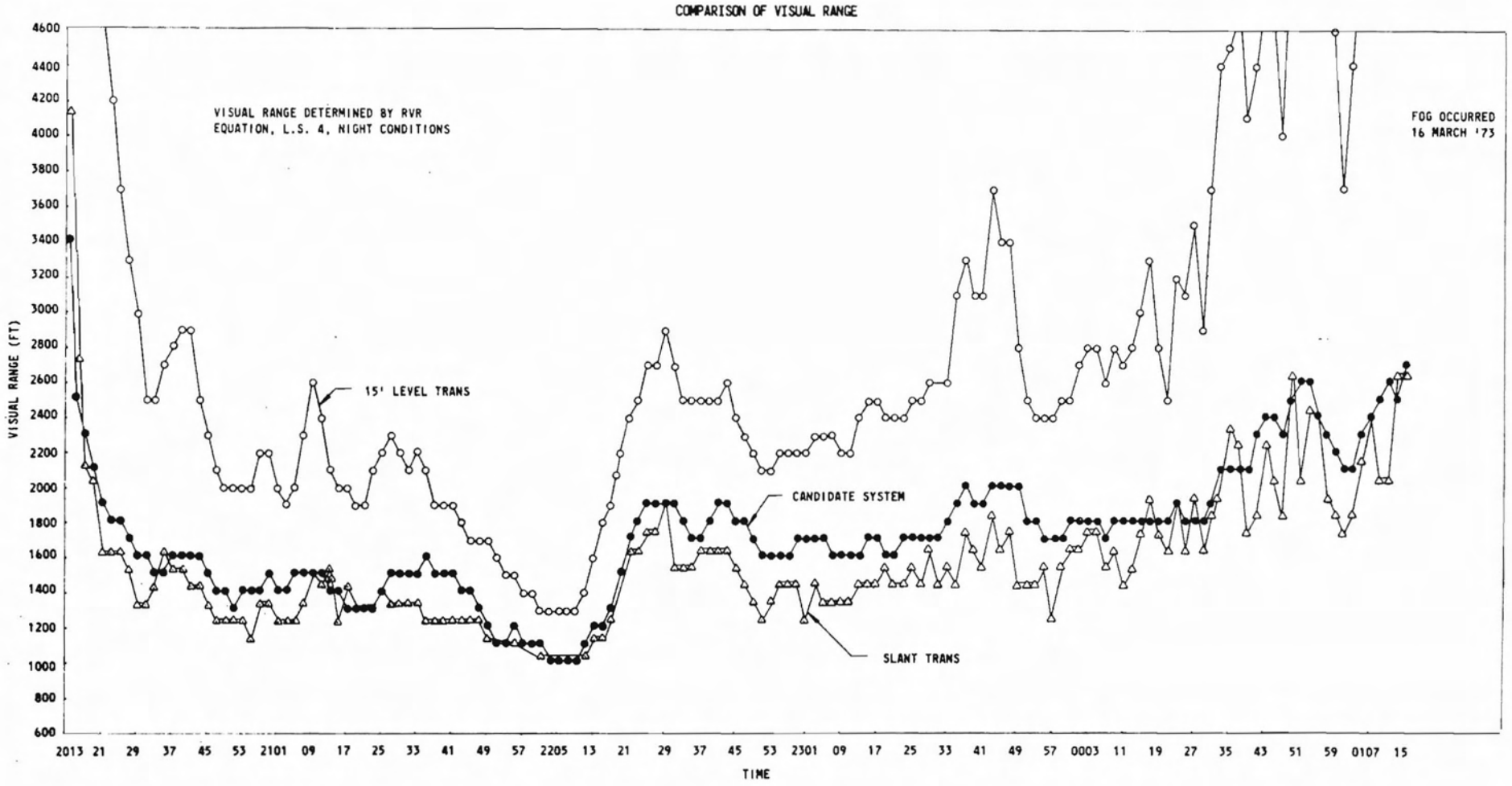
COMPARISON OF VISUAL RANGE
VISUAL RANGE DETERMINED BY RVR
EQUATION, L.S. 4, NIGHT CONDITIONS
FOG OCCURRED
16 MARCH '73
15' LEVEL TRANS
CANDIDATE SYSTEM
SLANT TRANS
VISUAL RANGE (FT)
4600
4400
4200
4000
3800
3600
3400
3200
3000
2800
2600
2400
2200
2000
1800
1600
1400
1200
1000
800
600
2013 21 29 37 45 53 2101 09 17 25 33 41 49 57 2205 13 21 29 37 45 53 2301 09 17 25 33 41 49 57 0003 11 19 27 35 43 51 59 0107 15
TIME

Figure 6-6

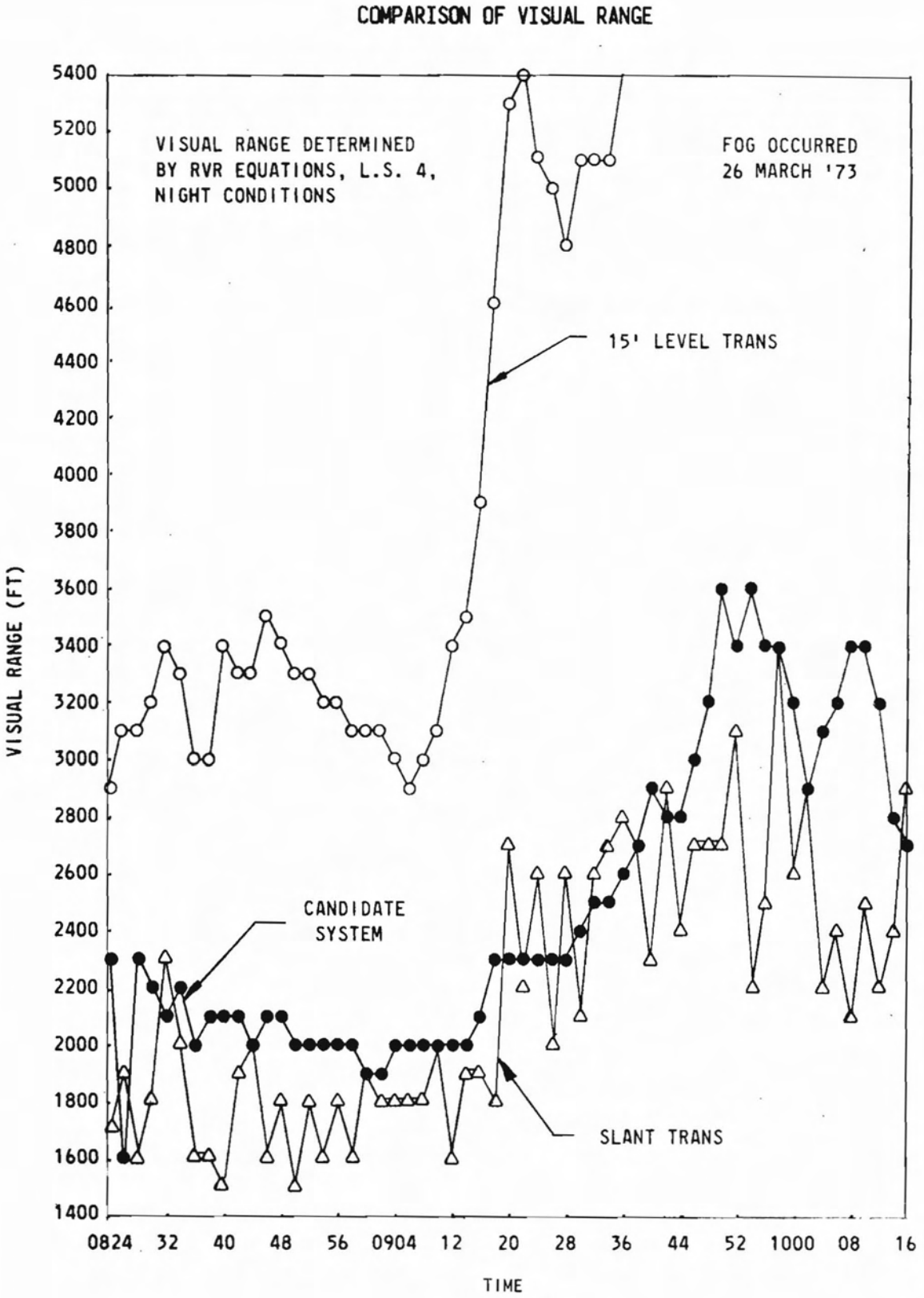
COMPARISON OF VISUAL RANGE
VISUAL RANGE DETERMINED
BY RVR EQUATIONS, L.S. 4,
NIGHT CONDITIONS
FOG OCCURRED
26 MARCH '73
15' LEVEL TRANS
CANDIDATE
SYSTEM
SLANT TRANS
VISUAL RANGE (FT)
5400
5200
5000
4800
4600
4400
4200
4000
3800
3600
3400
3200
3000
2800
2600
2400
2200
2000
1800
1600
1400
0824
32
40
48
56
0904
12
20
28
36
44
52
1000
08
16
TIME

FIGURE 6-7

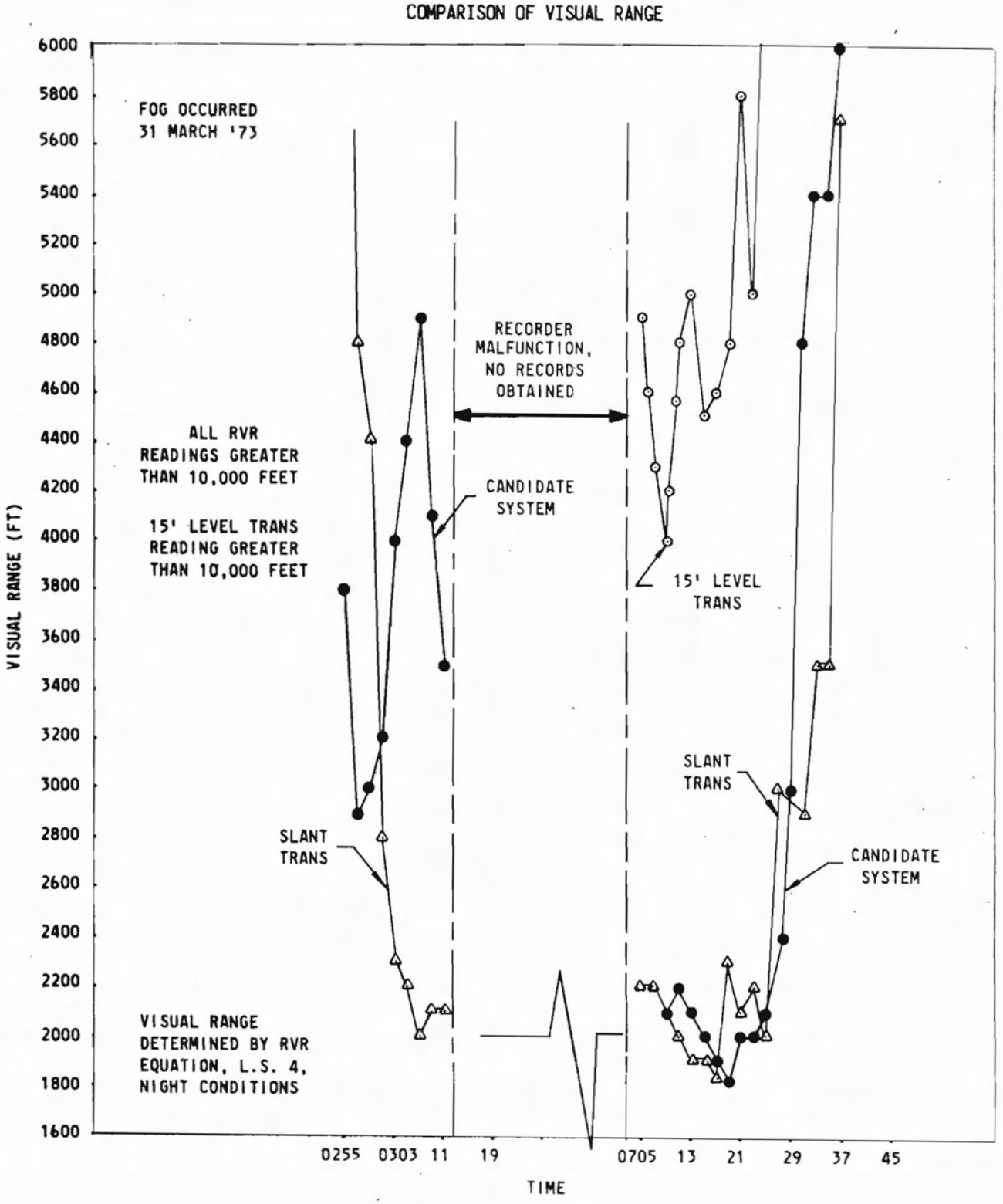
COMPARISON OF VISUAL RANGE
FOG OCCURRED
31 MARCH '73
RECORDER
MALFUNCTION,
NO RECORDS
OBTAINED
ALL RVR
READINGS GREATER
THAN 10,000 FEET
15' LEVEL TRANS
READING GREATER
THAN 10,000 FEET
CANDIDATE
SYSTEM
15' LEVEL
TRANS
SLANT
TRANS
SLANT
TRANS
CANDIDATE
SYSTEM
VISUAL RANGE
DETERMINED BY RVR
EQUATION, L.S. 4,
NIGHT CONDITIONS
VISUAL RANGE (FT)
6000
5800
5600
5400
5200
5000
4800
4600
4400
4200
4000
3800
3600
3400
3200
3000
2800
2600
2400
2200
2000
1800
1600
0255
0303
11
19
0705
13
21
29
37
45
TIME

Figure 6-8

For atmospheric conditions such that the slant visual range, as measured with the slant transmissometer, is 4,000 feet or less, the candidate system gave a good estimate of the slant visual range. Notable exceptions to this exist just at the onset or dissipation of advective fogs. The 1,500 feet separating the system from the slant transmissometer account for these discrepancies.

The data recorded at NAFEC, although far from exhaustive, indicates that the RVR as presently used provides only a very approximate prediction of the visual range that exists from the glide slope to the runway. In contrast, the system, employing a forward scatter meter on a 100-foot tower, a transmissometer five feet above the surface and luminance meters at 50 and 100 feet, yields reasonable estimates for the slant visual range.

7. LUMINANCE MEASUREMENTS AND ANALYSIS

NAFEC Measurements

The previous sections of this report have described atmospheric transmission data instrumentation and analysis on this data. Sections 7 and 8 will present analyses of the effect of adaptation luminance and describe the SVR/ALCH algorithm in terms of atmospheric and psychophysical parameters.

Daytime luminance meters were located at 15, 50, 100 and 150 feet at NAFEC. They were pointed 5° below horizontal at approximately 125° clockwise from true north. This particular aiming direction was chosen to simulate the pilot's direction of look on approach at NAFEC. Illuminance meters were located at five and 150 feet near and on the scaffold tower.

The luminance meters were installed to monitor the variation of luminance with time for different fogs. The luminance readings were to be compared with theoretical calculations which were entered into the SVR/ALCH system.

Figures 7-1 through 7-4 show how luminance changes with time. The gradual increase of luminance with time could be the result of increasing illumination on the fog or a decrease in fog density. As can be seen from Figures 7-1 through 7-4, luminance increases as altitude increases. This is the result of the decrease in optical depth that the sun's rays must penetrate before being scattered upward.

Figures 7-5 through 7-8 represent the absorption and scattering of light over a 250-foot baseline. In comparing Figure 7-2 with Figure 7-6 during the time interval 1143 - 1413, one can see an increase of luminance with a decrease in $1-T_{250}$. This can be attributed

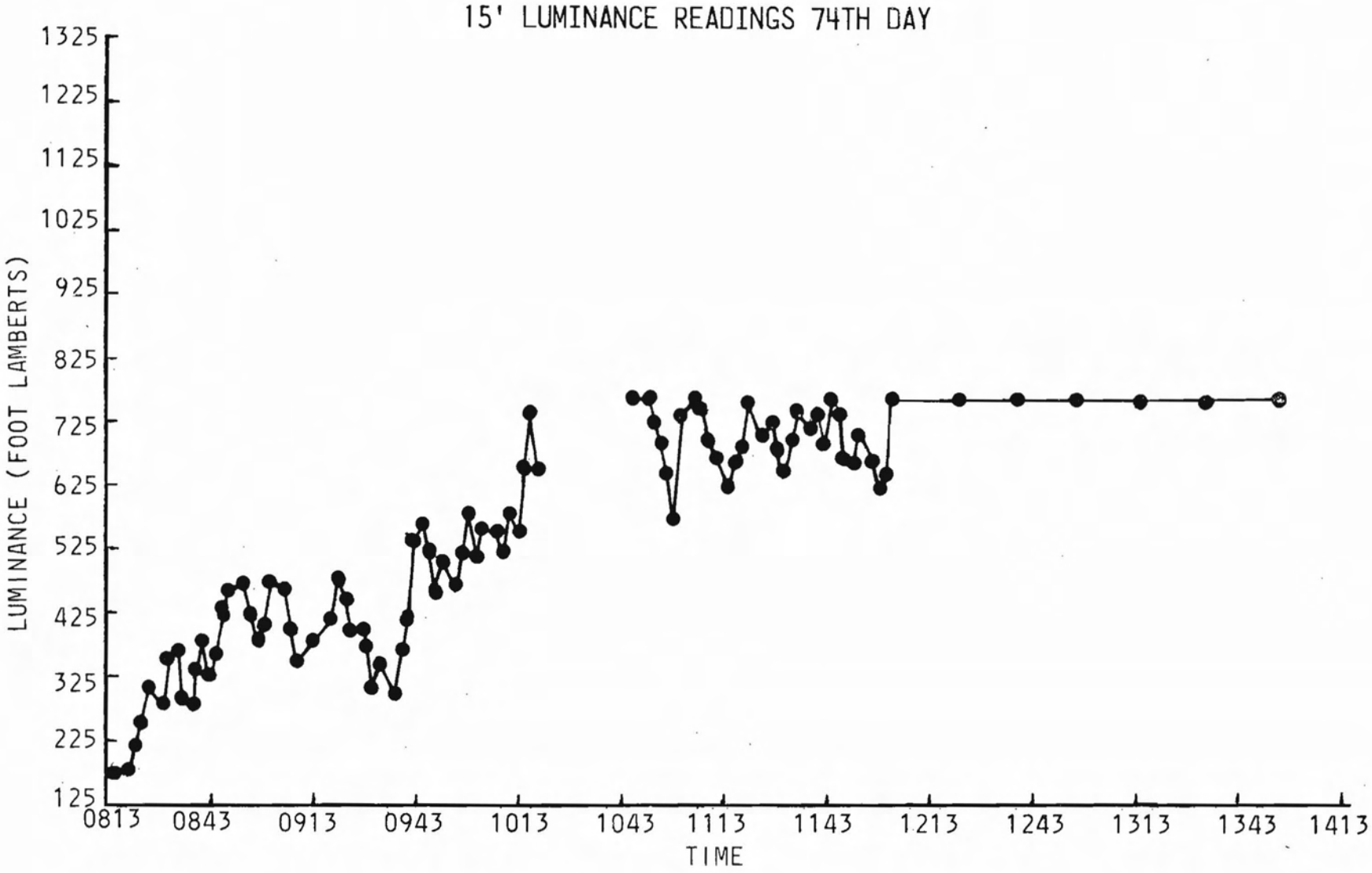
15' LUMINANCE READINGS 74TH DAY
LUMINANCE (FOOT LAMBERTS)
1325
1225
1125
1025
925
825
725
625
525
425
325
225
125
0813
0843
0913
0943
1013
1043
1113
1143
1213
1243
1313
1343
1413
TIME

Figure 7-1

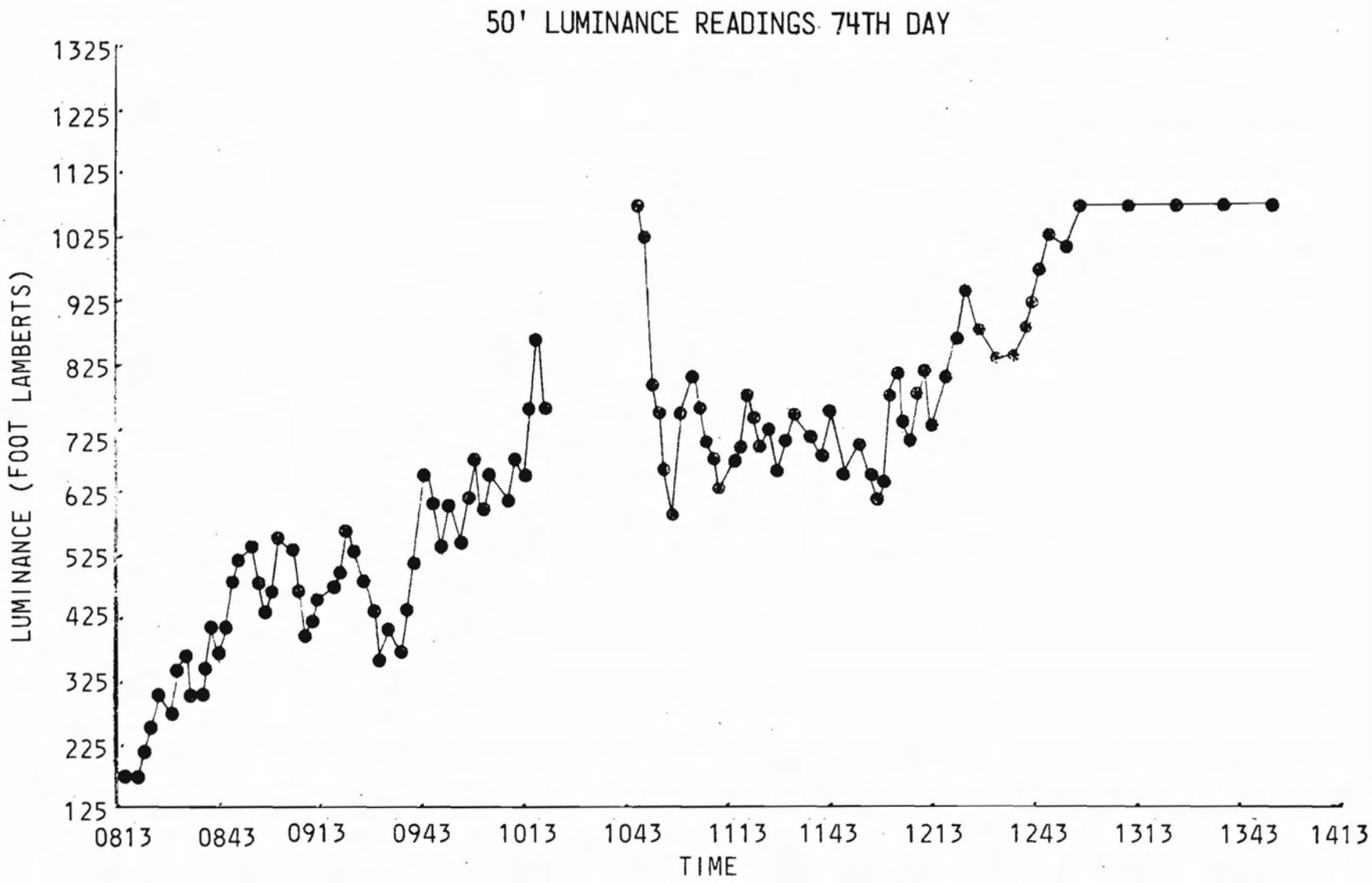
50' LUMINANCE READINGS 74TH DAY
LUMINANCE (FOOT LAMBERTS)
1325
1225
1125
1025
925
825
725
625
525
425
325
225
125
0813
0843
0913
0943
1013
1043
1113
1143
1213
1243
1313
1343
1413
TIME

Figure 7-2

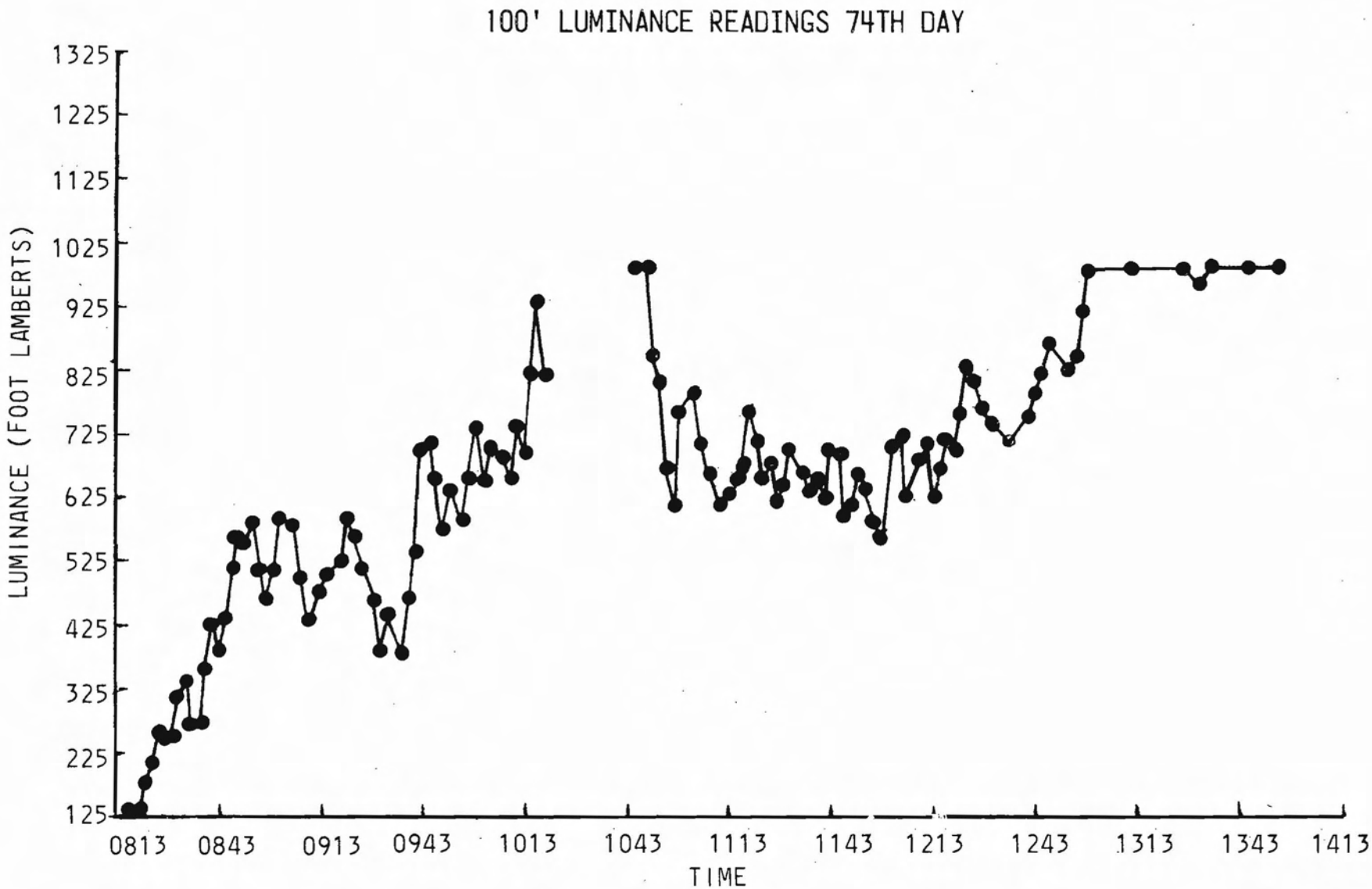
100' LUMINANCE READINGS 74TH DAY
LUMINANCE (FOOT LAMBERTS)
1325
1225
1125
1025
925
825
725
625
525
425
325
225
125
0813
0843
0913
0943
1013
1043
1113
1143
1213
1243
1313
1343
1413
TIME

Figure 7-3

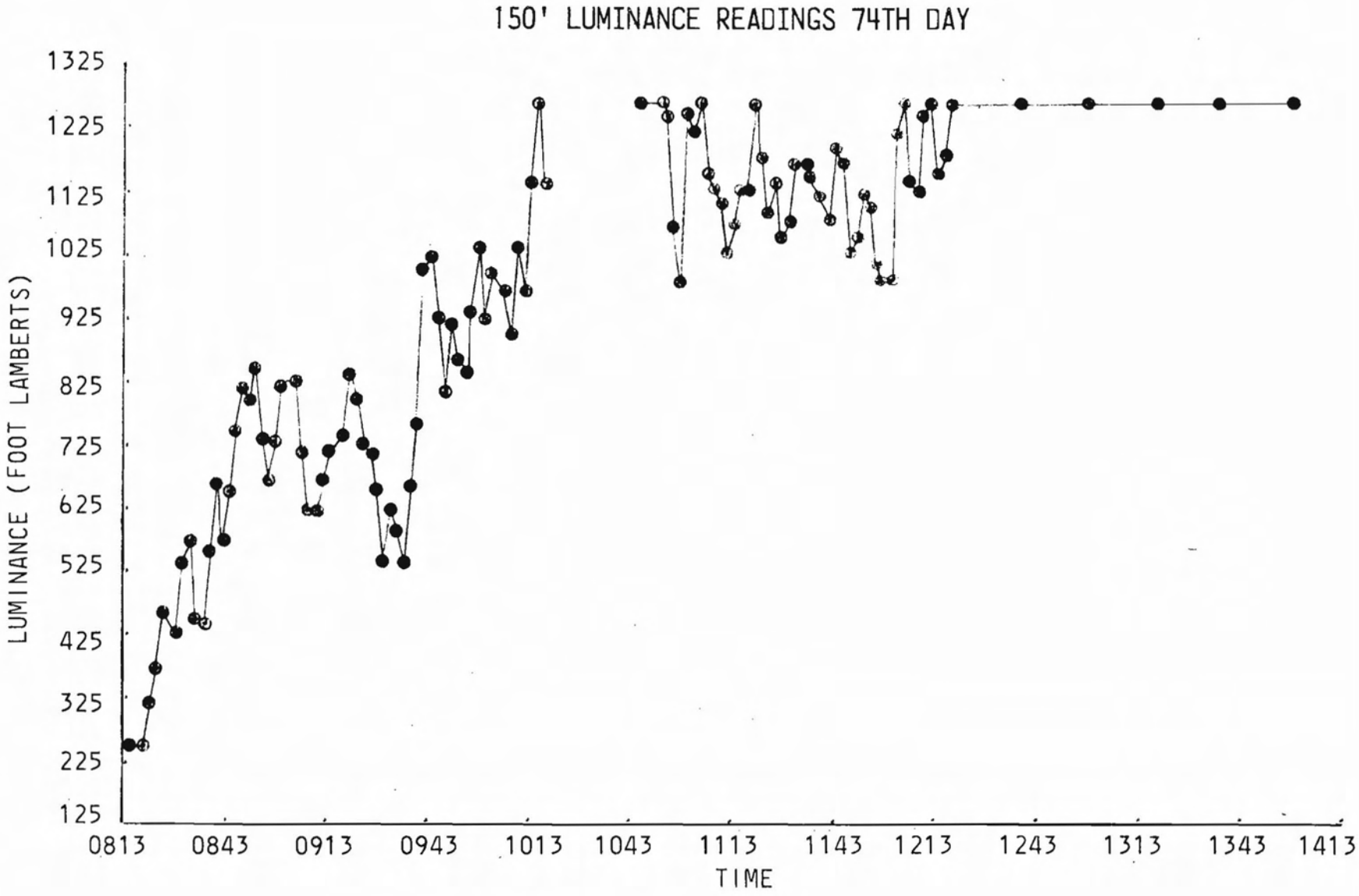
150' LUMINANCE READINGS 74TH DAY
LUMINANCE (FOOT LAMBERTS)
1325
1225
1125
1025
925
825
725
625
525
425
325
225
125
0813
0843
0913
0943
1013
1043
1113
1143
1213
1243
1313
1343
1413
TIME

Figure 7-4

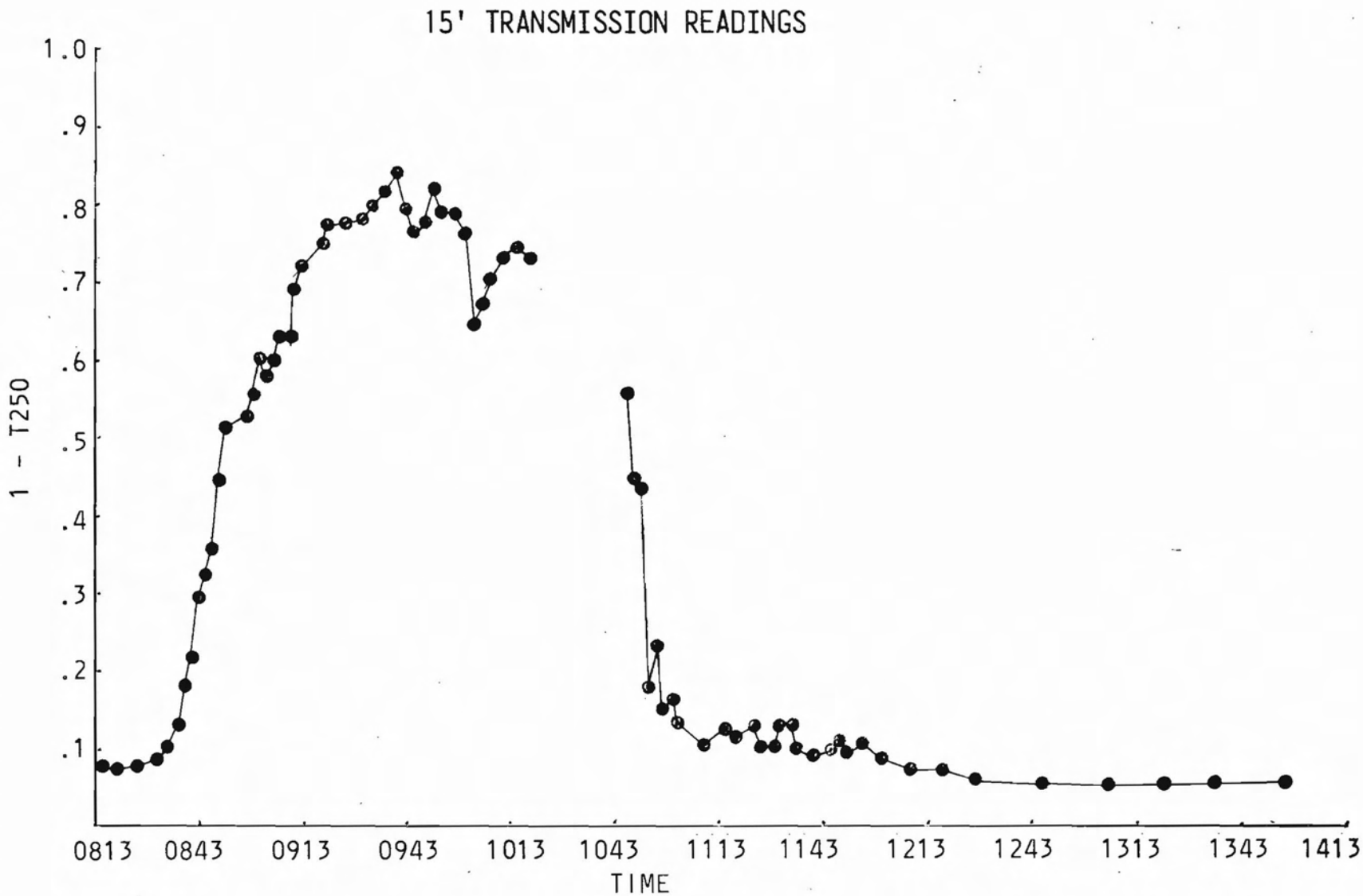
15' TRANSMISSION READINGS
1 - T250
1.0
.9
.8
.7
.6
.5
.4
.3
.2
.1
0813
0843
0913
0943
1013
1043
1113
1143
1213
1243
1313
1343
1413
TIME

Figure 7-5

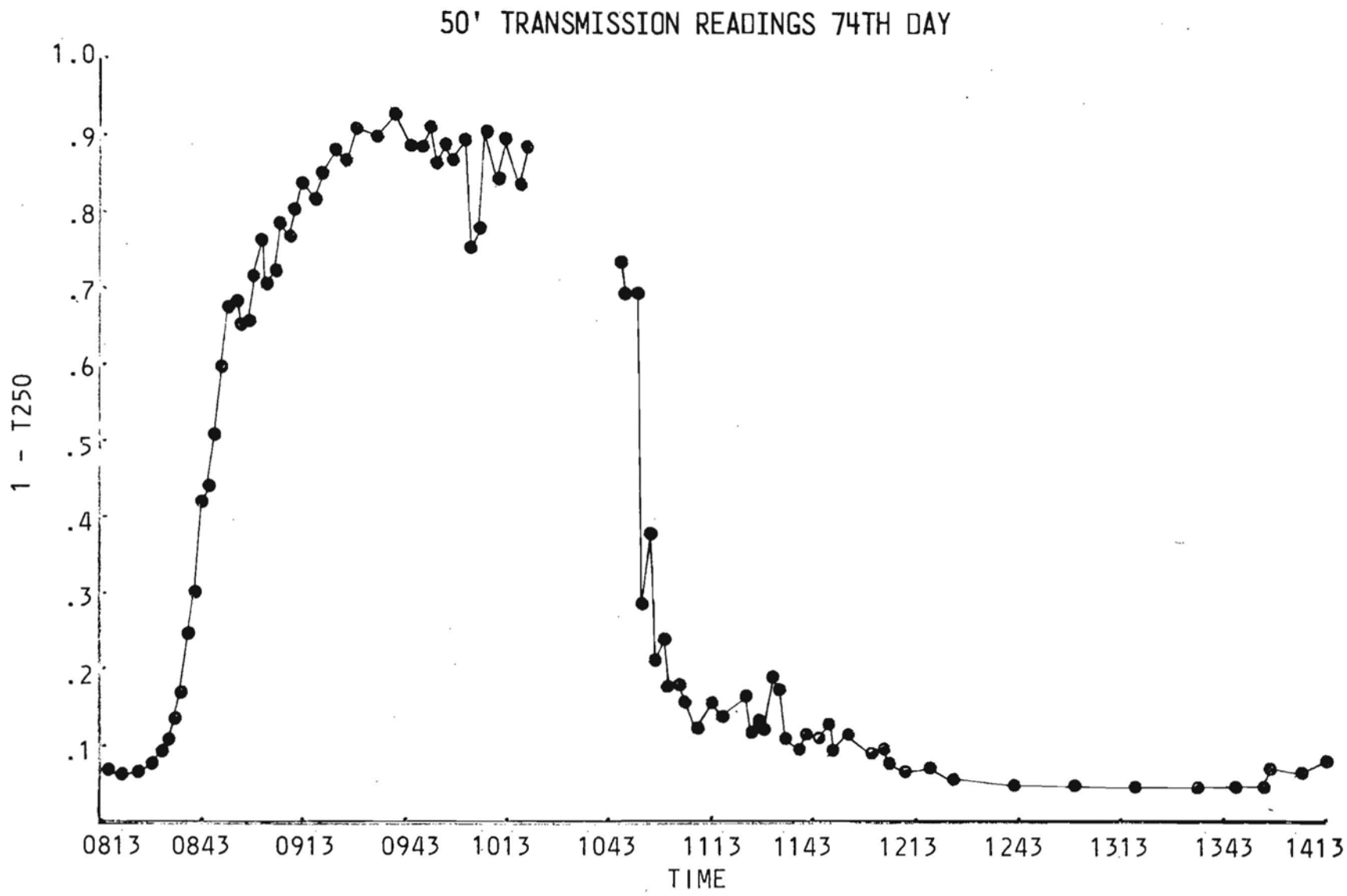
50' TRANSMISSION READINGS 74TH DAY
1 - T250
1.0
.9
.8
.7
.6
.5
.4
.3
.2
.1
0813
0843
0913
0943
1013
1043
1113
1143
1213
1243
1313
1343
1413
TIME

Figure 7-6

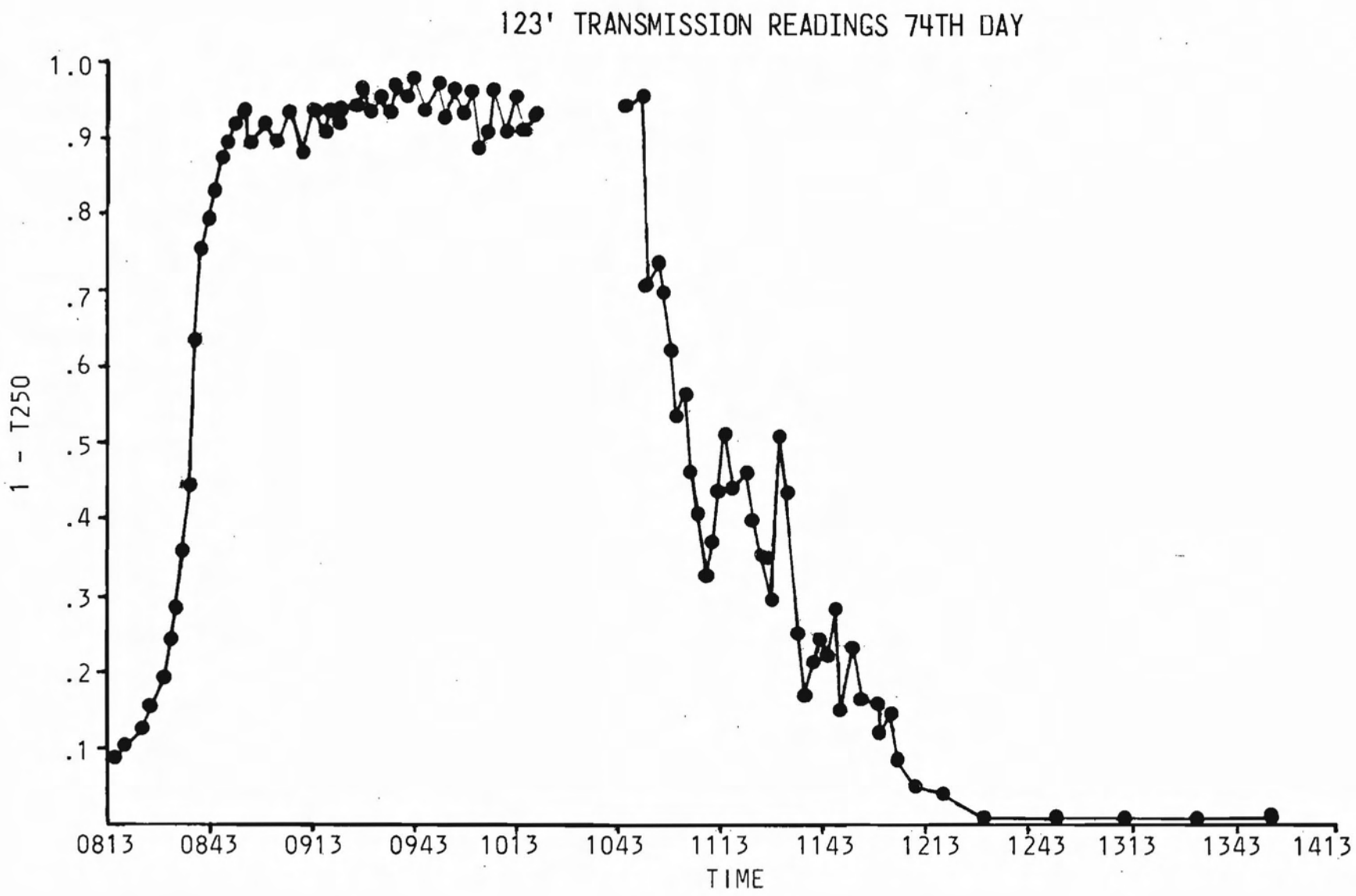
123' TRANSMISSION READINGS 74TH DAY
1 - T250
1.0
.9
.8
.7
.6
.5
.4
.3
.2
.1
0813
0843
0913
0943
1013
1043
1113
1143
1213
1243
1313
1343
1413
TIME

Figure 7-7

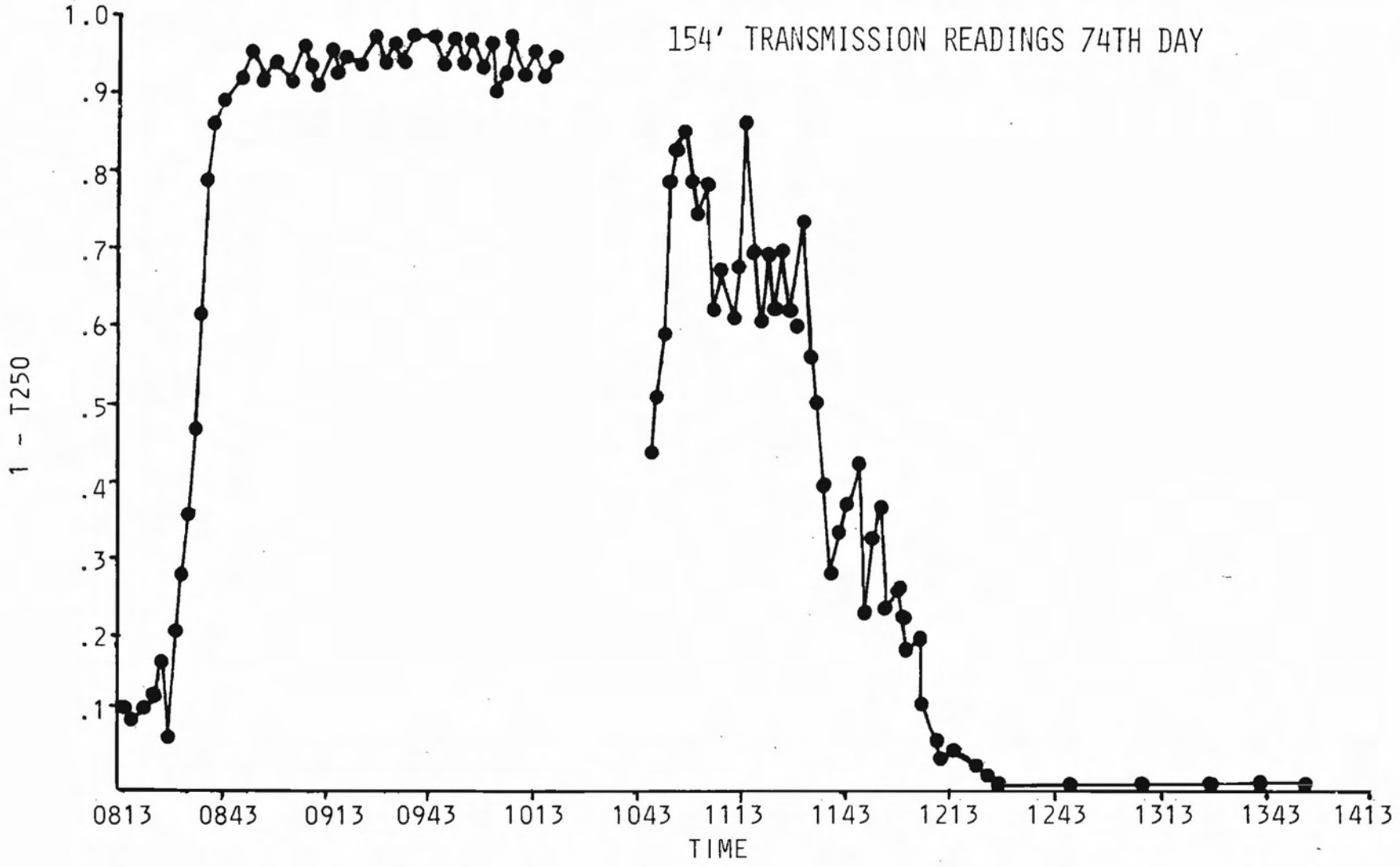
154' TRANSMISSION READINGS 74TH DAY
1 - T250
1.0
.9
.8
.7
.6
.5
.4
.3
.2
.1
0813
0843
0913
0943
1013
1043
1113
1143
1213
1243
1313
1343
1413
TIME

Figure 7-8

to an increase of illuminance on the ground and thus an increase in ground luminance. In fact, the time interval between 1143-1413 of Figure 7-2 probably represents mainly ground luminance and not fog luminance. The voids in the graph represent missing data.

Because of the low luminance levels of Figures 7-1 through 7-4, it is strongly suspected that the condition of the sky above the fogs was overcast, or the fogs continued to an altitude well above 150 feet. Luminance values well above 1,000 ft-lamberts are to be expected when the sky is clear above the fog and when the luminance meter is relatively close to the top of the fog. For this reason and since the present luminance meters at 15, 50, 100 and 150 feet have saturation points at 760, 1,000, 1,000 and 1,260 respectively, future luminance meters will range from one ft-lambert to 3,000 ft-lamberts.

In evaluating the effect of measuring luminance, the following analysis was performed. The slant transmissometer readings were used in computing the extinction coefficient. The 150-foot luminance meter readings were used in computing SVR by determining threshold illuminance (see Section 8) and then applying Allard's or Koschmieder's law to yield an SVR. SVR was also calculated using the 1,000 mile-candles as the illuminance threshold. A comparison was then made and the results are shown in Figure 7-9. As can be seen, the percent difference is not very great. Figure 7-10 gives the percent difference frequency distribution for Figure 7-9 and the majority of daytime fogs sampled at NAFEC. As can be seen from Figure 7-10, most of the errors fall in the 5 - 15% range.

Reliable data were not obtained from the zero and 150-foot illuminance meters at NAFEC. They were not environmentally hardened to withstand the weather at NAFEC. It was planned to try to correlate illuminance data with optical depth of the fog (as will be discussed later), but since there was no data available, this could not be done.

EFFECT OF THRESHOLD ILLUMINANCE ON SVR

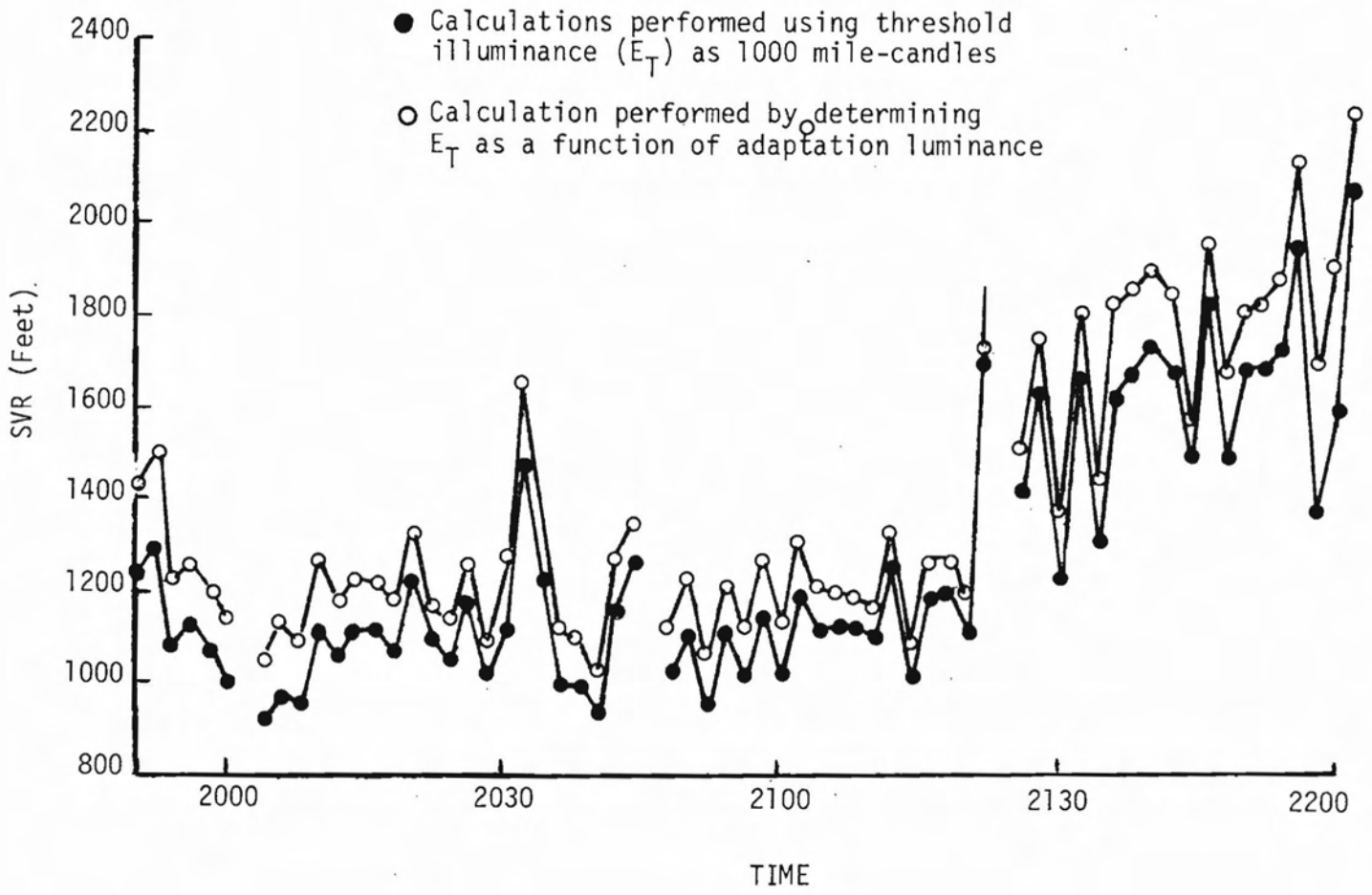

FIGURE 7-9

FREQUENCY DISTRIBUTION OF
SVR PERCENT ERRORS

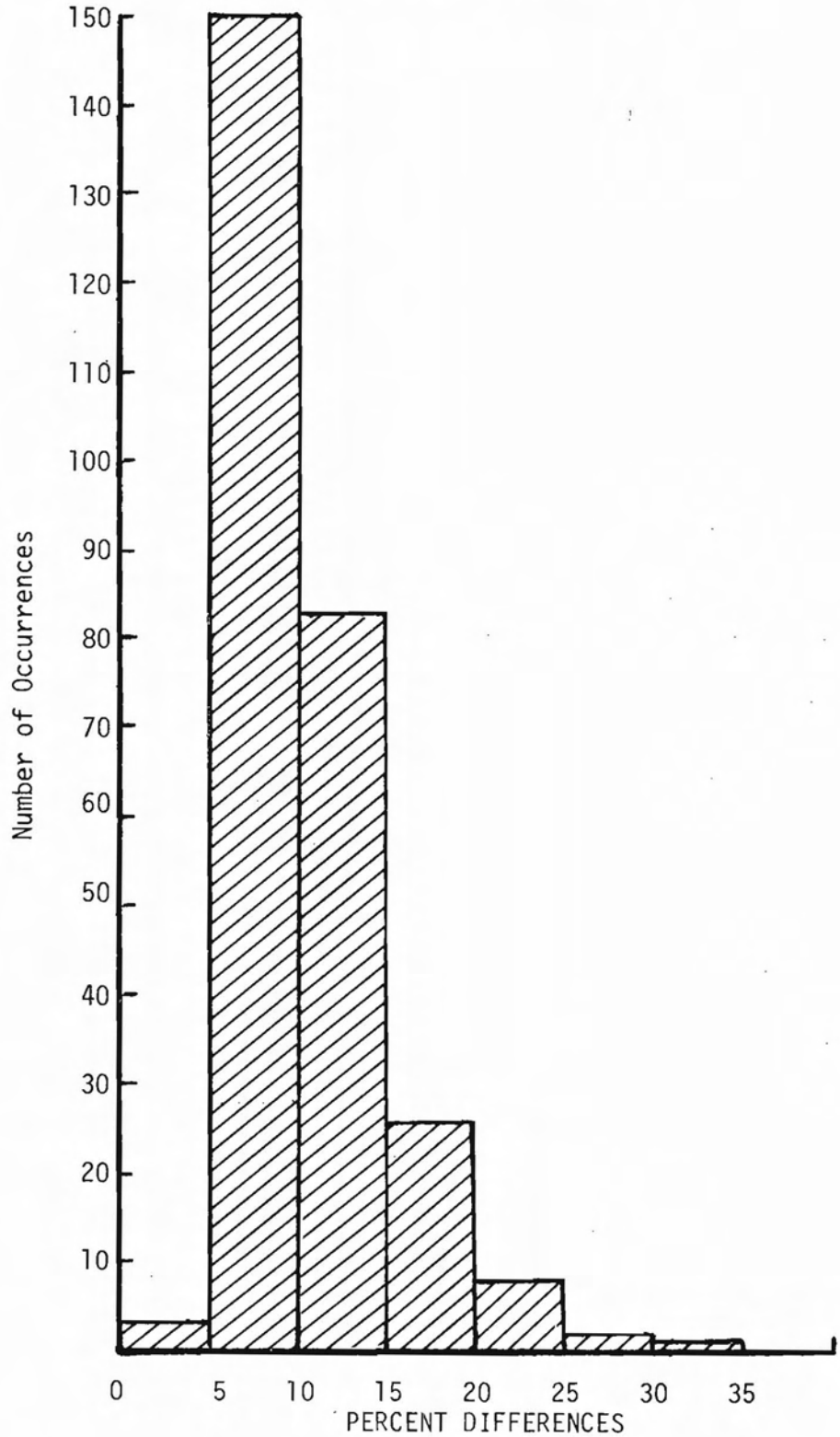

FIGURE 7-10

Determination of Background Luminance

Under daytime conditions, one of the inputs into the proposed SVR/ALCH system is the adaptation luminance of the pilot's eye. An ideal way of obtaining a value for this variable would be to measure it from inside the cockpit. However, due to logistics, this method is not feasible. Therefore, it is necessary to formulate a method of using physical measurements on or near the ground to predict the pilot's background luminance. The approach taken was the performance of a sensitivity study of the variables which determine fog luminance in reduced visibility conditions. The effect of fog parameters was evaluated using a modified radiative transfer computer program developed by Dr. Kattawar of Texas A&M University (Plass, Kattawar and Catchings, February 1973; and Kattawar, Plass and Catchings, May 1973).

Computer Program Description

The program assumes an atmosphere bounded by two infinite parallel planes. The atmosphere can be subdivided into two homogeneous layers, the top layer consisting of Rayleigh scattering and the bottom layer consisting of Mie scattering. The inputs into the program are the scattering phase functions of the Rayleigh and Mie layers, optical depth of Rayleigh and Mie layers, the solar and receiver zenith angles and the azimuth angle between sun and receiver. The solar and receiver angles range from 0° to near 90°. The azimuth angles between the sun and receiver range from 0° to 180° (see Figure 7-24).

The output of the program is the luminance in various directions for various sun incident angles and receiver positions within the atmosphere.

A typical example which was executed by the program had the following for inputs and outputs. The Mie layer had an optical depth of 8 (extinction coefficient times vertical depth = 8) with the Rayleigh layer possessing an optical depth of .098. Twenty-one sun zenith angles and nine azimuth angles were input into the program. The output consisted of luminances for each combination of sun zenith and azimuth angles, and at 10 equally spaced positions within the lower layer. Therefore, a spatial luminance pattern was obtained at each receiver altitude for each of the 21 solar zenith angles. In addition, the upward and downward diffuse illuminances were obtained at each of these combinations.

Analysis of Computer Generated Luminance Data

In using the radiative transfer program, the parameters which determine fog luminance were assumed to be: the total optical depth of the fog; the optical depth above the pilot; the position of the sun relative to the pilot's direction of look; the scattering phase function of the fog; the reflectivity of the ground and condition of the sky aloft (overcast or clear). The scattering function of the fog was assumed to be that defined by Deirmendjian as a haze M with a wavelength of .55 micron. Figure 7-11 shows the haze M scattering function as well as the Eldridge 48 scattering function, which was used in much of the analysis performed in Phase I (Lohkamp *et al.*, 1972). The differences in the curves can be attributed to the different particle size distributions from which the curves were derived. Deirmendjian's haze M function was used in the radiative transfer computer program because of the analytical representation of the haze M particle size distribution (Deirmendjian, 1969). Extensive modification of the computer program would have been required to include Eldridge 48 into the program. Furthermore, after comparing Eldridge and Deirmendjian's scattering functions in Figure 7-11, the differences between the curves seemed minimal.

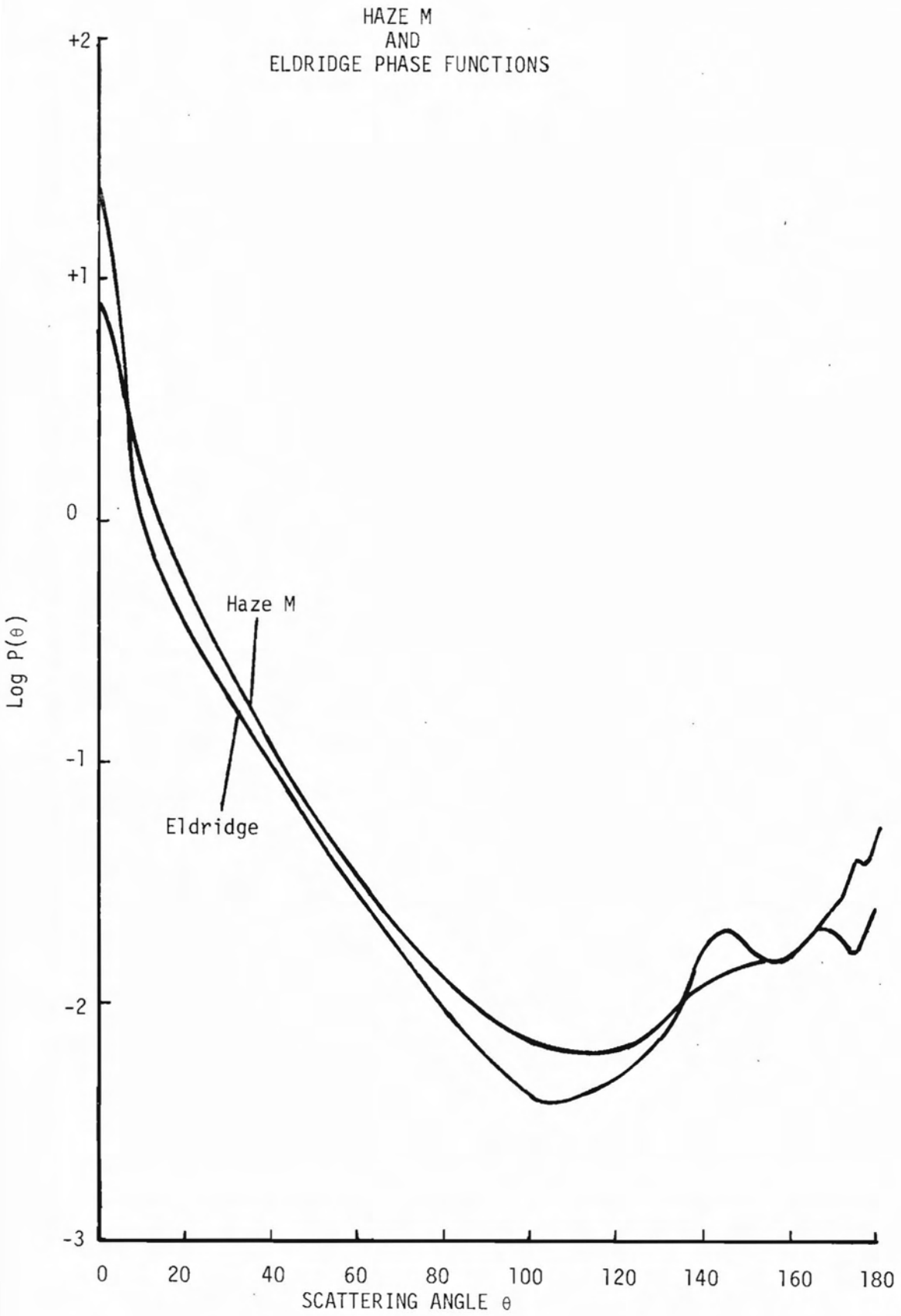
HAZE M
AND
ELDRIDGE PHASE FUNCTIONS
+2
+1
0
-1
-2
-3
Log P(θ)
Haze M
Eldridge
0
20
40
60
80
100
120
140
160
180
SCATTERING ANGLE θ

FIGURE 7-11

Four optical depths for fogs were run on the computer (.5, 2, 4, 8). Ground reflectivities of .05, .1 and .2 were run on the computer program. Concrete has a reflectivity ranging from .05-.1 over the wavelength band .4-.7 microns. A confierous environment has a reflectivity ranging from .05-.2 over the wavelength band of .4-.7 microns. Water reflectivity ranges from .05-.12 over the wavelength of .4-.7 microns. Therefore, it was decided that a reflectivity in the .05-.2 range would be fairly representative of the backgrounds encountered. The condition of the sky aloft was considered as clear with only Rayleigh scattering occurring above the fog layer. Solar zenith angles included 0°, 31°, 57°, 66° and 79°. The azimuth angles between sun and receiver were 0°, 22.5°, 45°, 67.5°, 90°, 112.5°, 135°, 157.5° and 180°. The receiver zenith angle considered was 84°.

Figure 7-24 shows the pilot-solar geometry. Plane CDE represents the principal plane of the sun. Plane ABC represents the plane containing the pilot's direction of look. The azimuth angle is the angle $\leq$180° defined by the intersection of the two planes. The solar zenith angle is defined to be $\leq$90° and is measured between a vertical line and the line defined by the solar rays.

The curve displacements on each of the Figures 7-12 through 7-15 represents the luminance differences for the zenith angles given. The effect of zenith angle becomes less important at the top of the fog. Generally speaking, the smaller the zenith angle, the larger the luminance, except near the top of the fog when the azimuth is 0° and 45°. Noting the haze M phase function of Figure 7-11, one observes a decrease in $P(\theta)$ with an increase in scattering angle for scattering angles between 0° and 90°. The pilot-solar azimuth angle of 0° and 45° correspondsto the pilot flying into the quadrant of the sun. A pilot-solar azimuth angle (Figure 7-24) of 0° and 45° would define a scattering angle between 0° and 90°. Therefore, as the sun zenith angle decreases from 79° to 31° (sun

EFFECT OF DIFFERENT SOLAR ZENITH ANGLES

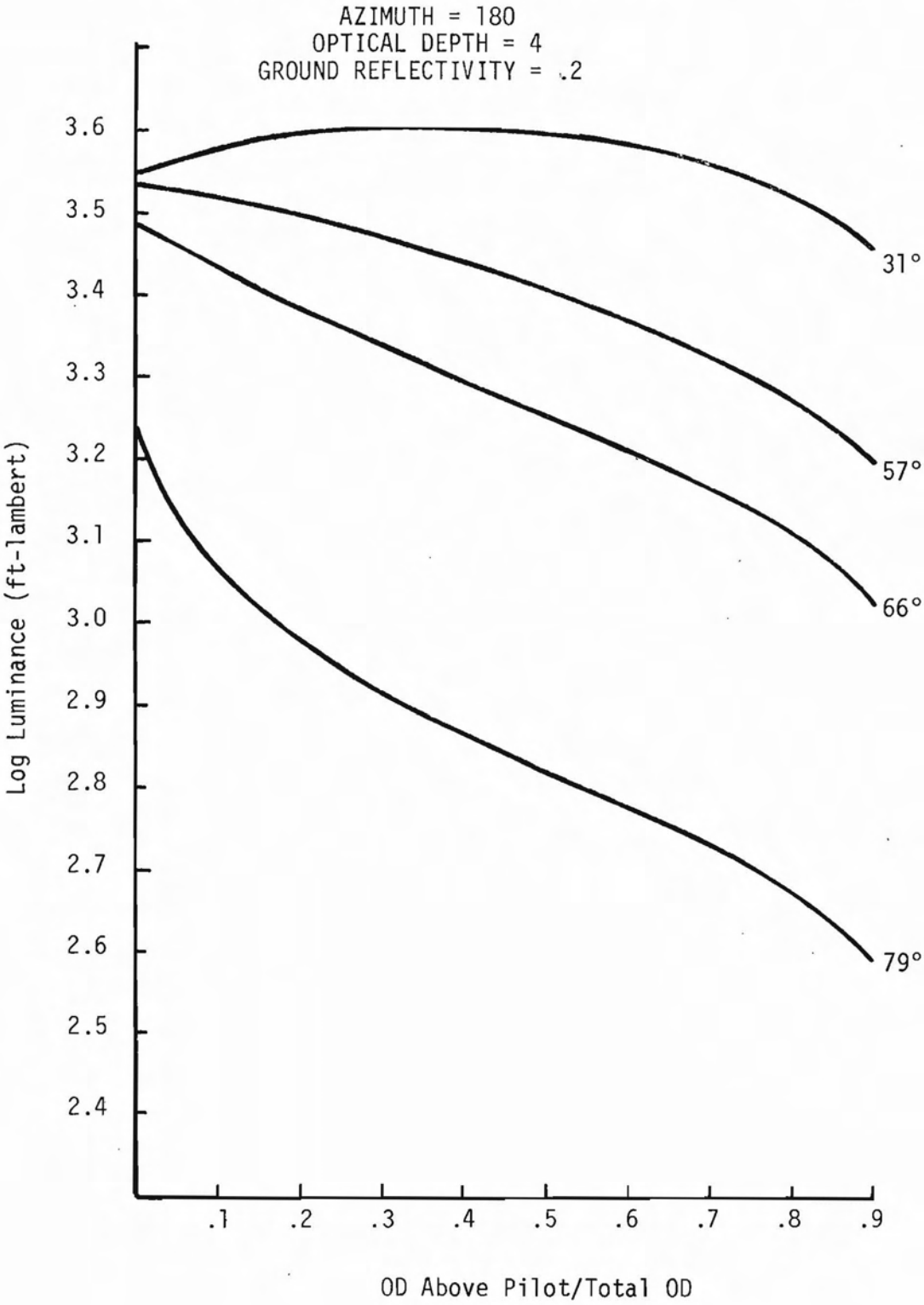

FIGURE 7-12

EFFECT OF DIFFERENT SOLAR ZENITH ANGLES

AZIMUTH = 0°
OPTICAL DEPTH = 4
GROUND REFLECTIVITY = .2

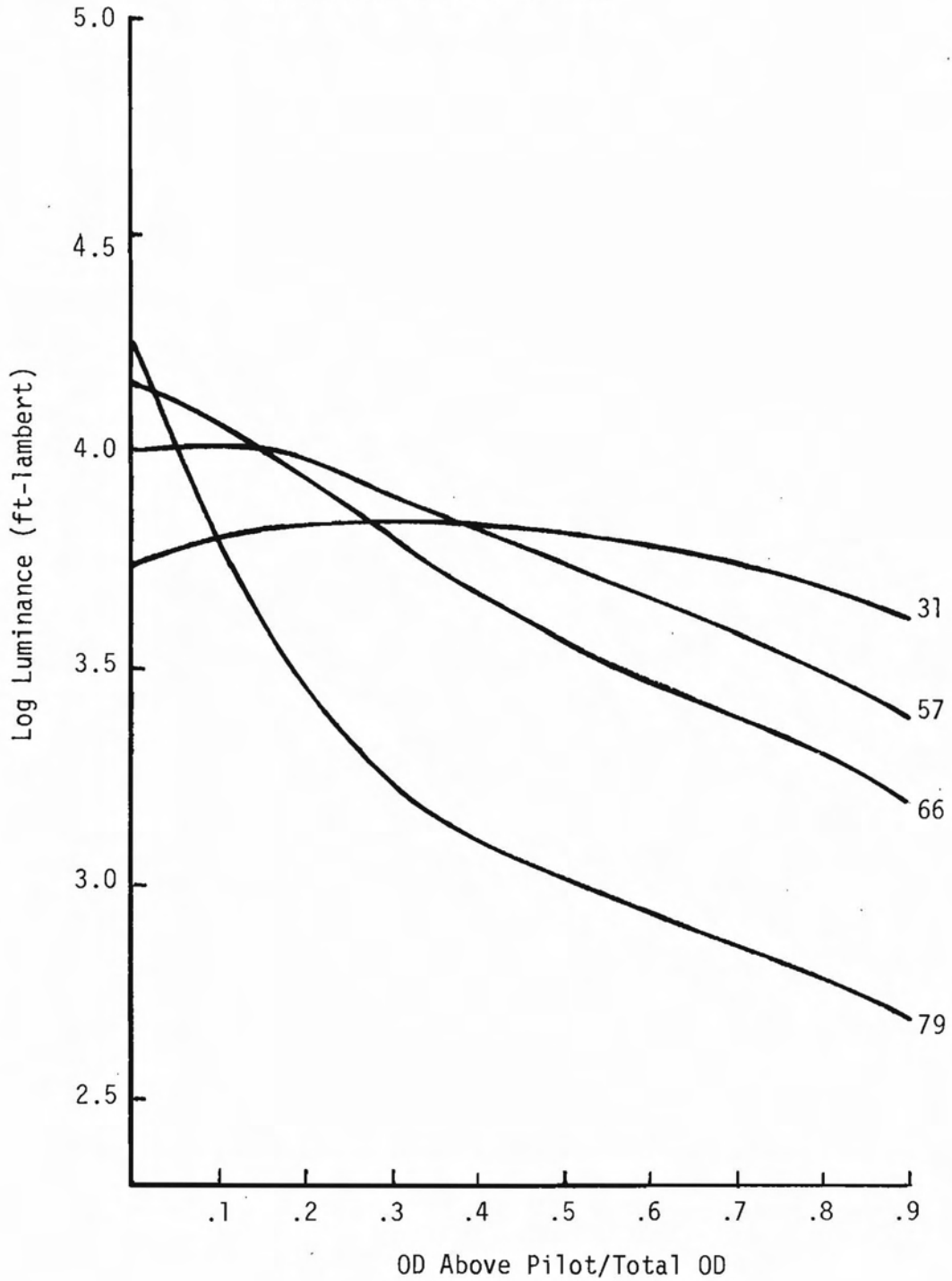

FIGURE 7-13

EFFECT OF DIFFERENT SOLAR ZENITH ANGLES

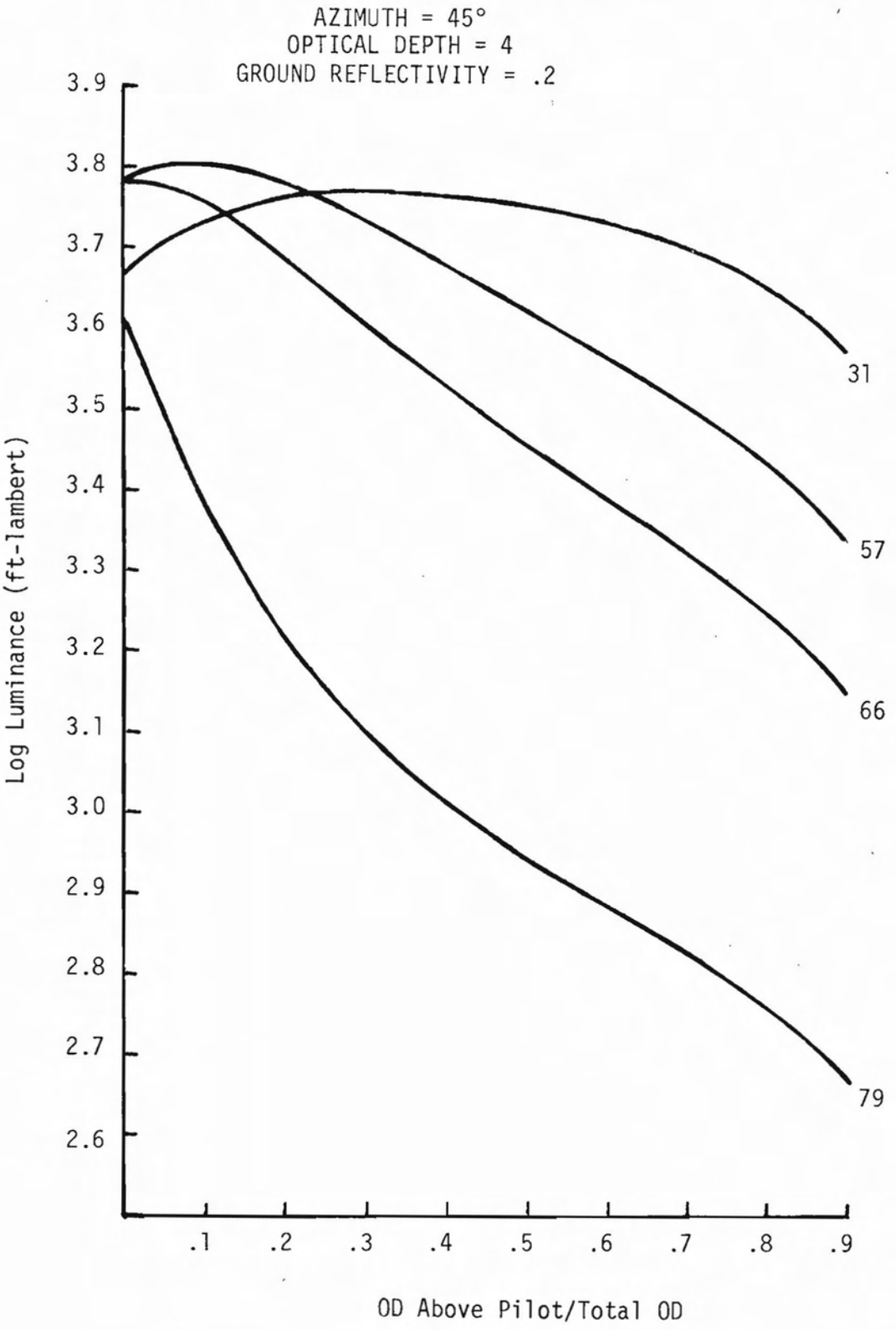

FIGURE 7-14

EFFECT OF DIFFERENT SOLAR ZENITH ANGLES

AZIMUTH = 180°
OPTICAL DEPTH = .5
GROUND REFLECTIVITY = .2

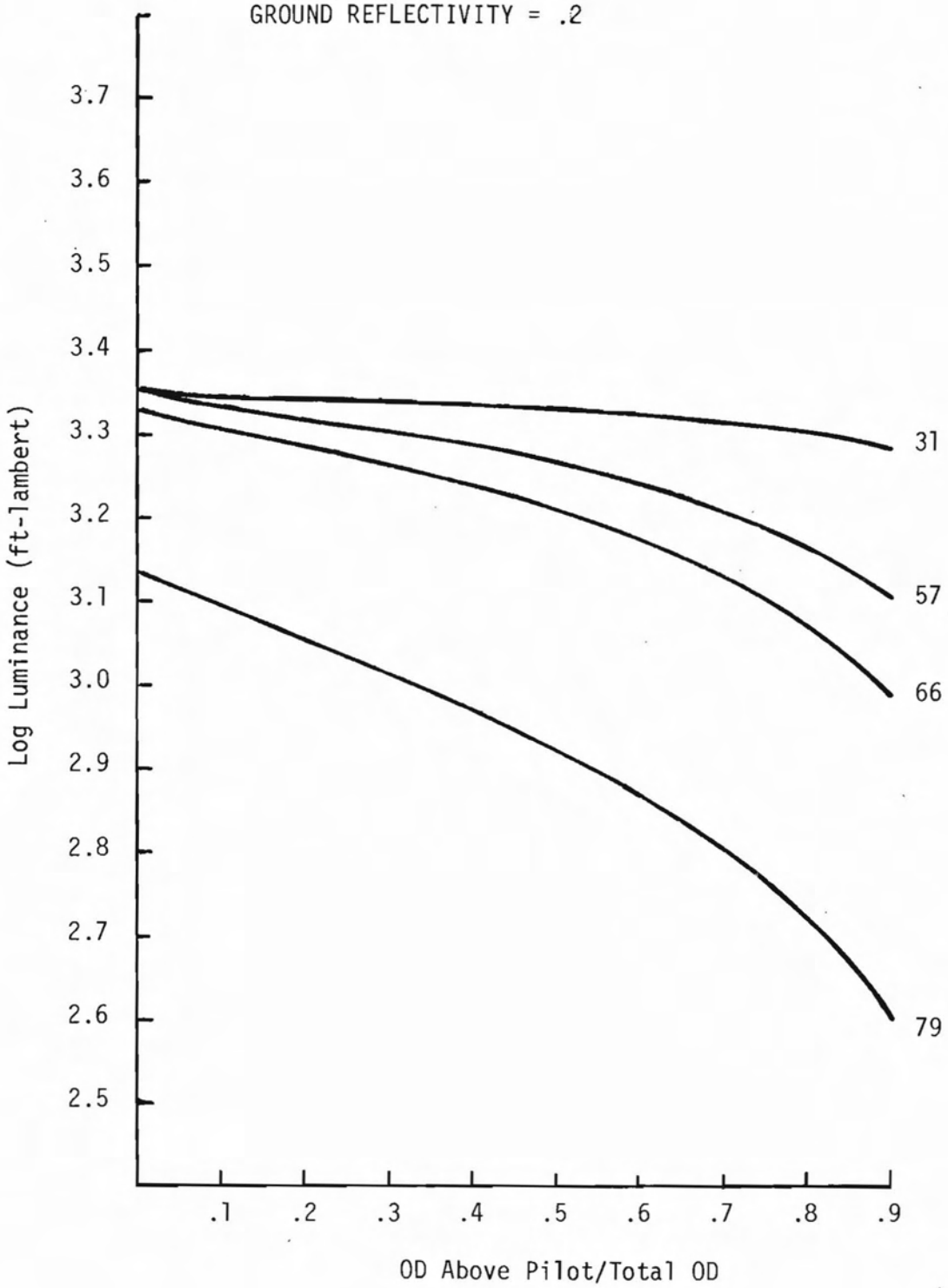

FIGURE 7-15

rising), the scattering angle is increasing, thus lowering $P(\theta)$ and the luminance the pilot perceives. This phenomenon reverses as the pilot descends through the fog. This is due to the diffusion of the light through multiple scattering.

Figures 7-16 through 7-19 represent the effect of different pilot-solar azimuth angles for various optical depths and solar zenith angles. As can be noted in all four figures, the luminance curves representing the 90°, 135° and 180° azimuth angles are close together, while the 0°, 45° and 90° curves show greater differences. The effect of solar azimuth angle is greatest near the top of the fog. The luminances are greatest for small azimuth angles. Again, this is the result of a large amount of scattering at small scattering angles.

Figures 7-20 through 7-22 represent the effect of varying optical depth. Optical depth has the greatest effect at the bottom of the fog for small azimuth angles. From the top to the bottom of the fog, the luminance varies a factor of 10.

Figure 7-23 shows the effect of ground reflectivity. Ground reflectivity does not appear to affect luminance significantly.

It was anticipated that from the computer runs, total optical depth of the fog could be correlated with illuminance on the ground. This information, along with an estimate of extinction coefficient(s), would enable the optical depth versus altitude to be defined. Thus, in effect, the optical depth above the pilot could be calculated, given the pilot's altitude. Since the luminance the pilot sees depends to a large extent on the location of the sun relative to the pilot's direction of look, computational formulas were obtained which predict the azimuth and zenith as a function of pilot's longitude and latitude, day of the year and time of day. Thus,

EFFECT OF DIFFERENT AZIMUTH ANGLES

SOLAR ZENITH = 79°
OPTICAL DEPTH = 4
GROUND REFLECTIVITY = .2

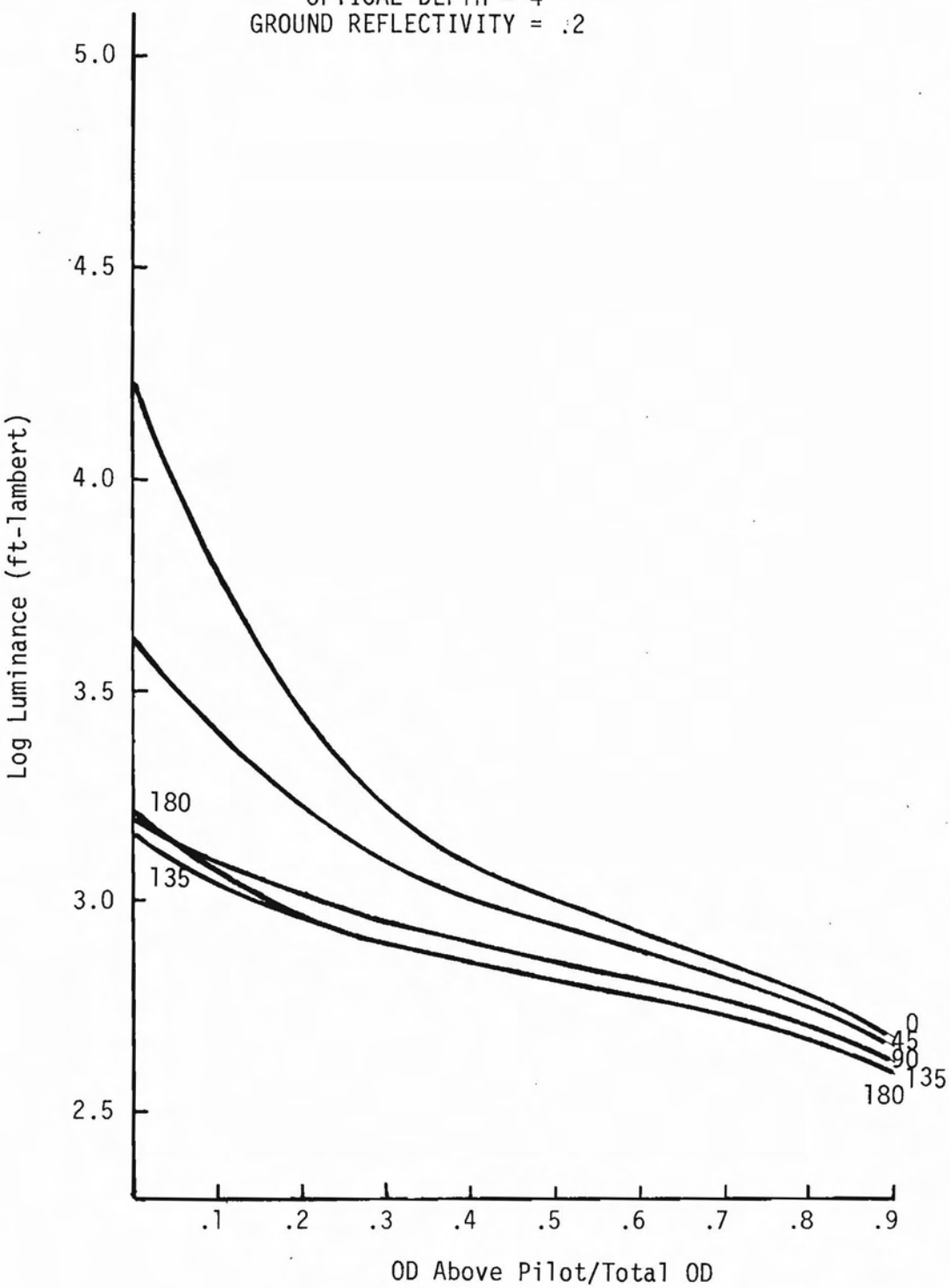

FIGURE 7-16

EFFECT OF DIFFERENT AZIMUTH ANGLES

SOLAR ZENITH = 31°
OPTICAL DEPTH = 4
GROUND REFLECTIVITY = .2

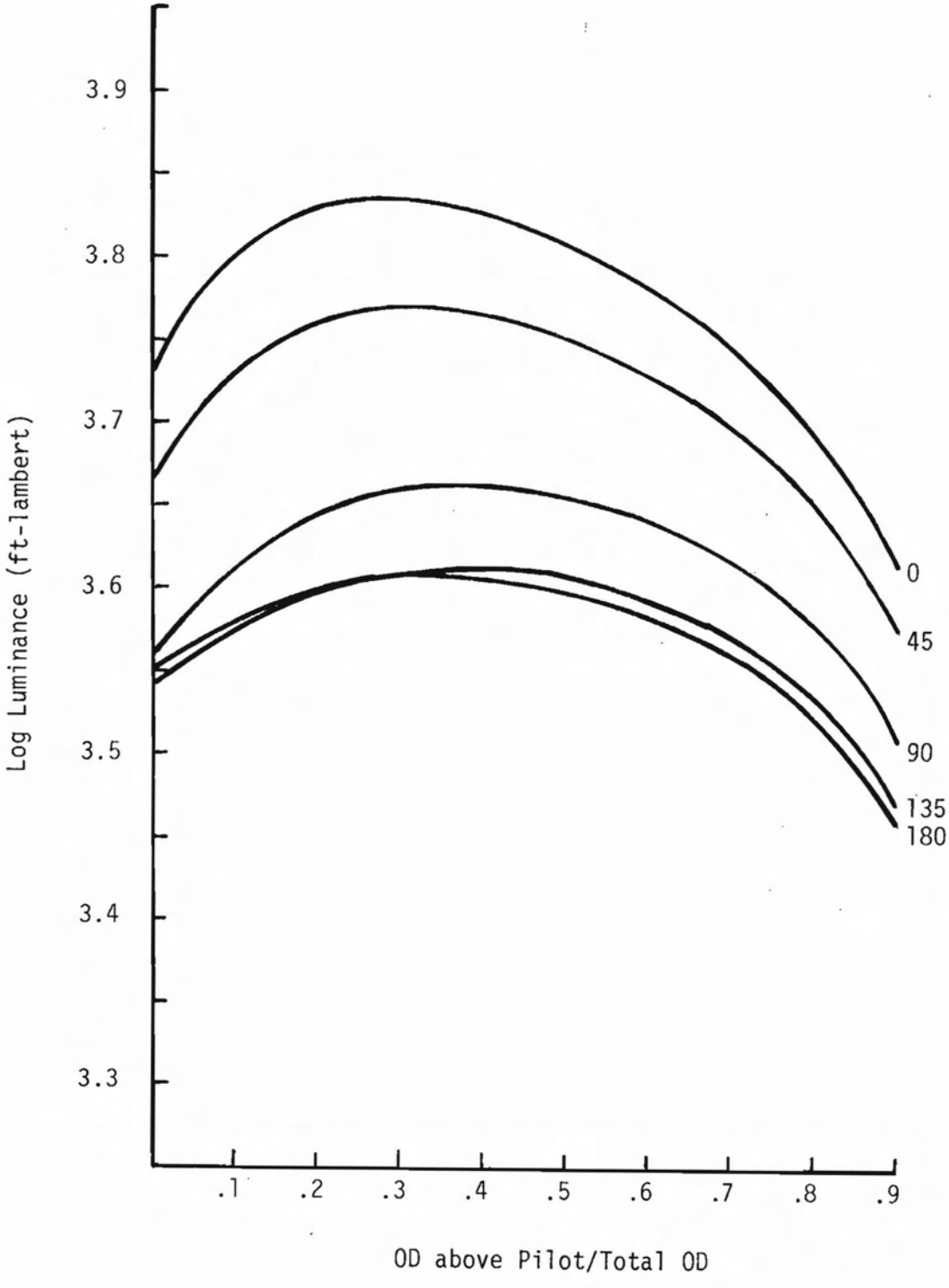

FIGURE 7-17

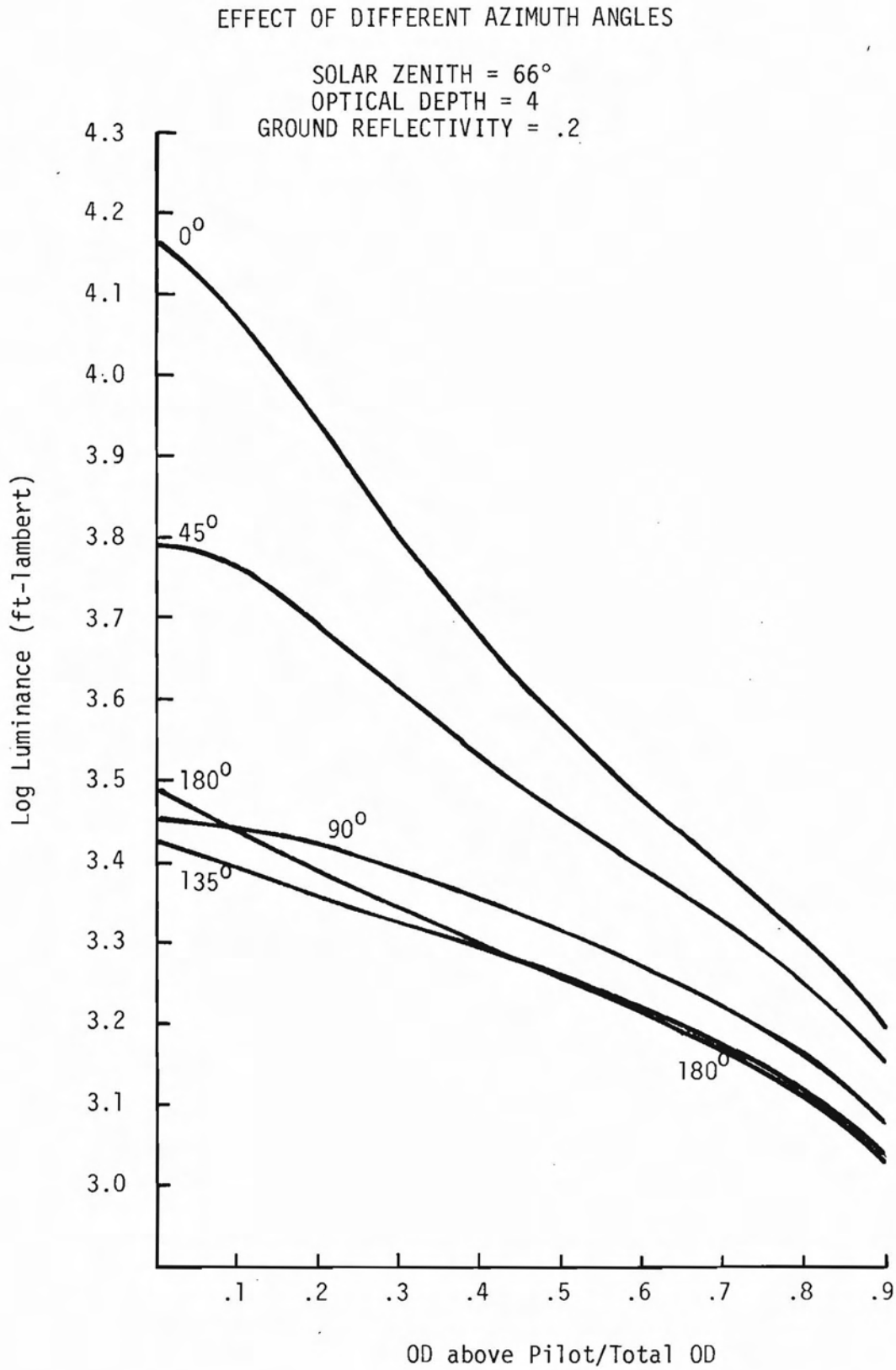
EFFECT OF DIFFERENT AZIMUTH ANGLES
SOLAR ZENITH = 66°
OPTICAL DEPTH = 4
GROUND REFLECTIVITY = .2
Log Luminance (ft-lambert)
4.3
4.2
4.1
4.0
3.9
3.8
3.7
3.6
3.5
3.4
3.3
3.2
3.1
3.0
0°
45°
180°
90°
135°
180°
.1
.2
.3
.4
.5
.6
.7
.8
.9
OD above Pilot/Total OD

FIGURE 7-18

EFFECT OF DIFFERENT AZIMUTH ANGLES

SOLAR ZENITH = 66°
OPTICAL DEPTH = .5
GROUND REFLECTIVITY = .2

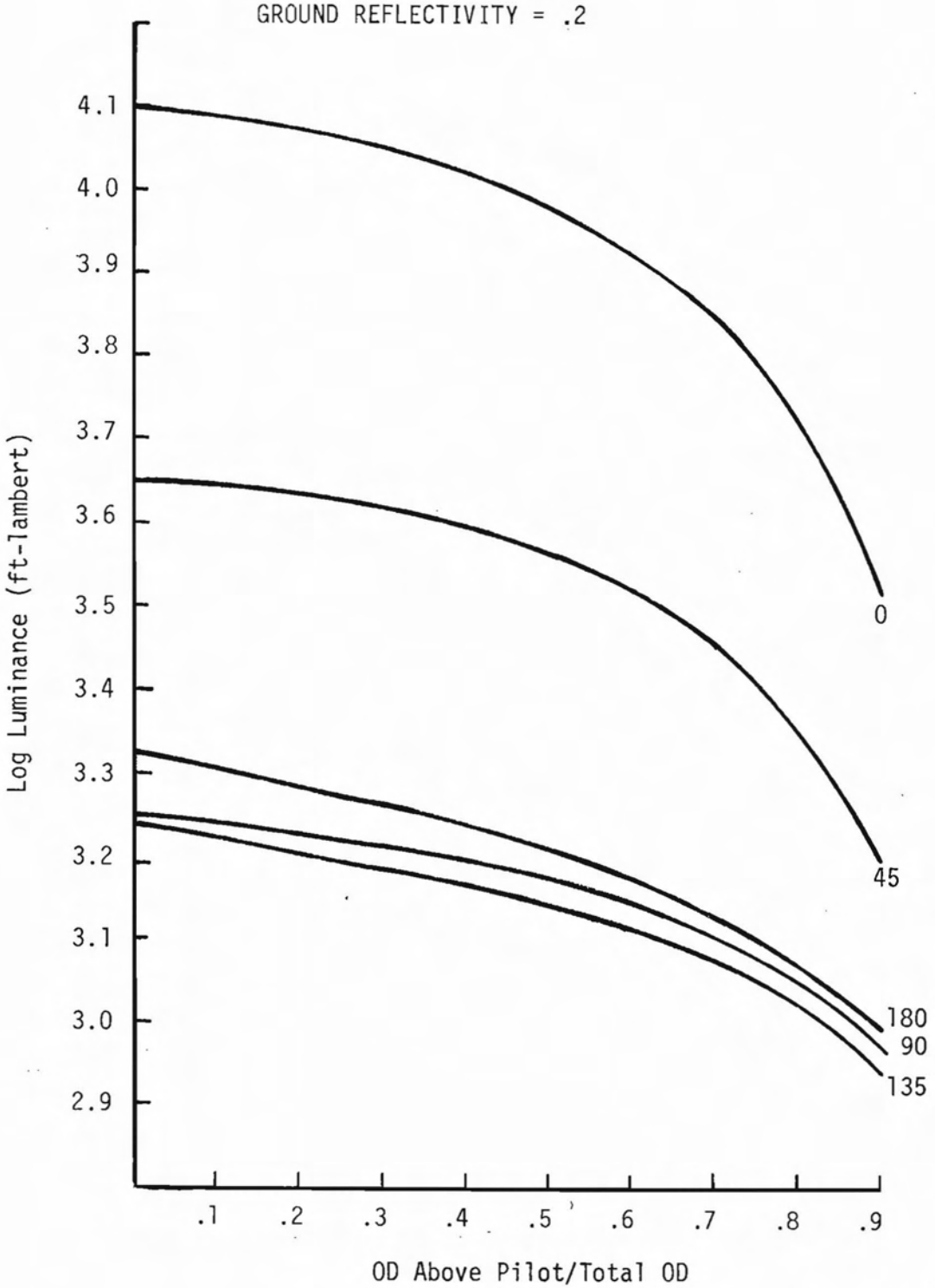

FIGURE 7-19

EFFECT OF DIFFERENT OPTICAL DEPTHS

SOLAR ZENITH = 66°
AZIMUTH = 180°
GROUND REFLECTIVITY = .2

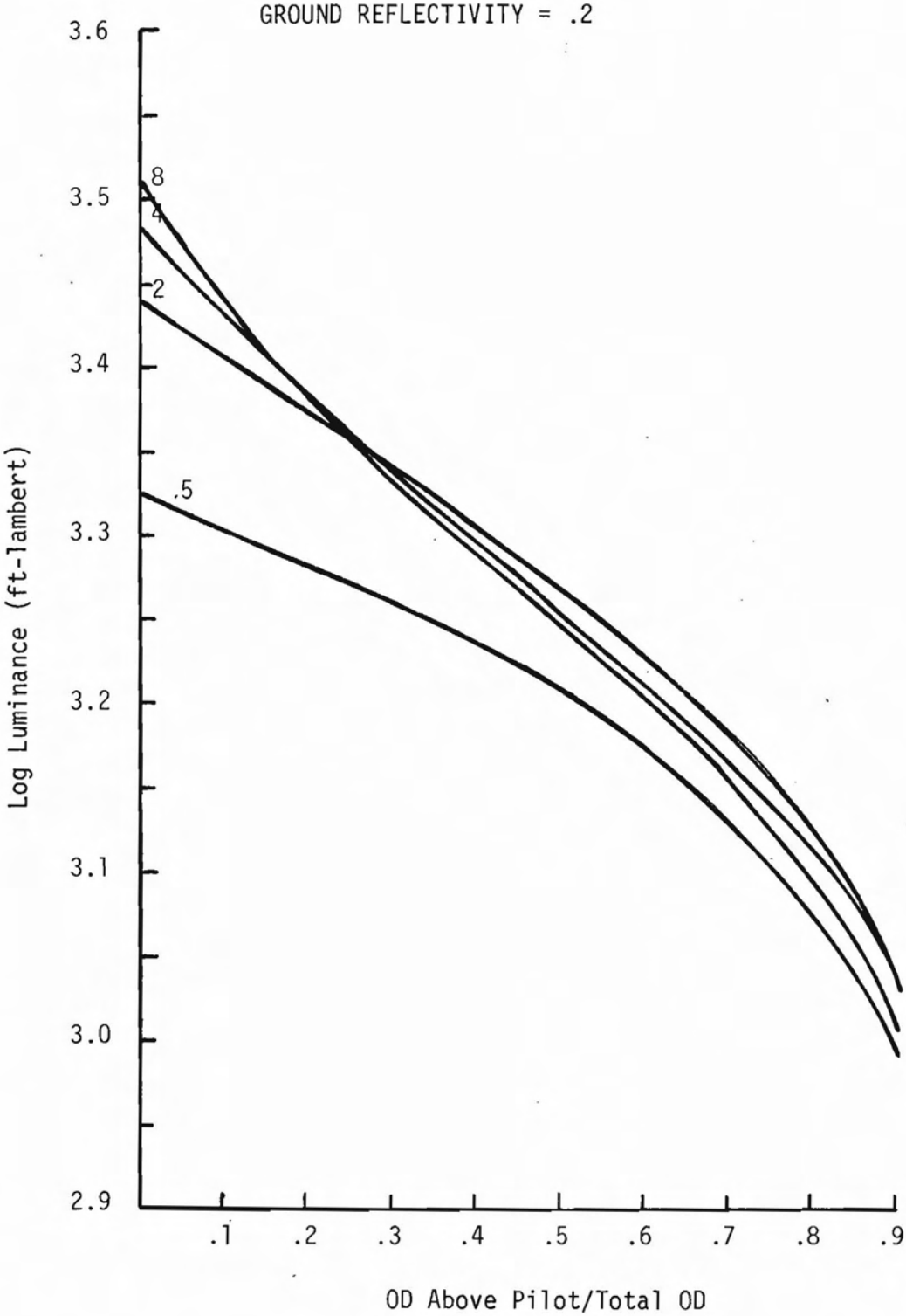

FIGURE 7-20

EFFECT OF DIFFERENT OPTICAL DEPTHS

SOLAR ZENITH = 66°
AZIMUTH = 45
GROUND REFLECTIVITY = .2

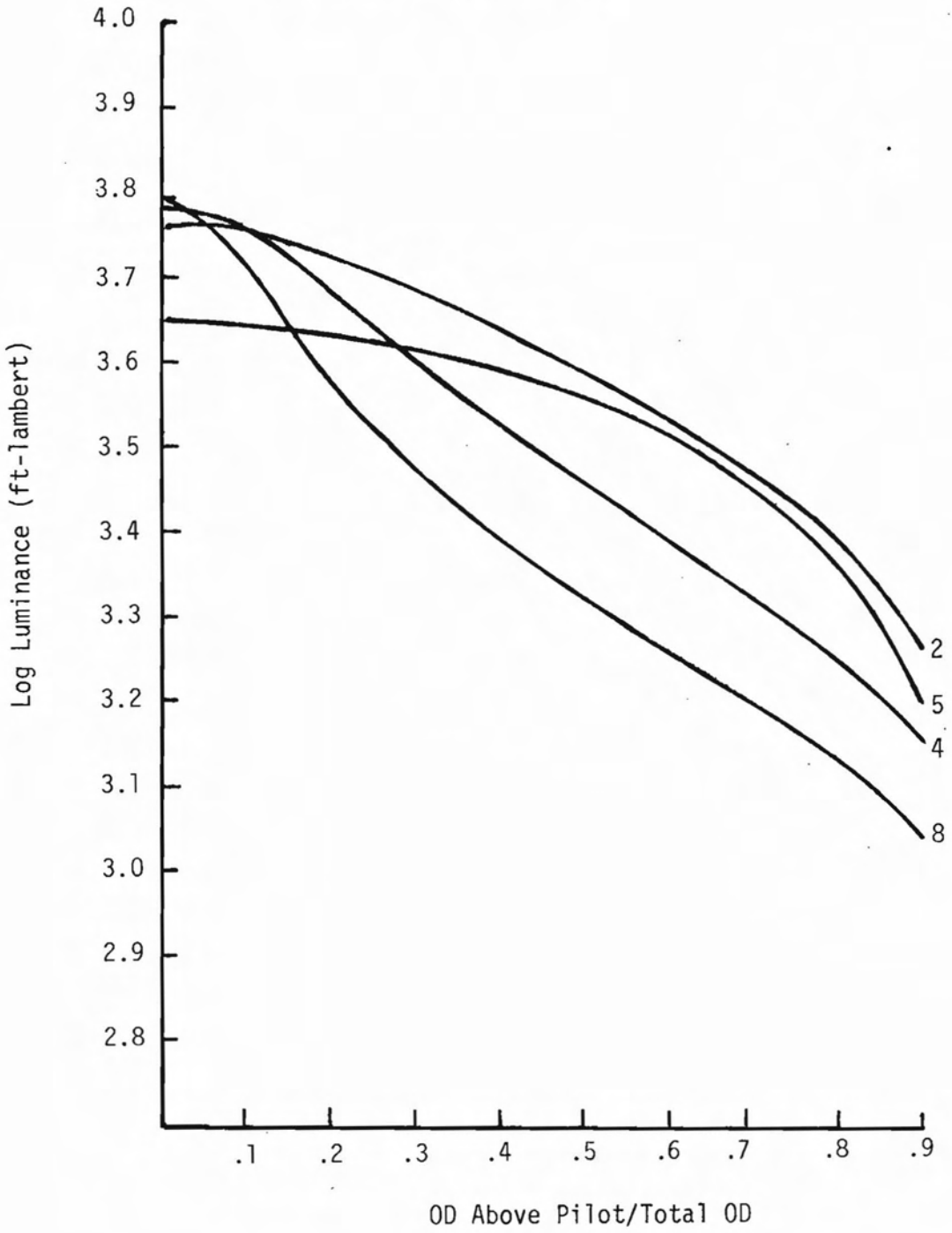

FIGURE 7-21

EFFECT OF DIFFERENT OPTICAL DEPTHS

SOLAR ZENITH = 66°
AZIMUTH = 0°
GROUND REFLECTIVITY = .2

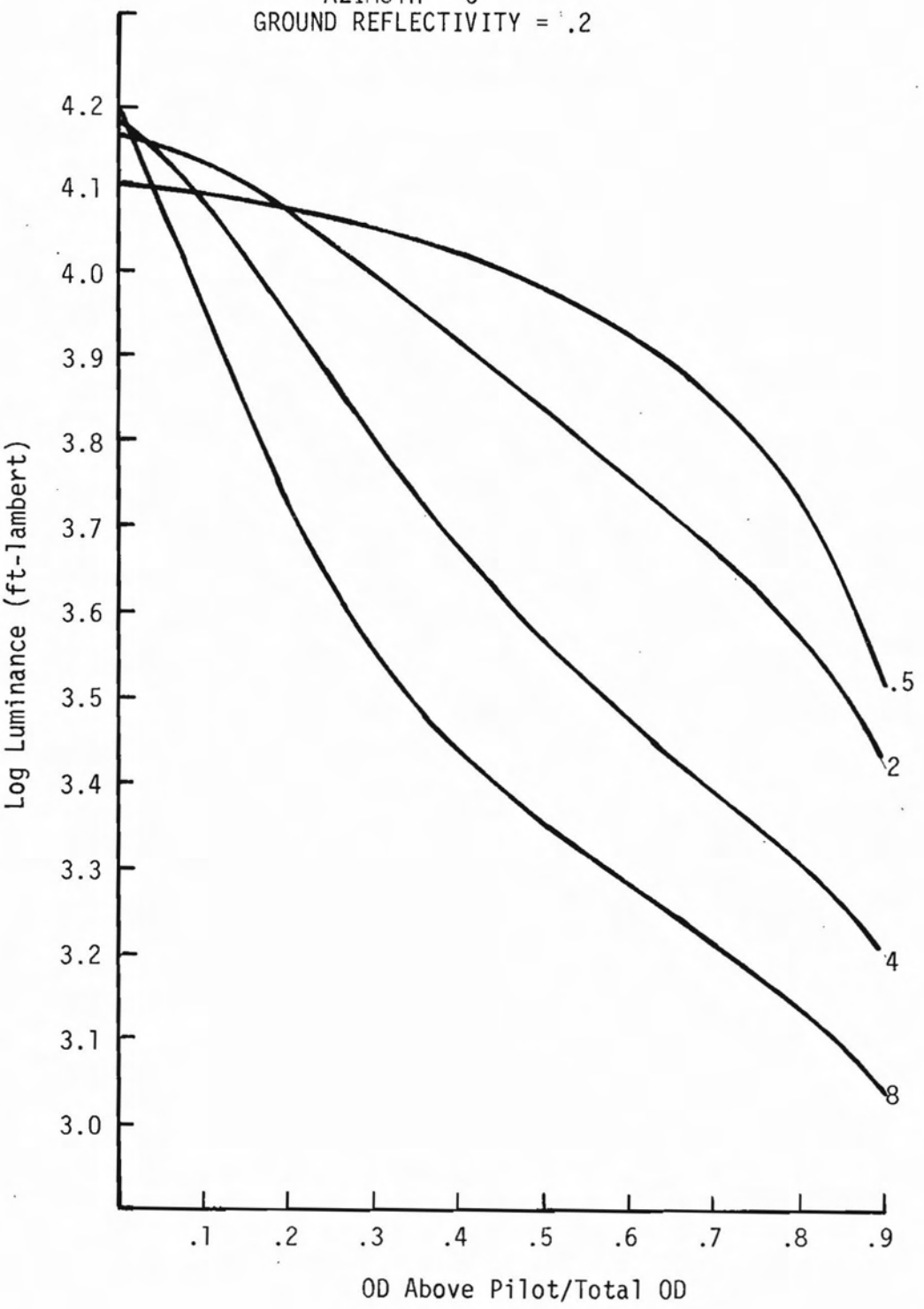

FIGURE 7-22

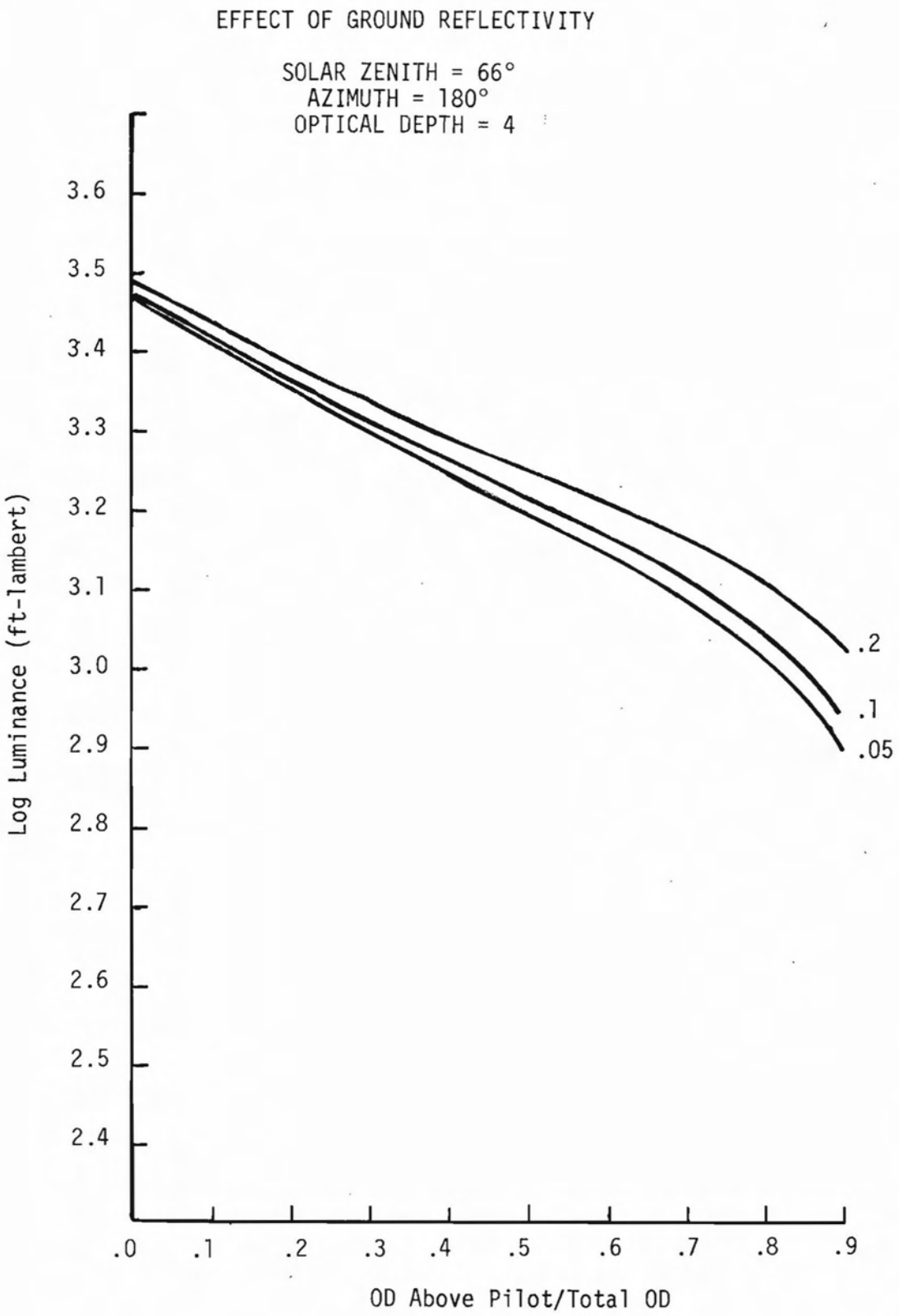
EFFECT OF GROUND REFLECTIVITY
SOLAR ZENITH = 66°
AZIMUTH = 180°
OPTICAL DEPTH = 4
Log Luminance (ft-lambert)
3.6
3.5
3.4
3.3
3.2
3.1
3.0
2.9
2.8
2.7
2.6
2.5
2.4
.2
.1
.05
.0
.1
.2
.3
.4
.5
.6
.7
.8
.9
OD Above Pilot/Total OD

FIGURE 7-23

PILOT-SUN GEOMETRY

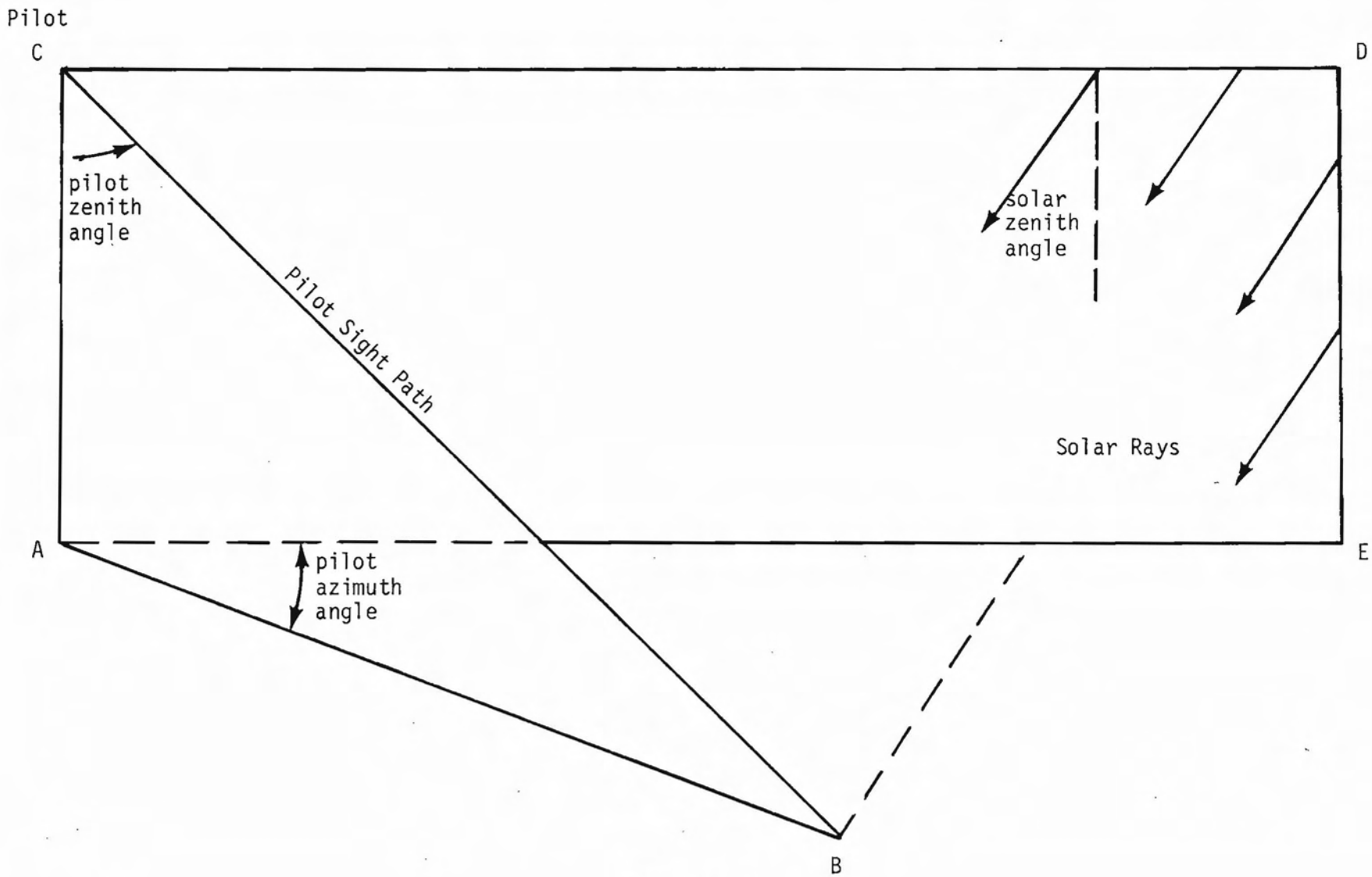

FIGURE 7-24

knowing the position of the sun, total optical depth, optical depth above the pilot and ground reflectivity, the computed luminance can be found from the computer output. Realizing the impracticality of looking up luminance from computer printouts, luminance values were fitted via linear regression techniques as a function of sun position, total optical depth, optical depth above pilot and ground reflectivity. This enabled luminance at each ALCH decision point to be computed quickly by substitution into the regression equation. The results of the regression fitted to the luminance data calculated by the computer program is given in Figures 7-25 and 7-26. The abscissa represents the actual data and the ordinate represents the predicted. The luminance prediction is made only for decision heights greater than 100 feet and then only when the condition of the sky above the fog is known as clear. When a cloudy condition occurs, the luminance is taken from the 100-foot luminance meter and is applied to decision heights of 150, 200, 300 and 400 feet. The luminance scale ranges from two ft-lamberts to 3,000 ft-lamberts for the SVR/ALCH system in the daytime case.

As mentioned above, the total optical depth and the optical depth above the pilot in daytime conditions must be input into the regression formula. To obtain these, an attempt was made to correlate total optical depth with the illuminance on the ground using the computer generated data. Figure 7-27 shows illuminance versus total optical depth. As can be seen, illuminance on the ground is very sensitive to solar zenith angle. Likewise, illumination on the ground is very sensitive to the total optical depth. Since optical depth equals the extinction coefficient times altitude ($\tau = \sigma h$), the height of the fog or breakout altitude can be found by knowing σ and assuming it constant with altitude. Likewise, the amount of optical depth above the pilot can be calculated assuming a constant σ and by knowing the altitude of the pilot. Therefore, knowing total optical depth, optical depth above pilot, solar zenith and azimuth angle, the regression formula will estimate fog luminance.

REGRESSION PREDICTION OF LUMINANCE

AZIMUTH 0-90°

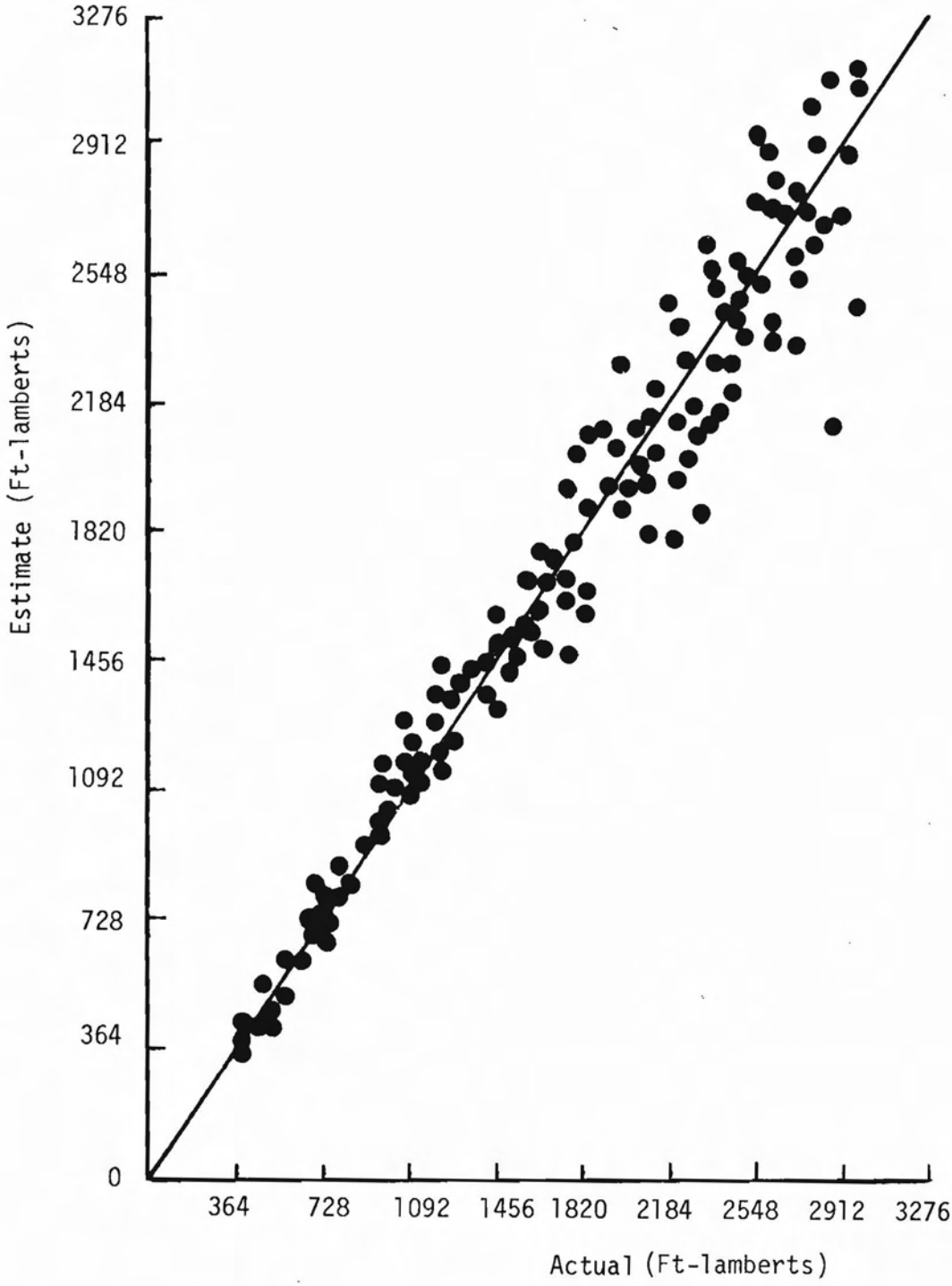

FIGURE 7-25

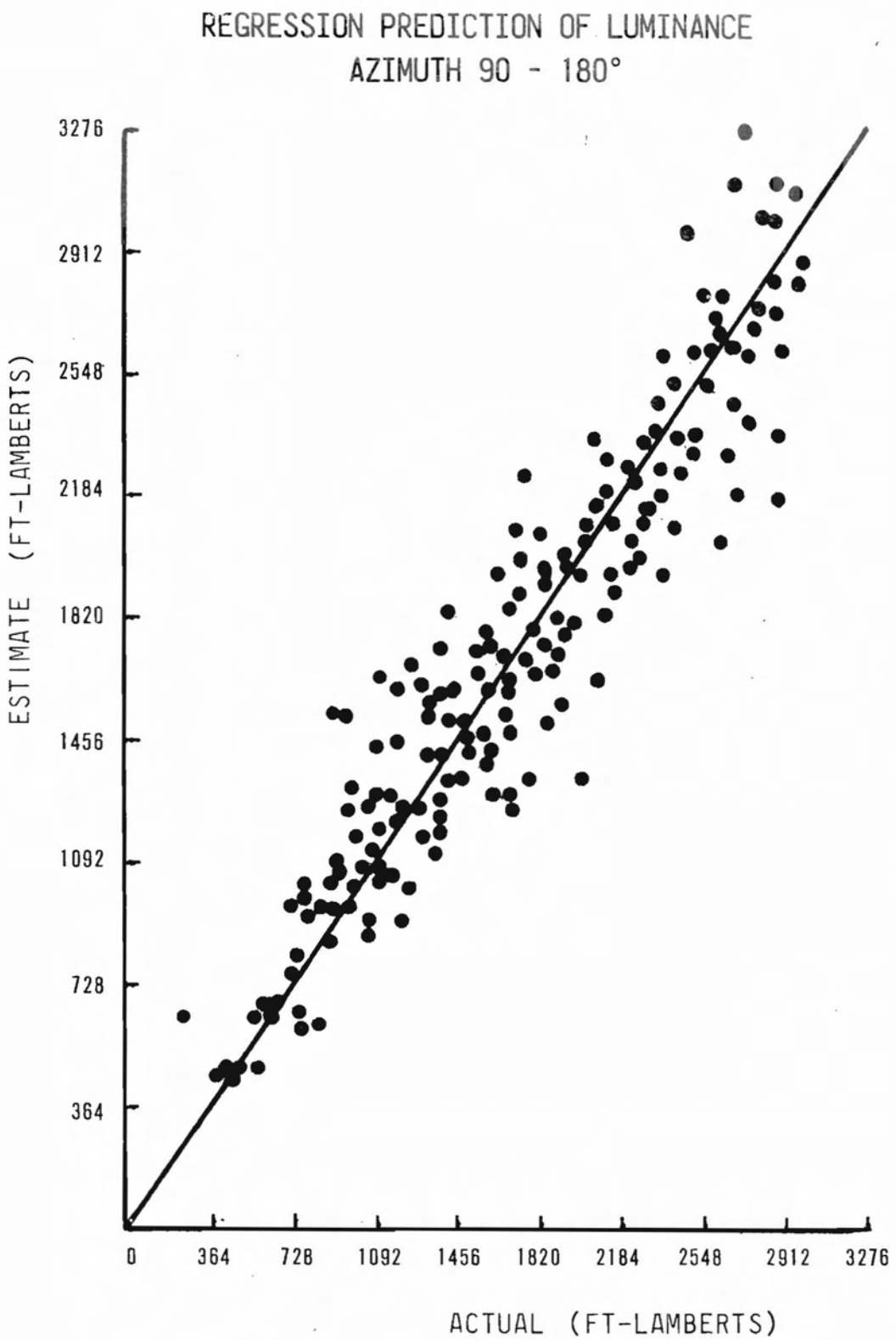
REGRESSION PREDICTION OF LUMINANCE
AZIMUTH 90 - 180°
ESTIMATE (FT-LAMBERTS)
3276
2912
2548
2184
1820
1456
1092
728
364
0
364
728
1092
1456
1820
2184
2548
2912
3276
ACTUAL (FT-LAMBERTS)

Figure 7-26

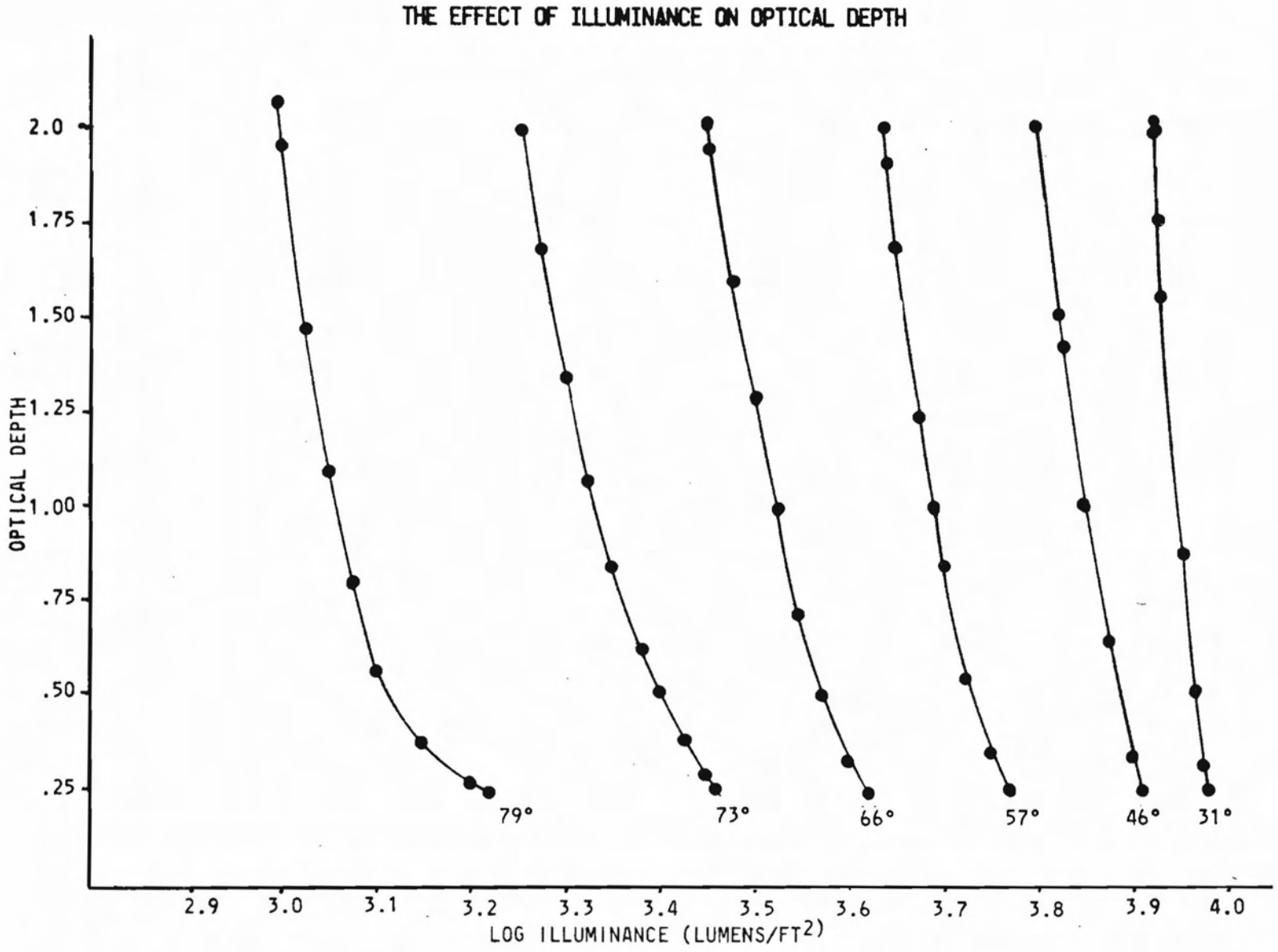
THE EFFECT OF ILLUMINANCE ON OPTICAL DEPTH
OPTICAL DEPTH
2.0
1.75
1.50
1.25
1.00
.75
.50
.25
79°
73°
66°
57°
46°
31°
2.9
3.0
3.1
3.2
3.3
3.4
3.5
3.6
3.7
3.8
3.9
4.0
LOG ILLUMINANCE (LUMENS/FT2)

Figure 7-27

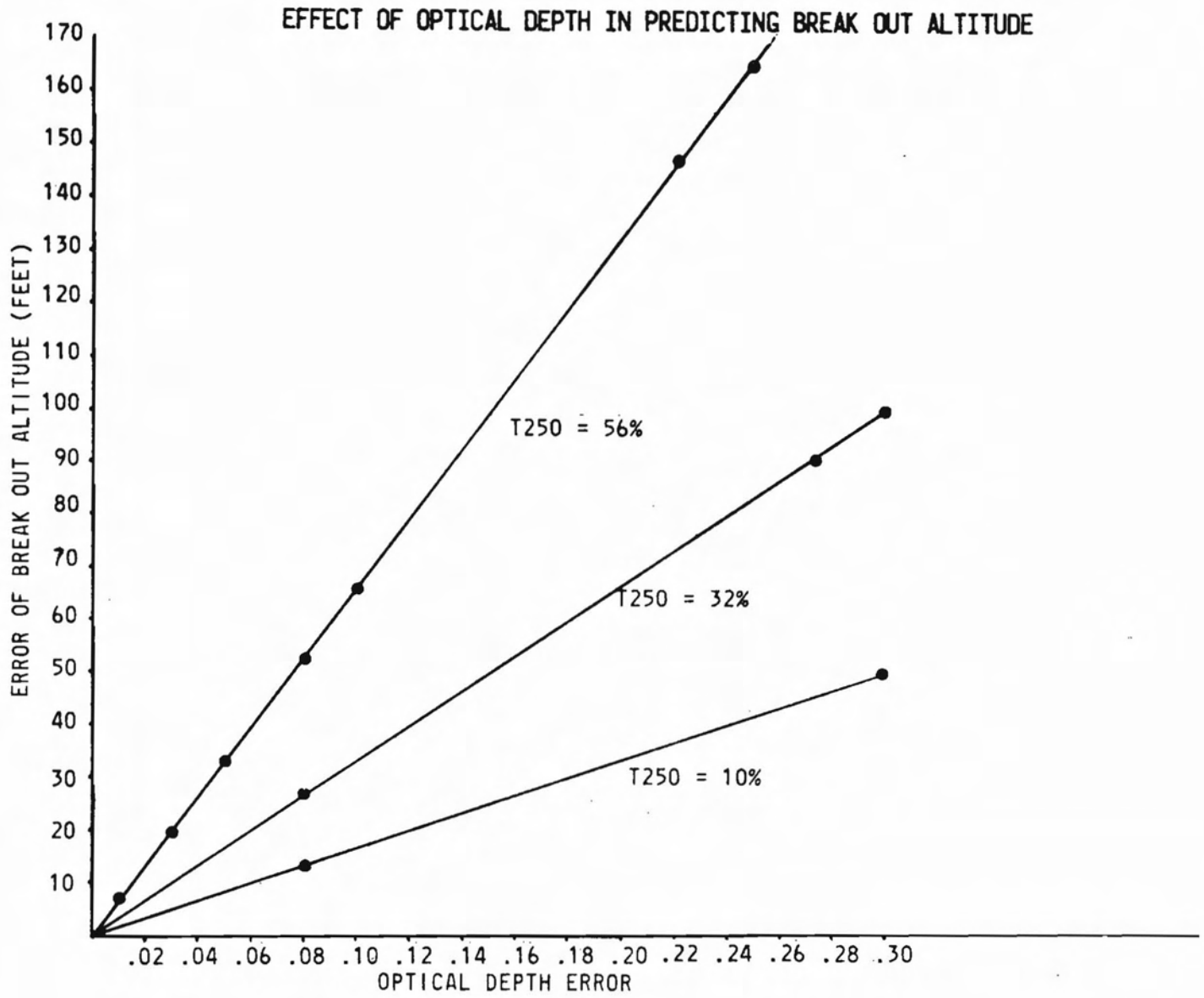
EFFECT OF OPTICAL DEPTH IN PREDICTING BREAK OUT ALTITUDE
ERROR OF BREAK OUT ALTITUDE (FEET)
170
160
150
140
130
120
110
100
90
80
70
60
50
40
30
20
10
T250 = 56%
T250 = 32%
T250 = 10%
.02 .04 .06 .08 .10 .12 .14 .16 .18 .20 .22 .24 .26 .28 .30
OPTICAL DEPTH ERROR

Figure 7-28

The effect of assuming σ constant with altitude is not completely known in terms of predicting fog luminance. This, to a great extent, depends on the assumption that fog luminance is determined primarily by the optical depth above the pilot and total optical depth. The first parameter is certainly affected by the constant σ assumption, while the total optical depth may or may not be affected. In other words, since total optical depth is determined from illumination on the ground and illumination on the ground may be fairly independent of the location of fog with altitude, it is possible that predicted total optical depth be independent of σ varying with altitude.

Figure 7-28 shows the breakout altitude error generated for the error in calculating total optical depth from the illuminance measurements described above. This graph can be expressed as follows: $\Delta h = \Delta\tau/\sigma$. Figure 7-29 is a composite of Figures 7-27 and 7-28. It shows the error generated in predicting the top of the fog (breakout altitude) for the error of measuring illuminance. As can be seen, the denser the fog, the less sensitive breakout altitude is to illuminance. To go one step farther, Table 7-1 shows the sensitivity of ALCH on breakout altitude. Column five represents the default value of ALCH for a 400-foot breakout altitude, which is used in the SVR/ALCH system if breakout altitude is not known.

TABLE 7-1

Effect of Breakout Altitude on ALCH

Approximate Adaptation Luminance	T_{250}	Actual Breakout Altitude (Ft.)	Actual ALCH (Ft.)	ALCH for Assumed 400 Ft. Breakout Altitude
100-500	.63	100	400	200
100-500	.63	200	300	200
100-500	.63	300	200	200
2-100	.25	100	400	200
2-100	.25	200	300	200
2-100	.25	300	200	200
100-500	.5	100	300	200
100-500	.5	200	200	200
1000-1500	.37	100	200	150
1000-1500	.37	200	150	150

As can be seen from comparing columns four and five, an error of at least 200 feet can be made in predicting ALCH. This indicates the importance of knowing breakout altitude.

At present, two alternatives exist for obtaining breakout altitude: (1) predicting breakout altitude as a function of the measured illuminance on the ground and an estimate of σ from the SVR/ALCH system and (2) pilot reports. Both of these methods will be used in predicting breakout altitude at the NAFEC experimental flight tests. Evaluation of the two methods will then be made to determine if one, both or neither of the methods will be entered into the ALCH system.

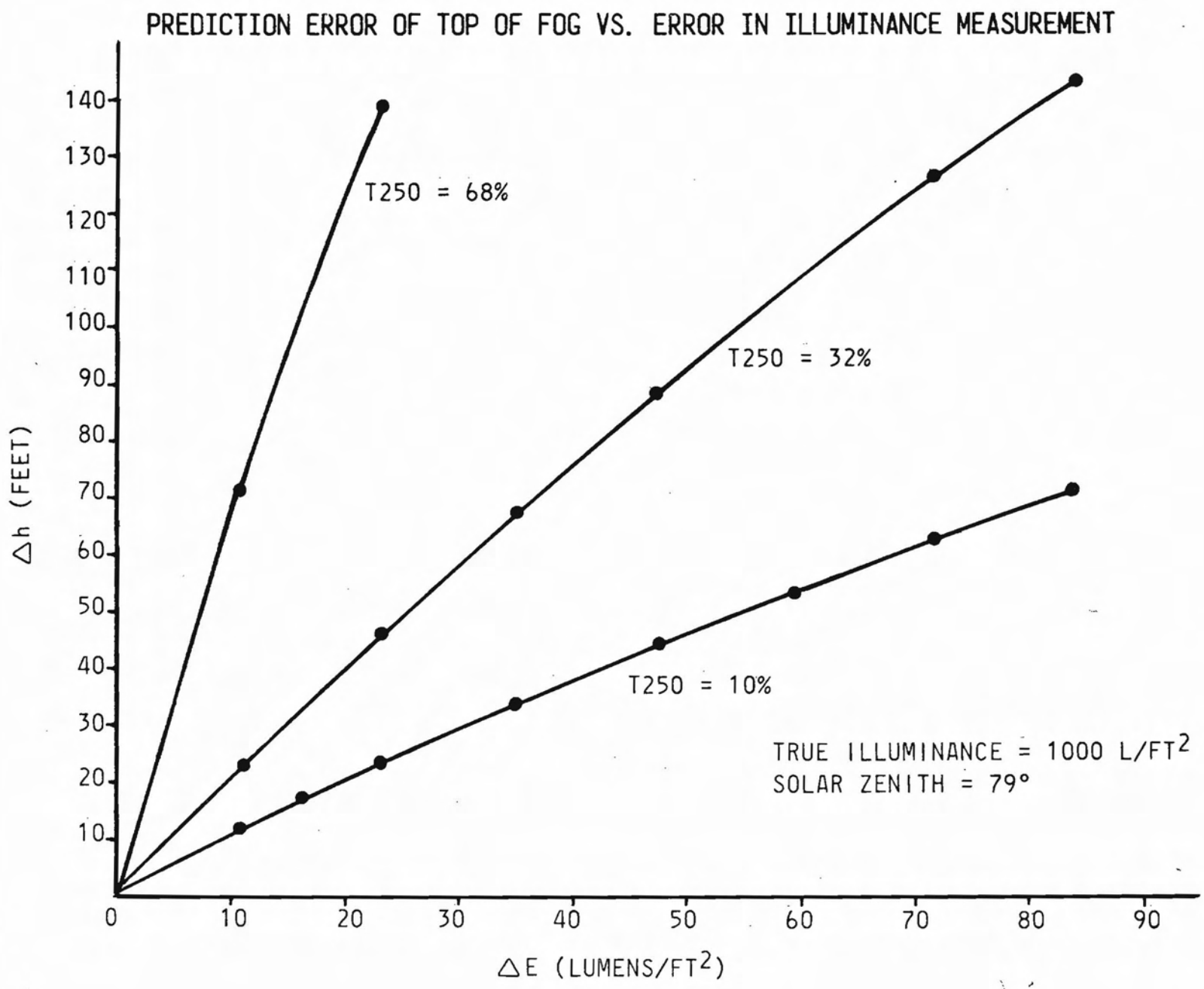
PREDICTION ERROR OF TOP OF FOG VS. ERROR IN ILLUMINANCE MEASUREMENT
T250 = 68%
T250 = 32%
T250 = 10%
TRUE ILLUMINANCE = 1000 L/FT2
SOLAR ZENITH = 79°
Δh (FEET)
ΔE (LUMENS/FT2)
0
10
20
30
40
50
60
70
80
90
100
110
120
130
140

Figure 7-29

8. ALCH/SVR CALCULATIONS

ALCH Algorithm

Day Case

ALCH predictions are based on data concerning: (1) the adaptation luminance being viewed by the pilot; (2) the amount of flux necessary upon the eye from a specific approach bar to enable the pilot to "see" the bar; (3) the condition of the atmosphere (extinction rate) between the pilot and the approach light bars of interest; and (4) the orientation of the approach lights relative to the pilot, i.e., the intensity vector in the direction of the pilot.

In the previous phase of this project, a psychophysical experiment (Lohkamp *et al.*, 1972) was conducted to determine the amount of flux on the eye necessary in order to "see" (E_T) the approach bar of interest at several distances and adaptation levels. The E_T used in all calculations is twice the actual threshold laboratory value. This data, fitted via regression analysis, is used to determine the illuminance necessary on the eye once the adaptation level is known.

The adaptation luminance being viewed by the pilot is obtained by one of two techniques. As discussed in Section 7, there are two luminance meters (50 - 100 feet) incorporated in the candidate system. The values measured are utilized for the 50 and 100-foot ALCH predictions. The adaptation necessary for the calculations at the other four ALCH prediction points is obtained from a regression equation fitted to multiple scattering data. The multiple scattering data is discussed in Section 7.

The necessity of adaptation being known is shown in the results of a sensitivity analysis. Figures 8-1 and 8-2 depict the results of the analysis for two different extinction rates (σ).

EFFECT OF LUMINANCE ON ALCH

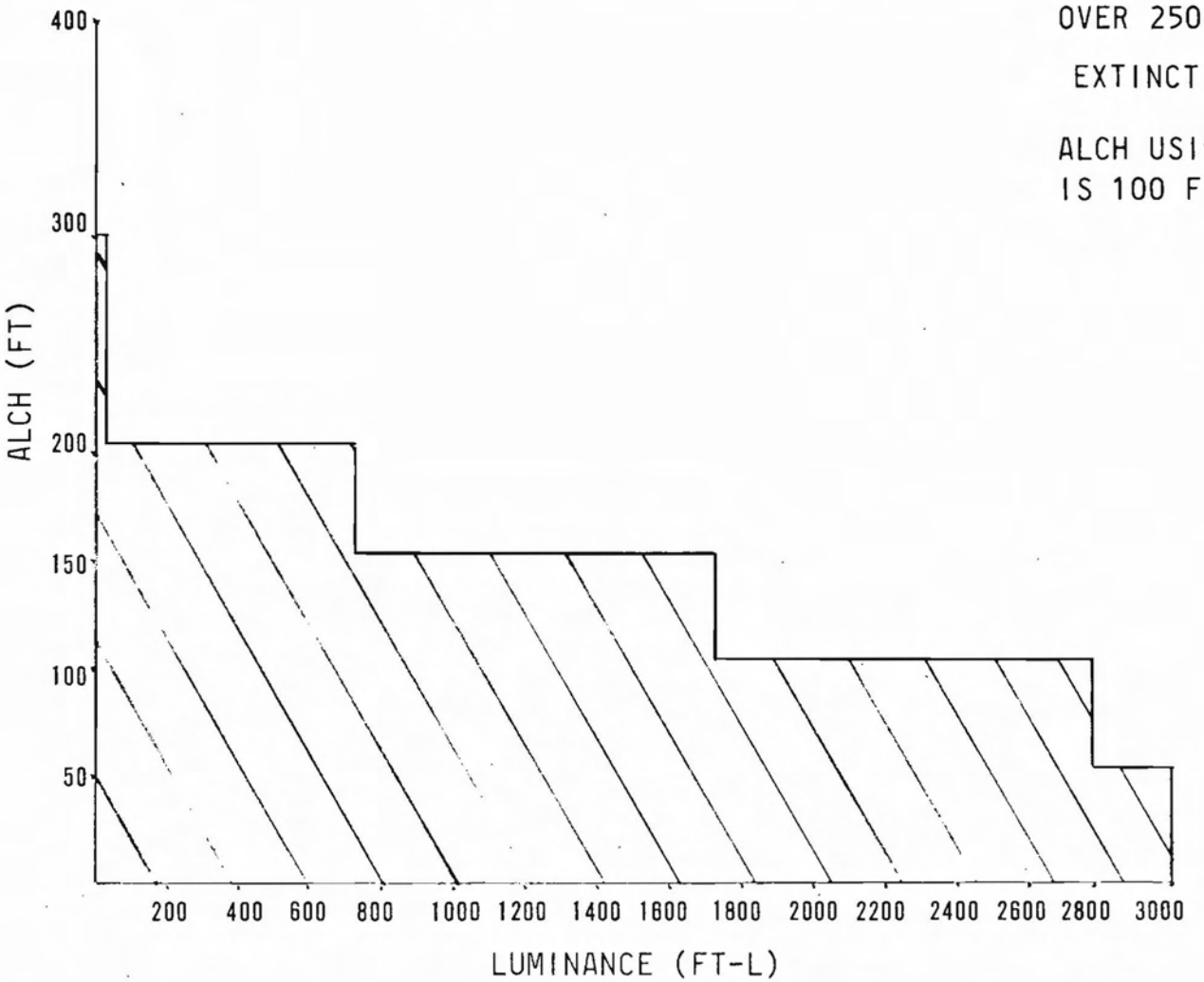

Figure 8-1

EFFECT OF LUMINANCE ON ALCH

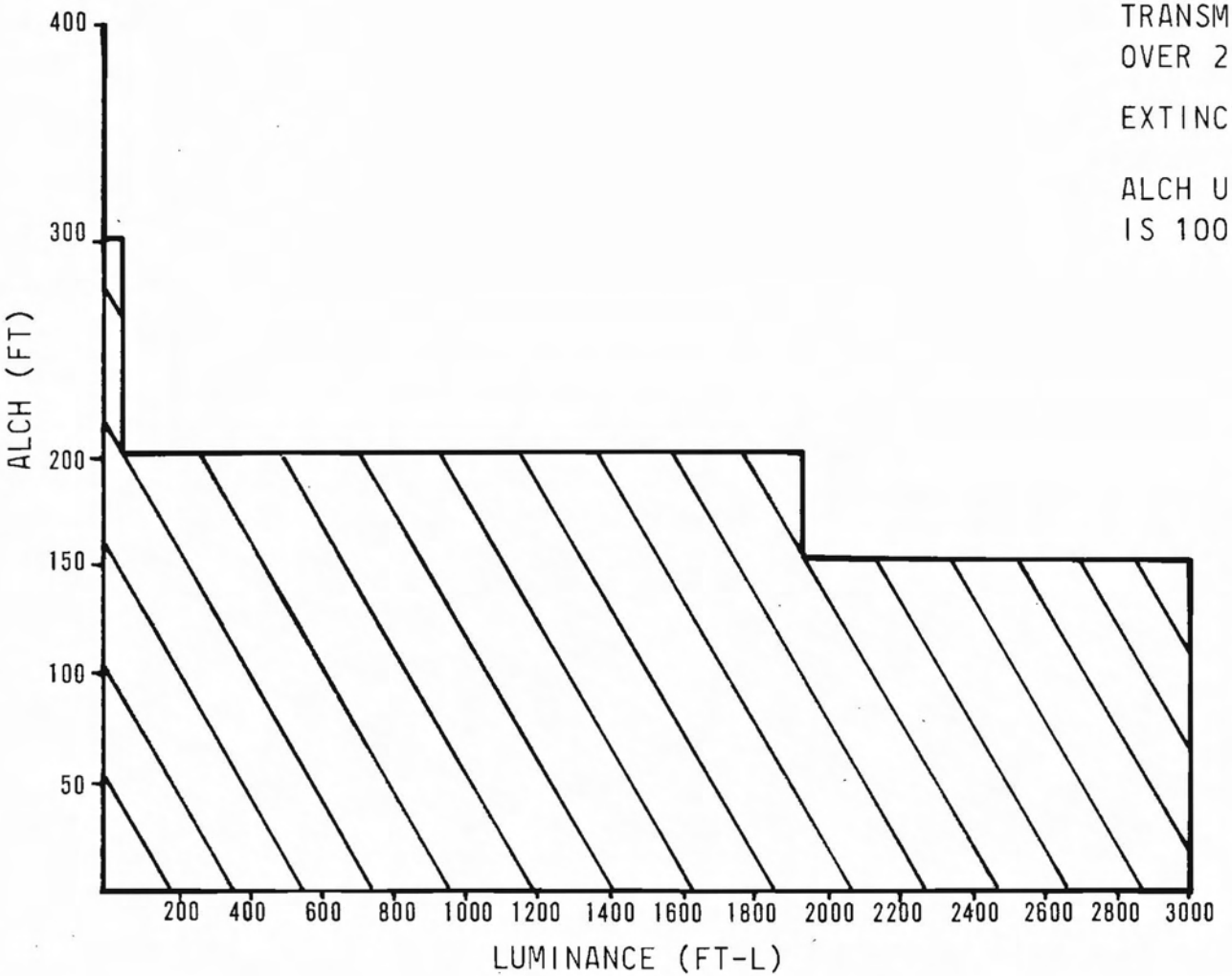

TRANSMISSION
OVER 250 FT = .5

EXTINCTION = 2.773×10^{-3}/FT

ALCH USING 1000 MILE CANDLES
IS 100 FT

Figure 8-2

To calculate the illuminance on the eye from an approach light, one must know the weighted average of the extinction rate ($\bar{\sigma}$) between the observer and the approach light of interest. The weighted average extinction rate is determined by the following equations.

When the top of the fog (HBO) is less than the ALCH prediction point of interest,

$$\bar{\sigma} = 100\left[(\sigma_{10} + \sigma_{100})/2 + (HBO - 100)\ \sigma_{100}\right]/ALCH$$

where ALCH is the height of the prediction point of interest.

When the ALCH prediction point is less than the height of the top of the fog,

$$\bar{\sigma} = 100\left[(\sigma_{10} + \sigma_{100})/2 + (ALCH - 100)\ \sigma_{100}\right]/ALCH.$$

For the 50 feet ALCH prediction point,

$$\bar{\sigma} = \left[\sigma_{10} + (\sigma_{10} + \sigma_{100})/2\right]/2.$$

σ_{10} = the extinction rate measured at a height of 10 feet.

σ_{100} = the extinction rate measured at a height of 100 feet.

HBO = height of the top of the fog in feet (assumed to be 400 feet if unknown).

As can be seen from examination of the equations, $\bar{\sigma}$ is calculated as if σ_{10} were the value at zero height and the extinction above 100 feet height was constant at the value measured at 100 feet.

The illuminance incident upon the eye (E) is calculated by the following equation:

$$E = 5I_{\theta}\ T\ \exp(-\ \bar{\sigma}\ D)/D^2$$

I_{θ} = the intensity of an approach lamp in the direction of the observer.

T = the transmittance of the aircraft windscreen.

D = the distance to the light bar of interest.

$\bar{\sigma}$ = the extinction rate between the observer and the lamp.

In determining the ALCH, the prediction points 400, 300, 200, 150, 100 and 50 feet are always used in the order given.

The value of the illuminance incident on the eye (E) is compared to the necessary illuminance for detection (E_T) for that ALCH prediction point. If the illuminance produced (E) is greater than the required E_T for the ALCH prediction point of interest, that prediction point is the correct ALCH.

Figure 8-3 gives an example of the extinction rates associated with each ALCH prediction point. The data in Figure 8-3 is for an adaptation level of 1,000 ft-lamberts.

The RVR values shown on the graph indicate the RVR's associated with the transition from one ALCH to another. As an example, an RVR of 1,450 is the smallest RVR that is allowable and still have an ALCH of 300 at the 1,000 ft-lambert adaptation level. In obtaining the RVR values, light setting 5 was used.

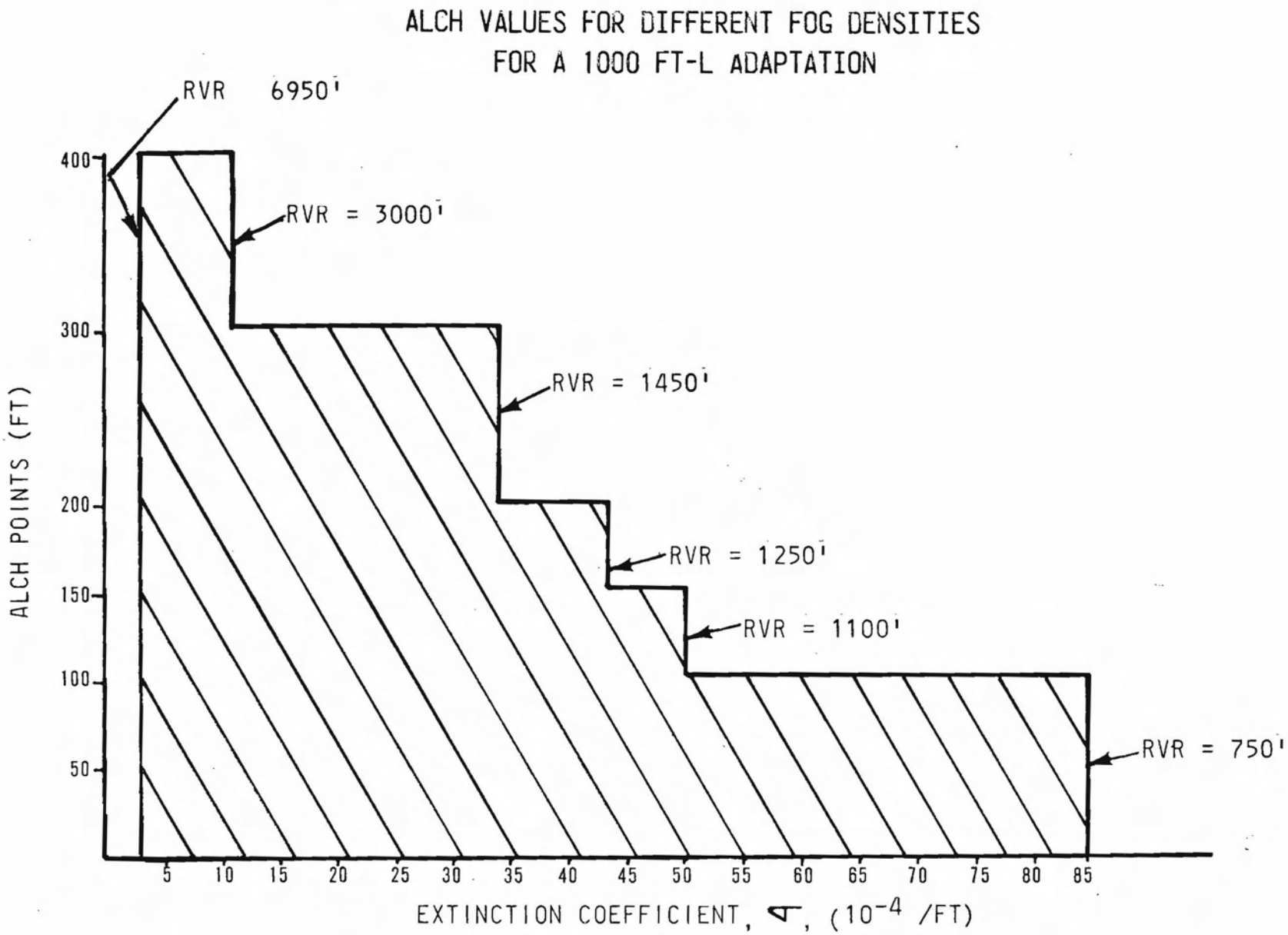
ALCH VALUES FOR DIFFERENT FOG DENSITIES
FOR A 1000 FT-L ADAPTATION
RVR 6950'
RVR = 3000'
RVR = 1450'
RVR = 1250'
RVR = 1100'
RVR = 750'
ALCH POINTS (FT)
400
300
200
150
100
50
5
10
15
20
25
30
35
40
45
50
55
60
65
70
75
80
85
EXTINCTION COEFFICIENT, σ, (10^-4 /FT)

Figure 8-3

As can be seen from Figure 8-3, the extinction rate can vary a large amount yet not change the predicted ALCH. As an example, under the conditions specified in Figure 8-3, the extinction rate can range from 11.3×10^{-4} per foot to 33.7×10^{-4} per foot for a predicted 300-foot ALCH. In terms of RVR, the values can vary from 3,000 feet to 1,450 feet for the 300-foot ALCH prediction.

For comparison, ALCH predictions based upon an illuminance threshold of 1,000 mile-candles are included as Figure 8-4. This illuminance threshold does not take into consideration the adaptation of the pilot. It is interesting to note the similarity of these two graphs. The unusual shape of the graphs is believed due to the approach light-pilot geometry associated with each ALCH prediction point.

Night Case

In Phase I of this project, calculations were made to determine the maximum extinction rate which would allow an observer at each ALCH prediction point to see five approach light bars. Lohkamp, *et al.* (1972), discusses the calculations and the values obtained. The maximum extinction rate is related to an illuminance threshold by Allard's law. The illuminance minimum necessary for detection (E_T) is then compared to the illuminance (E) produced upon the eye by the approach light bar when at an ALCH prediction point. The value of the weighted average extinction coefficient ($\overline{\sigma}$) obtained from the tower measurement is utilized to calculate illuminance on the eye (E).

The ALCH prediction point selected is determined by finding the one where E is closest to E_T yet E is larger than E_T.

ALCH PREDICTIONS FOR DIFFERENT FOG DENSITIES
FOR AN ILLUMINANCE THRESHOLD OF 1000 MILE CANDLES

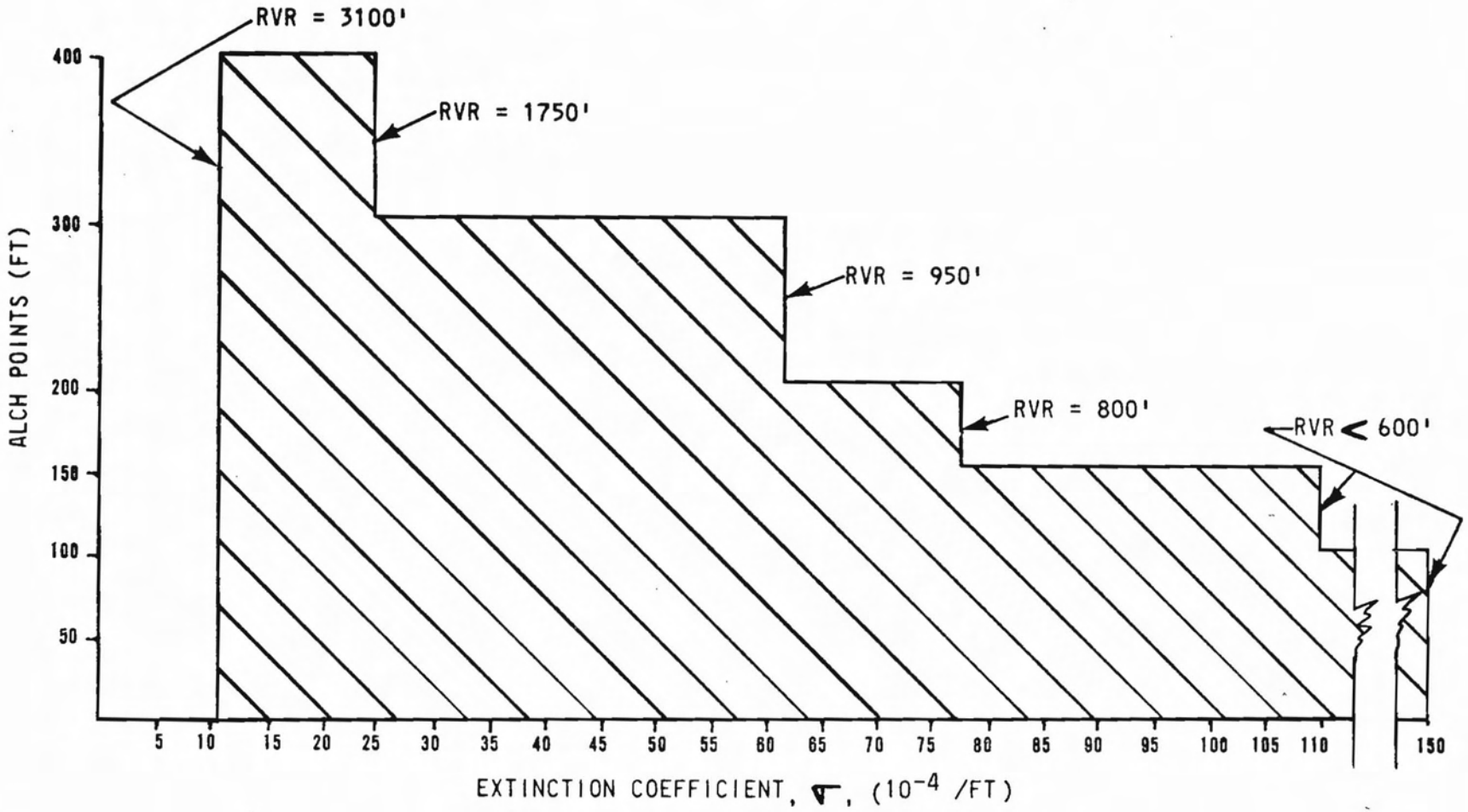

Figure 8-4

Figure 8-5 is a block diagram of the logic and steps in both the day and night ALCH calculations.

SVR Algorithm

Day Case

SVR is the larger of the following two distances: the distance over which .055 contrast is transmitted, or the distance to the furthest selected light which illuminates the pilot's eye to a prescribed level.

The first distance is calculated by Koschmieder's law with a .055 contrast threshold.

$$D = 2.9/\bar{\sigma}$$

$\bar{\sigma}$ = weighted average extinction coefficient (see section on ALCH).

The alternate distance is calculated via Allard's law.

$$E_T = TI_\theta \exp(-\bar{\sigma} D)/D^2$$

E_T = illuminance threshold of the pilot at his adaptation level.

I_θ = the intensity of the light source in the direction of the pilot (taken as 20,000 candelas for runway lights).

T = transmittance of the aircraft windscreen (taken as .8 in all calculations).

ALCH ALGORITHM

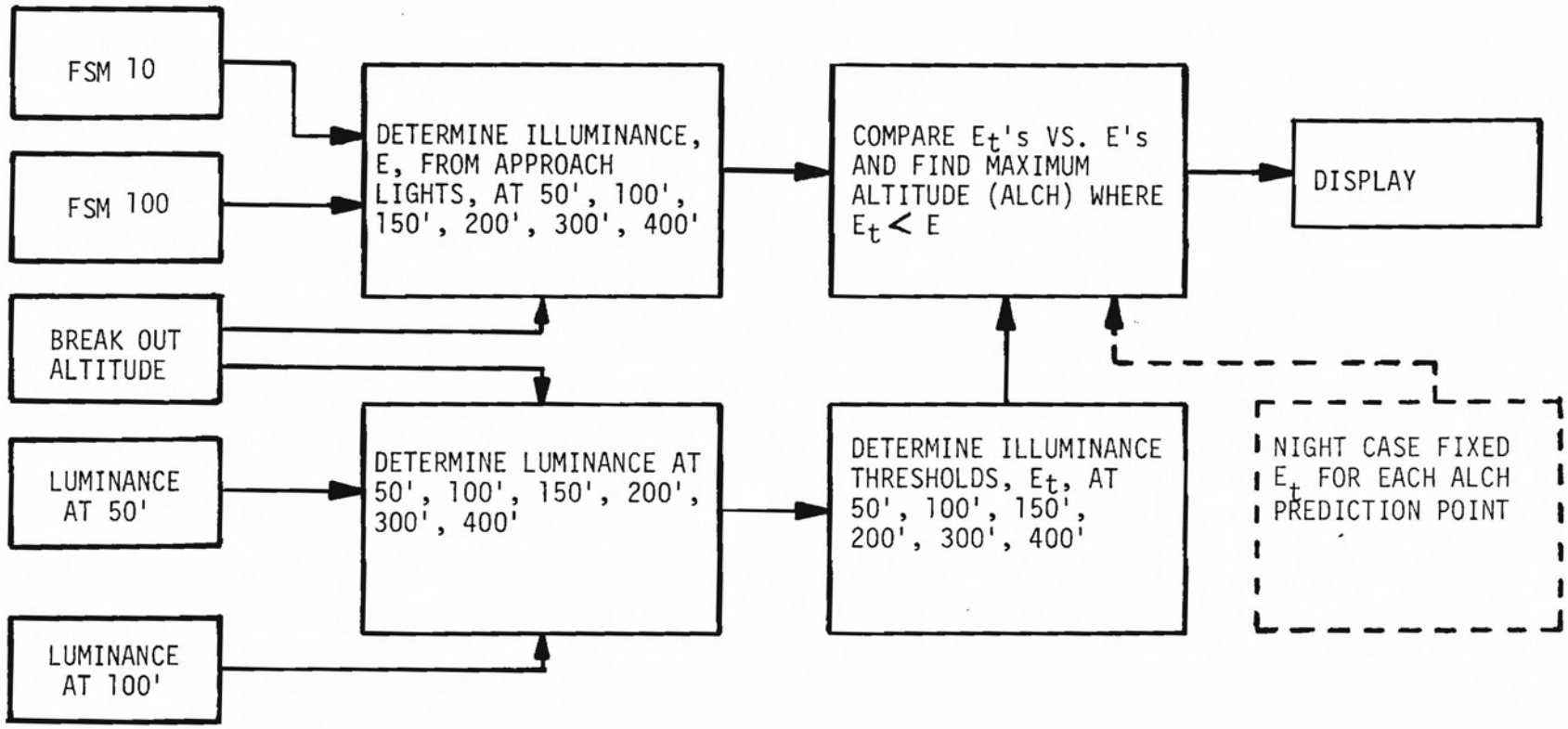

Figure 8-5

When the high intensity runway edge lights are used as the light source, point source data by Blackwell (1946) are used. The illuminance threshold data was multiplied by a factor of two for use in this application to raise it to what Blackwell refers to as a "common sense level of seeing."

The pilot's adaptation must be known in order to determine the illumination threshold. The adaptation is determined through the use of a luminance meter mounted on the tower at a height of 100 feet. The effect of luminance on SVR predictions are shown in Table 8-1.

TABLE 8-1

Adaptation Effect on SVR

Transmission over 250 ft. = .3
RVR = 1,100 ft.

Luminance (Ft-lamberts)	SVR (Feet)
3000	1100
2000	1200
1000	1200
500	1300
250	1400
20	1800

Transmission over 250 ft. = .5
RVR = 1,650 ft.

3000	1600
2000	1700
1000	1900
500	2100
250	2300
20	2900

When the pilot is at 100 feet altitude, he is 1,100 feet from the first runway edge light. This would mean that predictions of SVR less than 1,100 feet would require the use of imaginary lights. To avoid this case, the approach light bars (one through five)

are used as light sources. The data on the illuminance necessary for detection of approach light bars was obtained in a psychophysical study completed earlier in this project.

Night Case

The prediction of the detection of high intensity runway edge lights or of approach lights (one through five) at night is a problem; this is primarily due to the lack of information on the adaptation of the pilot. The luminance meters located on the remote tower cannot yield useful data since they are not viewing the lighted area viewed by the pilot.

In previous experiments conducted for the Federal Aviation Administration (Eggert, 1960) and in the RVR calculation (Larsson, 1970), an illuminance threshold (E_T) of two mile-candles was either found or selected. Using an illuminance of two mile-candles and the Blackwell (1946) data, one can determine the appropriate adaptation level. For a common sense level of seeing the two mile-candles, E_T yields a 2.4 ft-lambert adaptation level.

In the detection of the high intensity runway lights, the two mile-candles E_T is utilized. For the detection of approach light bars one through five, 2.4 ft-lamberts adaptation level was utilized to determine E_T for each bar.

The $\bar{\sigma}$ used in the SVR calculation is determined by the following equation:

$$\bar{\sigma} = \left[\sigma_{10} + \sigma_{100} \right] /2$$

where σ_{10} and σ_{100} are the extinction rates at heights of ten and 100 feet respectively.

Included in this equation is the assumption that σ_{10} represents σ_0 and that the variation with height of σ between σ_{10} and σ_{100} is linear. With only a two-point measurement and limited historical data, one can not justify the use of a more complex form of interpolation.

A block diagram of the day and night calculation of SVR is shown in Figure 8-6.

SVR ALGORITHM

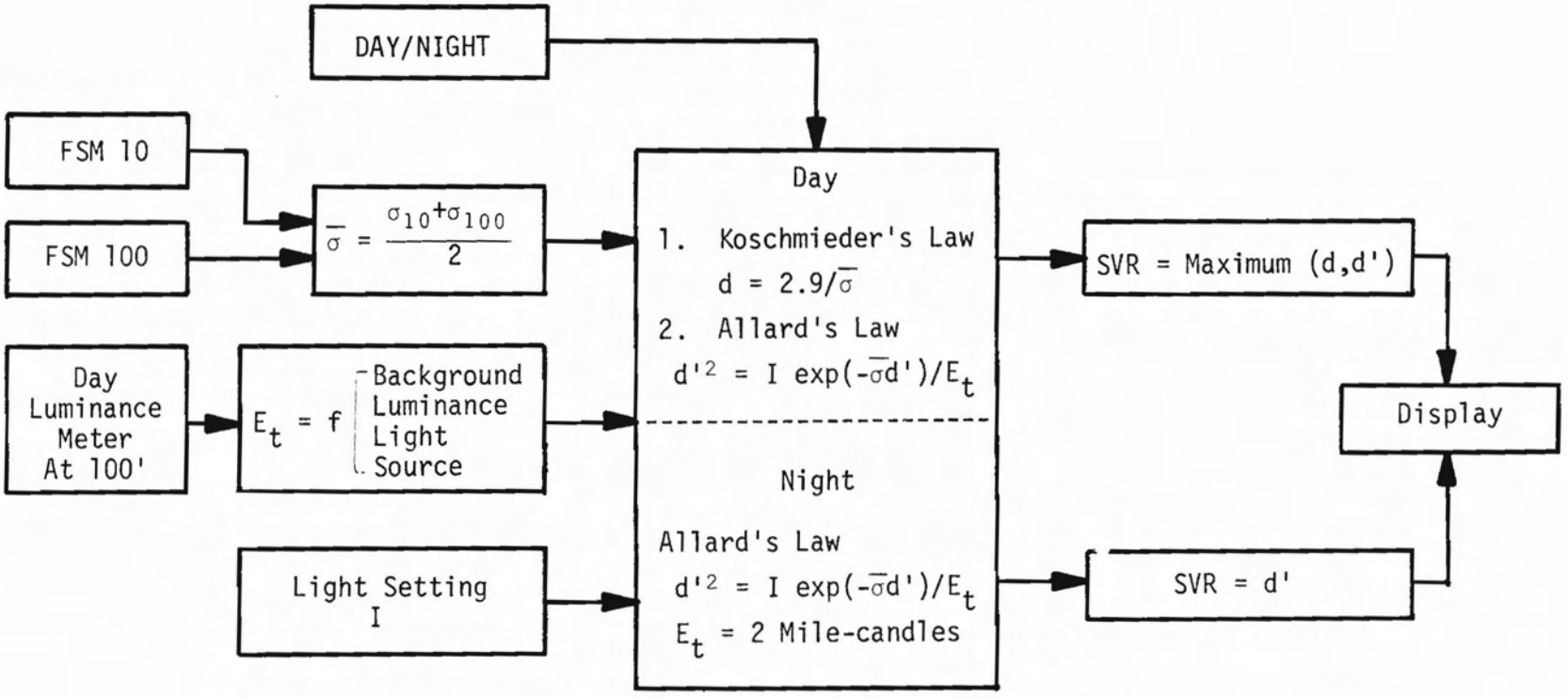

Figure 8-6

9. SYSTEM DEMONSTRATION

The proposed slant visual range system was demonstrated at NAFEC on 23 August 1973. Although the system was fully operational, it was necessary to simulate fog by using data previously recorded. The system demonstrated, therefore, had an extra panel of electronics and did not use the FSM or luminance meters for real time data input.

ALCH/SVR System

The computer, programmed with the ALCH and SVR algorithms, was used with the fog data measured at NAFEC. Several examples were demonstrated by preparing data tapes for use with the system. An example of a fog occurring during daylight used measurements recorded on the morning of 26 March 1973. Transmission measurements from the remote tower at five and 100 feet, luminance recorded at 50 and 100 feet and time of day were entered in the system.

Additional inputs not entering the SVR/ALCH calculations were the transmission record of the 15-foot transmissometer located at the met tower complex. This data was used in the RVR calculations; the results were displayed.

The data used in the demonstration of the night case calculations was recorded on 16 March 1973. The data input, via paper tape, was the transmission recorded from the remote tower at the five-foot and 100-foot levels and the transmissometer readings at the 15-foot level recorded at the met tower complex.

As an additional part of the demonstration, variables such as the transmissions measured at the remote tower, luminance measured at the 50 and 100-foot levels, breakout altitude, cloud cover and light

setting, could be varied with controls on a separate panel, allowing test cases of any type to be investigated.

With the above variable parameters, the effects of changes in luminance, transmission, etc., were shown. As an example, data similar to that contained in Figure 8-1 and 8-2 were visually displayed on the readout panel.

Display Panel

A solid state display panel converts the computer output to a digital readout. Figure 9-1 shows the layout of the panel. The data displayed by the panel are:

1. ALCH in feet, three digits
2. SVR in hundreds of feet, three digits
3. RVR for touchdown, midpoint and rollout in hundreds of feet, two digits each
4. Background brightness coded in steps from 0 - 7
5. Approach light setting, steps 1 - 5
6. Runway light intensity, steps 1 - 5
7. Day/night status

In addition to these displays, a "." is included in ALCH, SVR and the three RVR's indicating when values are below prescribed minima. The display panel has error detection capability, and when an error is encountered, a light signals the observer that the readings displayed should be ignored. The panel automatically resets on the next update of data. The panel at present does not indicate which readings are in error, only that an error is present.

The solid state display panel has several associated advantages. It allows a more concise presentation of the information and is

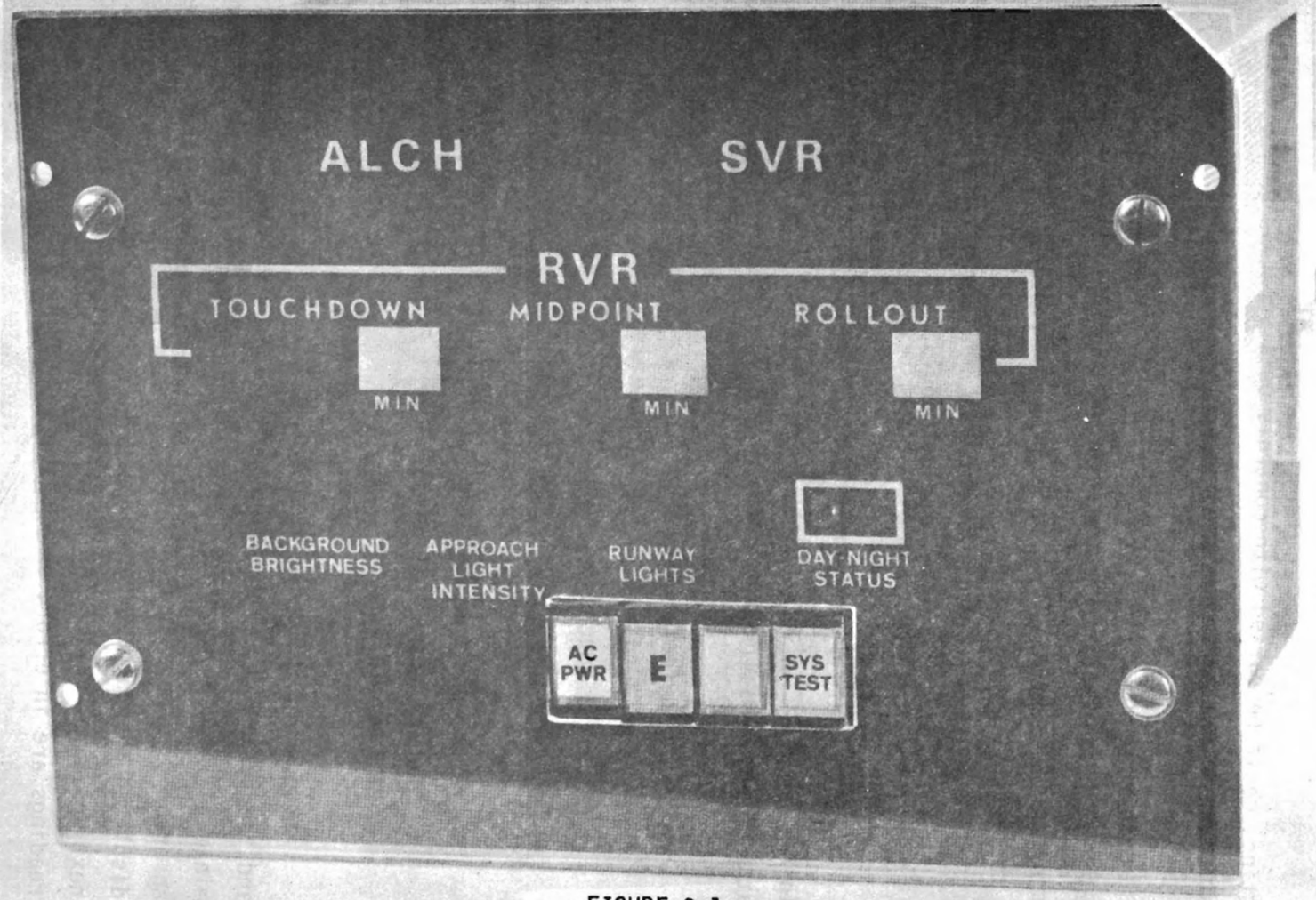

FIGURE 9-1

DISPLAY PANEL

readily expandable for displaying meteorological or other variables. This type of display can be easily connected to a central computer facility through standard teletype interface. The data coding is in a serial format allowing the use of telephone lines and acoustic couplers for transmission of data; therefore, remote display of control tower data is a simple matter.

This demonstration illustrated the operation of the proposed system as well as displaying the instruments and data processing hardware which will be used in the flight tests at NAFEC starting in October 1973. It is hoped that these tests will provide further validation of the instrumental portion of the system, and provide a test of the algorithms used in computing ALCH and SVR with results compared to human observations.

10. REFERENCES

H. R. Blackwell, *Contrast Thresholds of the Human Eye,* J. Opt. Soc. Am. 36, 624-646 (1946).

D. Deirmendjian, *Electromagnetic Scattering on Spherical Polydispersions,* American Elsevier, New York (1969).

C. A. Douglas and L. C. Young, *Development of a Transmissometer for Determining Visual Range,* National Bureau of Standards, Report No. 47, Washington, D.C. (February 1945).

W. E. Eggert, *Approach Visibility Studies at Newark,* Weather Bureau AMB, Project D-1-902 (1960).

W. S. Hering, H. S. Muench and H. A. Brown, *Field Test of a Forward Scatter Visibility Meter,* Air Force Cambridge Research Laboratories, Bedford, Massachusetts (May 1971).

F. C. Hochreiter, *Analysis of Design Characteristics of Meteorological Tower Facility,* Observations and Methods Branch, Weather Bureau, AD 684 864 (January 1968).

G. W. Kattawar, G. N. Plass and F. E. Catchings, *Matrix Operator Theory of Radiative Transfer. 2: Scattering from Maritime Haze,* Appl. Opt. 12, 1071-1084 (1973).

A. Larsson, J. Marut and R. Northedge, *Tables of Runway Visual Range Values as a Function of Transmittance and Various Values of Pilot's Illuminance Threshold and Light Targets,* FAA-RD-70-58 (1970).

C. Lohkamp, G. Bradley, R. Chipman, F. Bagrash, D. Montgomery and L. Wheelock, *Slant Visual Range/Approach Light Contact Height Measurement System,* prepared for FAA by NAD Crane, Indiana, FAA-RD-72-42 (1972).

G. N. Plass, G. W. Kattawar and F. E. Catchings, *Matrix Operator Theory of Radiative Transfer. 1: Rayleigh Scattering,* Appl. Opt. 12, 314-329 (1973).

11. APPENDIX

The list of fog occurrences that served as the data base for this work is shown. Included in the listing is an indication of the form in which the data is recorded.

Fog Occurrence	Computer Data Available	Strip Chart Data Available
12 Sep 1972		X
16 Sep 1972		X
17 Sep 1972		X
18 Sep 1972		X
4 Dec 1972		X
10 Dec 1972		X
12 Dec 1972		X
25 Dec 1972		X
1 Jan 1973		X
22 Jan 1973		X
26 Jan 1973	X	X
28 Jan 1973		X
7 Mar 1973	X	X
9 Mar 1973	X	X
11 Mar 1973	X	X
15 Mar 1973	X	X
16 Mar 1973	X	X
26 Mar 1973	X	X
29 Mar 1973		X
31 Mar 1973	X	X
1 Apr 1973		X
2 Apr 1973		X
27 Apr 1973	X	X
9 May 1973	X	X
23 May 1973	X	X
29 May 1973	X	X
30 May 1973	X	X
31 May 1973		X
3 Jun 1973		X
8 Jun 1973	X	X

The format of the computerized data is illustrated below. Time is shown as Julian date and hours and minutes for a 24-hour clock. The transmittance measured by each transmissometer is shown in percent. The readings for the slant transmissometer are adjusted to a 250-foot baseline.

Date	Hr	Min	T_5	T_{15}	T_{51}	T_{87}	T_{123}	T_{159}	T_S
75	19	32	95.6	98.3	90.8	81.2	59.3	34.3	74.2
75	19	34	93.6	96.9	86.3	70.6	36.4	18.8	60.2
75	19	36	95.2	97.6	91.4	81.0	46.6	19.4	70.4
75	19	38	95.2	97.6	90.7	79.1	41.8	18.4	65.8
75	19	40	94.3	97.0	88.6	73.5	38.6	19.9	63.1
75	19	42	94.8	97.5	90.8	81.6	51.9	31.2	68.9
75	19	44	95.6	98.1	92.3	86.0	73.3	47.5	83.0
75	19	46	95.4	97.8	92.1	86.0	74.1	48.0	83.0
75	19	48	94.0	96.6	89.7	80.6	63.4	39.4	76.8
75	19	50	96.0	98.0	93.1	86.3	73.1	44.8	83.4
75	19	52	96.4	98.8	93.6	88.0	76.3	49.9	86.5
75	19	54	96.8	99.1	94.4	90.3	81.9	56.9	89.3
75	19	56	97.1	99.3	94.9	91.4	86.3	75.0	92.3
75	19	58	97.2	99.4	94.8	91.5	87.8	82.9	93.8
75	20	0	96.7	98.9	94.4	90.6	85.6	77.2	92.1
75	20	2	96.2	98.5	93.5	89.0	81.9	67.1	89.7
75	20	5	96.0	98.8	93.0	88.7	82.8	70.3	90.5
75	20	7	96.1	98.8	92.9	88.3	79.9	62.0	88.1
75	20	9	95.4	98.3	90.9	82.9	59.8	37.2	75.1
75	20	11	93.9	97.3	86.6	73.1	49.7	36.3	68.9
75	20	13	93.9	97.3	87.5	74.2	39.1	19.0	64.0
75	20	15	89.3	93.9	76.6	52.9	26.2	14.5	48.7
75	20	17	90.8	95.1	77.8	35.9	10.4	6.6	33.6
75	20	19	77.2	85.0	52.9	29.6	15.8	8.8	31.9
75	20	21	68.4	77.1	41.0	18.8	8.6	6.4	21.6
75	20	23	65.1	74.4	40.1	20.6	11.2	7.9	22.7
75	20	25	60.8	69.9	36.4	18.8	9.6	6.6	21.3
75	20	27	57.0	66.5	34.6	19.1	9.2	6.3	19.2
75	20	29	53.2	63.8	26.3	12.3	6.0	4.2	15.1
75	20	31	43.2	53.5	22.8	12.6	8.6	6.4	15.7
75	20	33	43.7	53.6	25.6	15.7	8.5	6.6	16.0
75	20	35	48.6	58.0	29.1	17.8	11.1	8.3	20.7
75	20	37	49.8	59.2	33.2	19.9	10.4	7.0	20.0
75	20	39	51.0	60.8	28.5	15.9	9.3	6.8	19.0
75	20	41	50.6	60.3	27.3	15.9	8.8	6.4	17.3
75	20	43	44.8	54.5	25.1	14.5	8.2	6.1	16.0
75	20	45	38.8	48.4	19.4	11.0	6.4	5.0	13.8
75	20	47	34.2	43.5	15.0	9.4	5.1	4.0	12.0
75	20	49	32.1	41.1	14.1	9.5	5.7	5.2	12.0
75	20	51	31.3	39.5	16.0	11.1	6.7	5.3	12.9
75	20	53	33.2	41.8	16.2	10.3	5.9	4.7	12.4
75	20	55	32.9	41.5	15.6	9.5	5.1	3.6	11.6
75	20	57	36.4	44.6	21.8	13.4	7.2	5.3	14.8
75	20	59	36.1	44.9	18.7	11.9	7.4	5.8	14.2
75	21	1	31.8	40.0	14.6	9.4	6.1	4.4	12.5
75	21	3	30.6	38.1	13.8	10.4	7.3	6.3	13.5
75	21	5	32.1	41.0	15.4	9.8	5.7	4.9	11.9
75	21	7	39.1	47.2	25.1	14.6	7.6	5.6	15.4

34958